AN ELECTRICAL RESISTIVITY SURVEY IN THE AREA SOUTH OF SUSWA VOLCANO

BY

OMONDI C. JUMA

A thesis submitted in partial fulfilment for the degree of Master of Science (Geology) in the University of Nairobi

NAIROBI 1992

DECLARATION
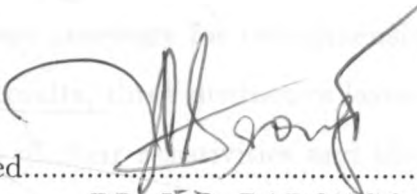
This is my original work and has not been submitted for a degree in any other University

Signed..
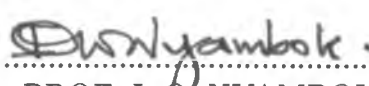OMONDI C. JUMA

The thesis has been submitted for examination with our knowledge as University supervisors

Signed..
DR. J. O. BARONGO

Signed..
PROF. I. O. NYAMBOK

ABSTRACT

The area south of Suswa volcano is underlain by volcanic and volcano-sedimentary rocks of the Pliocene-Pleistocene-Recent Periods. These rock types are common water-bearing formations, especially the weathered, fractured or transition zones along faults and at interfaces of the various volcanic flows. Consequently, any groundwater investigations are usually based on methods aimed at detecting such underground structures. Electrical resistivity studies conducted in the area have indicated low resistivities which appear to be associated with geothermal fluids migrating from the Suswa volcano region. Hot grounds and fumaroles within the perimeter of Suswa caldera indicate that the geothermal system is likely to be directly beneath Suswa volcano. The resistivities are further noted to increase southwards. The low resistivities are attributed to high fluid temperatures and/or conductive minerals within the water-bearing units which are either weathered or fractured. The actual temperatures of these reservoirs are between 70^0 and 100^0 C which are considerably below those expected for high temperature geothermal systems. High temperature geothermal areas normally border low temperature geothermal areas and the present area of study borders the more productive high temperature Olkaria geothermal fields.

The analysis of resistivity data was first done by partial curve matching prior to the use of linear inverse theory in the determination of the most probable physical parameters of the subsurface layers necessary for two-dimensional interpretation of the underlying geology. From the results, three distinctive layers overlying a resistive half-space were recognized in terms of their resistivities and thicknesses. The main conductive layer, which is one of those three layers, immediately overlies the resistive half-space.

ACKNOWLEDGEMENT

Contents

CHAPTER 6   DISCUSSION AND CONCLUSIONS

List of Figures

List of Tables

List of Plates

Chapter 1

INTRODUCTION

1.1   General

Adequate water supply and rural electrification are among the top priorities in the Kenya government's development goals. Many projects have been initiated with an aim of achieving these two goals. In this respect, foreign contracted firms and governments have aided the country in several ways to try and meet these goals. Groundwater is of vital importance, particularly to the rural communities who are disadvantaged by lack of clean piped water. Unlike stream water, groundwater is readily available for consumption since it needs less, if any, treatment. Further, streams do not occur in every area whereas chances of striking groundwater may be fairly good. Geothermal steam is presently being utilized in Kenya to generate electric power. The Olkaria geothermal project, situated in the Kenya Rift Valley, at present supplies 45 Megawatts (MW) of electric power to supplement the other sources of electricity. However, there is still need for more electric power to enable the government meet the demands of the rural electrification programme.

The need for more water supply from the subsurface and electric power from geothermal reservoirs has made it necessary for more subsurface investigations to be conducted. This should involve detailed studies of shallow subsurface structures that control groundwater movements and delineation of the actual aquiferous zones and deep subsurface investigations for geothermal reservoirs. Several geological, geophysical, geochemical and hydrogeological methods are known which are used to carry out these studies. The present investigation was concerned with the geophysical method of verti-

1

cal electrical sounding (VES) the results of which were correlated with those from other resistivity studies of the adjacent areas.

The location of the present study area is within a zone of young volcanism and has a concentration of temperature and thermal upflow, features which are appropriate for a geothermal field. The vertical electrical sounding method is used to determine the ability of rocks to conduct an electric current (i.e., their conductivity) and to delineate zones sharing similar electrical properties. These properties largely depend on the amount of water present, salinity of the water, temperature and the way in which the water is distributed within the rocks (Keller and Frischknecht, 1966). Prediction of groundwater and geothermal resources depends on fixing the subsurface configuration. It is, therefore, the aim of this study to carry out these investigations and to come out with geoelectric models of the area south of Suswa volcano. The instruments used for the resistivity survey were readily available and portable.

The method used in the analysis is the inversion of ground resistivity data. This method has been applied elsewhere in the rift valley where the conditions are similar to the present area. The results obtained by such studies were correlated by the use of integrated geophysical surveys in the earlier work. An integrated survey could, however, not be applied in the present work due to lack of funds.

1.2   Location and accessibility

The study area which occurs to the south of Mount Suswa is situated in the Rift Valley, between Mount Suswa and Lake Magadi, in the Kajiado District of the Rift Valley Province. It measures about 200 square kilometres and is bounded by longitudes 36^0 $19'$ E and 36^0 $25'$ E and latitudes 1^0 $10'$ S and 1^0 $20'$ S (Fig 1.1) and lies further south of the much explored and exploited Olkaria geothermal field.

The area can be reached through the Nairobi - Narok tarmac road or the Nairobi - Ngong - Narok tarmac/murram road. The latter is shorter but not as good as the former. The Nairobi - Narok road runs round the northern side of Mount Suswa while the Nairobi - Ngong - Narok road runs north-south on the eastern side of the area.

2

0^0 30′ S

35^0 30′ E 36^0 00′ E 36^0 30′ E 37^0 00′ E

EBURRU
GEOTHERMAL
FIELD

L. NAIVASHA

KIJABE

OLKARIA
GEOTHERMAL
FIELD

LONGONOT

1^0 00′ S

VOLCANO

NAROK

SUSWA
VOLCANO

NAIROBI

AREA OF
STUDY

1^0 30′ S

NGONG

SCALE 1:1 000 000

0   10   20 Km

Main roads

MOSIRO

Rift boundary

L. MAGADI

2^0 00′ S

KAJIADO

MAGADI
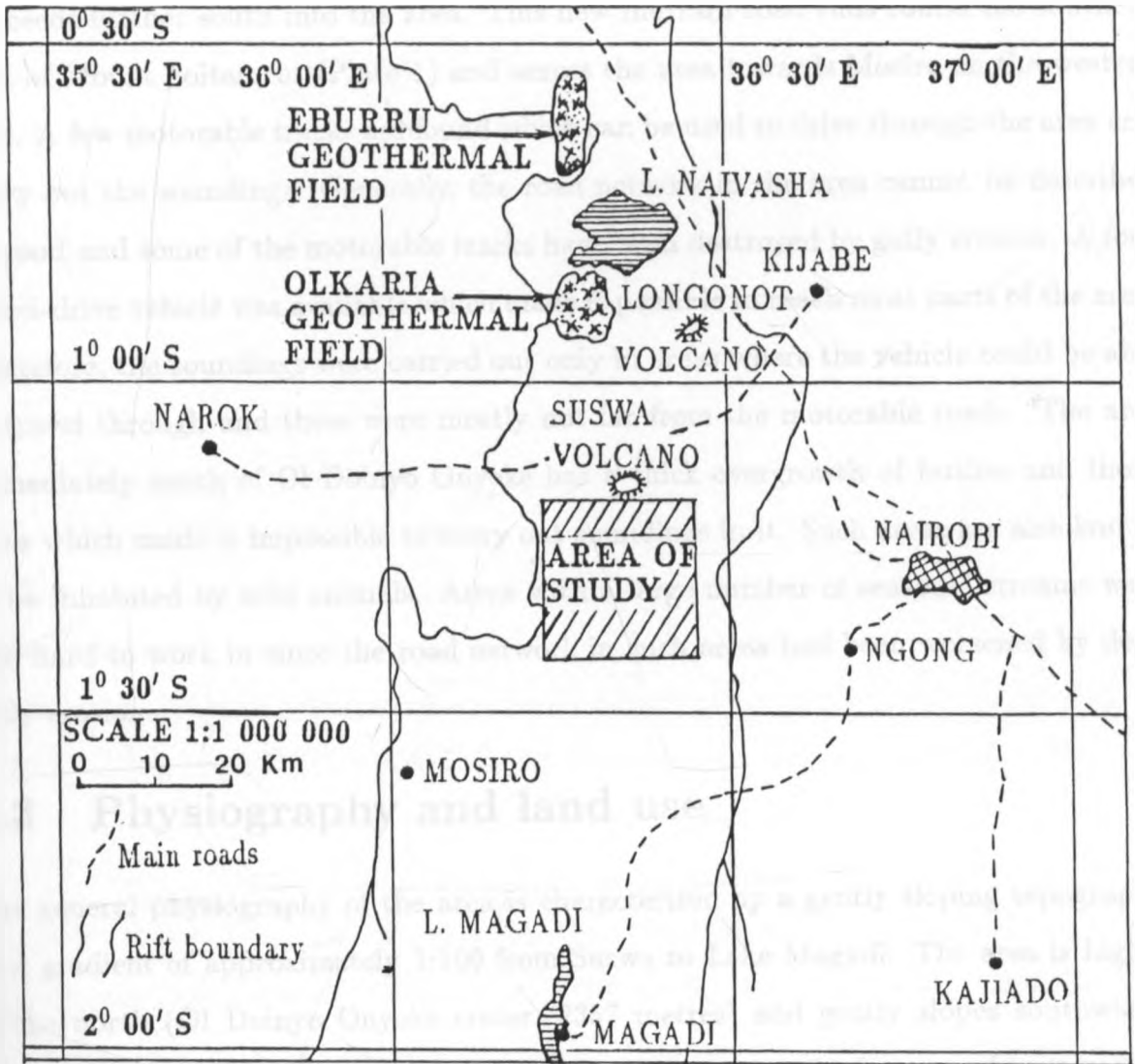
Figure 1.1   Location map of the area south of Suswa volcano and other geothermal areas within the Kenya Rift valley.

3

However, there is a new murram road that branches off from the Ngong - Narok road to the Ewaso Kedong shopping centre, which is just on the outskirts of the area, and proceeds further south into the area. This new murram road runs round the southern foot of Mount Soitamrut (Plate 1) and across the area towards Mosiro on the western side. A few motorable tracks are found which can be used to drive through the area and carry out the soundings. Generally, the road network in the area cannot be described as good and some of the motorable tracks have been destroyed by gully erosion. A four wheel-drive vehicle was available which made it possible to reach most parts of the area. Therefore, the soundings were carried out only in areas where the vehicle could be able to travel through and these were mostly not far from the motorable roads. The area immediately south of Ol Doinyo Onyoke has a thick overgrowth of bushes and thorn trees which made it impossible to carry out soundings in it. Such areas are also known to be inhabited by wild animals. Areas with a large number of seasonal streams were also hard to work in since the road network in such areas had been worsened by deep gully erosion.

1.3 Physiography and land use

The general physiography of the area is characterized by a gently sloping topography at a gradient of approximately 1:100 from Suswa to Lake Magadi. The area is higher in the north (Ol Doinyo Onyoke crater, 2357 metres) and gently slopes southwards towards Lake Magadi. However, there are a few interruptions in the general topography. Soitamrut crater on the south-eastern side of Mount Suswa (Plate 2) rises to about 1600 metres above sea level and is surrounded by a flat plain which stands at about 1400 metres above sea level. Mount Kalelerue on the southern side of the area rises to about 1400 metres above sea level and is surrounded by a flat plain of about 1200 metres above sea level. The low southern parts of the area are characterized by isolated depressions. Some of these depressions, however, have been filled with pyroclastics. Volcanic cones and domes which were plenty in the central parts of the area previously are not visible (Baker, 1958; Baker and Wohlenberg, 1971). The cones have been eroded and the domes

filled up with pyroclastics such that the topography along the central regions of the area is characterized by a gently sloping plain. Their presence has, therefore, been marred by the recent deposits.

The drainage pattern closely follows the topographical set-up. The area has seasonal streams which flow from the foot of Ol Doinyo Onyoke crater towards south. They terminate at what used to be depressions where they have now formed swamps. A dendritic pattern is evident where the streams originate. The seasonal streams have greatly contributed to gully erosion in the area.

Natural vegetation includes dry forms of woodland and savanna or derived semi-deciduous bushland (Kenya Atlas, 1970). Grass is scant and low thorn bushes are plenty. The area immediately south of Ol Doinyo Onyoke crater has a thick cover of thorn trees and bushes with an uneven surface due to gully erosion.

The area comprises land of marginal agricultural potential. The characteristic soil types are light brown to black loam with a poor sub-angular blocky structure showing little or no profile development and confined to depressions on the lava surfaces (Baker, 1958; Kenya Atlas, 1970). These soils are derived from volcanic materials. The soil profile is not thick enough and, as such, it is not rich in humus.

The area receives low rainfall for the greater part of the year and temperatures are high (32^0 C) in the months of April and May. Usually, about 130 millimetres mean monthly rainfall is received (Kenya Atlas, 1970; Kenya Met. Dept. data, 1931-1980).

Due to poor soil cover and low rainfall, the Maasai who live here are mainly pasturalists and keep large herds of cattle. The area is a potentially productive rangeland.

1.4 Geological exposure

The eastern Rift System is tectonically active and dates back to between Plio-Pleistocene and Recent. The stratigraphy is characterized by a sequence of volcanic rocks associated with recent volcanism.

The geology of the area is divided into seven main formations and their differences are attributed to their mode of formation, volcanic events, relative age, appearance

and composition. The geology, as noted by Torfason (1987), does not differ from what was noted by earlier geologists (Baker, 1958; Thompson and Dodson, 1963; Randel and Johnson, 1970; Saggerson, 1971; Kagasi, 1983). The main formations are not very conspicuous in the field as their presence has been covered by recent deposits, i.e., volcanic soil. They have been covered by pyroclastic material erupted later from the Suswa volcano. The main formations are described below in their stratigraphical order and are also indicated in Figure 1.2.

1.4.1   Qv: Volcanic soil and pyroclastics

These formations cover the plains on the southern part of the area. The volcanic soils and alluvium are derived from reworked pyroclastics from Suswa volcano (Torfason, 1987). The volcanic soils are light brown in colour with a weak sub-angular blocky structure showing little or no profile development (Baker, 1958; Kenya Atlas, 1970). These volcanic soils and pyroclastics were probably washed down from Suswa southwards by the Kedong flood at about 0.1 Ma. They were consequently confined in depressions on the lava surfaces in the southern end of the area and beyond.

1.4.2   Sa: Ol Doinyo Onyoke lavas

These formations are widespread on the immediate southern regions surrounding the Ol Doinyo Onyoke crater. Small patches of these lavas are noted in the central parts of the area. The volcano produced lavas which are distinctly K-feldspar porphyritic and form a very distinct group. The volcanic event that produced these lavas is distinct in that the volcanic centre is well defined and all the lavas were erupted from radial fractures centred on the Ol Doinyo Onyoke volcano which then grew up to be the highest point of the volcano (2357 metres).
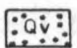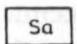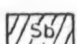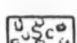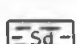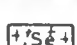
1.4.3   Sb: Agglutinates and lavas

These rock types are widespread on the south-eastern flanks of Ol Doinyo Onyoke volcano, but are also found on the central parts of the area. The formations consist of numerous fine-grained flows some of which are glassy and very vesicular, almost pumice-
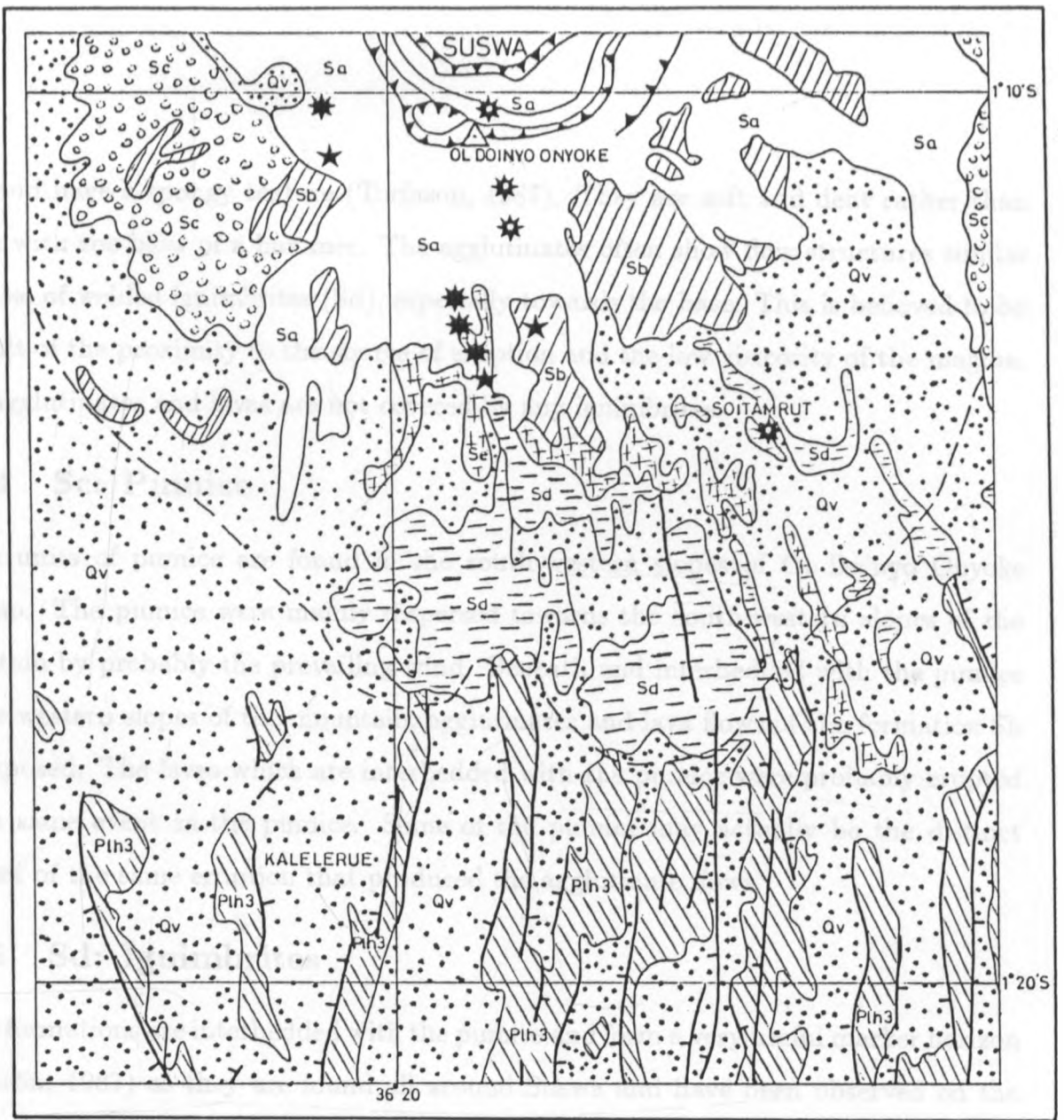
LEGEND

:Qv:	Volcanic soil and Pyroclastics
Sa	Ol Doinyo Onyoke lavas
Sb	Agglutinates and lavas
Sc	Pumice
Sd	Ignimbrites
Se	Lavas not faulted
Plh3	Plateau Trachytes

Eruption Centres and
Volcanic craters

Normal faults

Caldera faults

SCALE

0   1   2   3 Km.

Figure 1.2   Geological map of the area south of Suswa volcano.

like, and have a spongy texture (Torfason, 1987). They are soft and dent rather than break with the blow of a hammer. The agglutinates often show flow structures similar to those of welded ignimbrites (Sd), especially towards the base. This is believed to be a result of the proximity to the source of eruption and the low visicosity of the magma. The agglutinates and lavas are not covered by any ignimbrites.

1.4.4   Sc: Pumice

Thick units of pumice are found in the south-western slopes of Ol Doinyo Onyoke volcano. The pumice were mainly dispersed towards the south-western slopes of the mountain by probably the prevailing wind. Beneath and interbedded with the pumice on the western slopes of the mountain, agglutinates and lava flows of the formation Sb are exposed. The lavas which are interbedded with the pumice were probably erupted in the same event as the pumice. Some of the pumice may actually be the distinct product of the same eruption that produced the agglutinate flows.

1.4.5   Sd: Ignimbrites

These formations are interbedded with the pumice and form a very useful marker horizon (Torfason, 1987) as they are found all around Suswa and have been observed on the plains south of Suswa. The welded ignimbrites have been renamed as 'Globular lava flow' by Baker (1958) and Randel and Johnson (1970). They are dark greyish in colour, usually not thicker than 1 to 3 metres and contain abundant rounded to oval pumice. There is a decreasing amount of welding towards the top of this unit . The unwelded ignimbrites, also known as 'non-globular lava' (Baker, 1958 and Randel and Johnson, 1970) are yellowish in colour, 0.5 to 3 metres thick, and are mostly concentrated on the eastern parts of the area.

1.4.6   Se: Lavas not faulted

These are lavas which were not affected by the regional north-south tectonic fracture system. They are poorly exposed and too thin. They incorporate the base of the volcano (Torfarson, 1987) and consist of lavas, agglutinate flows and minor pyroclastics.

They are defined as rocks formed after the major faulting system. Lavas affected by the regional faulting (also known as 'Faulted Lava') are not widespread in the area. They form the base of the volcano and are covered by younger volcanics and are likely to be observed on the southern and eastern sides of Suswa. Soitamrut crater probably belongs to this formation.

1.4.7 Plh3: Plateau trachytes

These formations include the orthophyre trachytes and the alkali trachyte series. The orthophyre trachytes conformably overlie the alkali trachytes with little or no intervening sediments (Baker, 1958; Thompson and Dodson, 1963). The plateau trachytes are considered younger than the neighbouring Limuru trachytes on the eastern side of the area. The plateau trachytes are exposed throughout the entire southern parts of the area except where the volcanic soils and pyroclastics occur in depressions.

1.5 Stratigraphy

The surface geology of the Suswa area gives little indication of the subsurface geologic succession. Due to the absence of the deep boreholes in the area, the subsurface stratigraphy and the thickness of the various volcanic rock types have been inferred from geologic studies in the surrounding regions. Such studies include the chronology and the areal volume distribution of the volcanics in the central Kenya rift region by Saggerson (1971), Baker et al. (1972), Kagasi (1983) and others.

The rift valley is associated with large volumes of Cainozoic lavas and pyroclastics which become younger towards the rift centre (Saggerson, 1971; Baker et al., 1972) There seems to exist some bilateral symmetry about a central axial graben marked by recent caldera, namely Suswa and Longonot. The Kedong floor and the entire area south of the Suswa volcano is dominated by volcanoclastic sediments and lavas. These rocks have been deposited unconformably over those that form the eastern margin of the rift (Kagasi, 1983). This is evident from the altered surfaces, probably due to weathering between the older rocks and the recent deposits. The surface of the area south of Suswa is covered by lacustrine sediments and other Recent deposits including

volcanic soils, dust and ash (Table 1.1). These sediments were derived from the pre-existing volcanics which were then transported by the Kedong flood and deposited in a lacustrine environment, probably during the Upper Pleistocene Period (Thompson and Dodson, 1963). The sediments were not affected by any of the faulting that cut the other rocks. The sediments unconformably overlie the yellow to buff pumiceous tuffs, some rhyolites and ignimbrites whose thicknesses do not exceed 200 metres (Baker et al., 1972; Kagasi, 1983). These are underlain by Pliocene to Pleistocene trachytes and rhyolites with intercalations of tuffs and the whole series forms the uppermost volcanic sequence. These are consequently underlain by a sequence consisting predominantly of phonolites of Middle Pleistocene to Lower Pliocene age. Thicknesses of up to 900 metres have been revealed at the rift margins (Saggerson, 1971; Baker et al., 1972; Kagasi, 1983). The basement system consists of Precambrian migmatites and high grade metasediments of the Mozambique belt (Baker et al., 1972; Baker et al., 1987).

Table 1.1   Stratigraphic sequence of the area south of Suswa volcano

	FORMATIONS	PERIOD
4	Recent pyroclastic rocks (ash and dust)	Recent
3	Yellow-buff pumiceous tuffs, fluvial sediments and lacustrine sediments.	Middle-Upper Pleistocene
		Intense Faulting
2	(iii) Trachytes and rhyolites (ii) Welded tuffs and pyroclastics (i) Phonolites	Upper Pliocene to Middle Pleistocene

1.6   Previous work

The Kenya Rift Valley has been the subject of intensive investigations for the last three decades. Earlier exploratory work mainly involved geological mapping and geochemical sampling. Geophysical investigations, involving mainly the galvanic resistivity method of exploration, were first carried out in the mid 60's. These were mainly done in the

search for groundwater supplies (Keller, 1971).

The geology of the area around the Suswa volcano was first described by McCall and Bristow (Torfason, 1987) and then later by Johnson in 1966 and 1969 (Geotermica Italiana, 1988). Kagasi also carried out petrological studies of the areas surrounding Suswa volcano. The most recent geological mapping was carried out by Baker, Mitchell and Williams (1987). Randel and Johnson (1970) have printed a geological map sheet (scale 1 : 125 000) of the area covering the Suswa volcano and the surrounding vicinity.

The first geothermally related work was carried out in 1945 (Geotermica Italiana, 1988) in which observations on the steam jets in Suswa area were made. This work, however, did not involve any kind of geophysical exploration. However, theories on the possible geophysical and geological characteristics of the area were formulated. It was postulated that the steam originate from meteoric water augmented by juvenile water associated with the underlying magma (Thompson and Dodson, 1963) and trapped beneath the hard rocks by some pressure release mechanism. Some fumaroles have also been reported in the area by other geologists (Torfason, 1987).

Between 1963 and 1975, several resistivity surveys were carried out in the Rift Valley for the search of geothermal reservoirs by various groups and firms. This is considered the period when intensive geophysical work was initiated to investigate the geothermal potential of particular areas within the Rift Valley. Balfour, Beatty and Co. (1968) was the first to carry out Wenner soundings in 1968 with the aim of establishing the structural geology of the geothermal area between Lakes Nakuru and Bogoria which also cover the Menengai area. Keller (1971) re-interpreted their data in which the survey failed to show the presence of low resistivity zones within the first 500 metre from the surface. Group Seven Incorporated (1971) carried out resistivity surveys at Lake Bogoria, Eburru and Olkaria on behalf of East Africa Power and Lighting Company Limited (E.A.P.L.Co. Ltd.) and contracted by United Nations Development Program (U.N.D.P.). Their purpose was to outline the geothermal systems potentially useful for the generation of electrical power. Their survey also included electromagnetic soundings. They noted low resistivities beneath steaming ground. Furgerson (1972) carried out 30 Schlumberger soundings at Olkaria to map both vertical and lateral resistivity

changes. He noted that the southern and eastern sides of Olkaria were potential areas for geothermal reservoirs and that the depth to the basement ranges from just less than 2 kilometres to 4.5 kilometres. The resistivities drop with depth from 100-500 Ωm at the surface to about 5 to 11 Ωm at a probing depth of 2 kilometres. Baker and Wohlenberg (1971) noted an axial gravity high in the Rift Valley and attributed this to the intrusion of mantle material to the shallow depths beneath the Rift Valley. Fairhead (1976) further suggested a combination of volcanic infill and a relatively narrow dyke to account for the gravity high along the axis of the Rift Valley. Skinner (1977) postulated that a deep heating source at about 2500 metres exist along the axis of the Rift Valley where the mantle derived intrusion coincides with the depth of the crystalline basement (herein referred to as the 'resistive substratum' or the 'electric basement').

Several individuals have also worked in the area between Lake Naivasha and Suswa volcano for educational purposes. Bhogal (1978) used the roving polar-dipole method to study the geoelectrical characteristics of the areas around Lake Bogoria, Eburru and Olkaria and to provide scientific framework for the evaluation of the hot water and steam and to aid in siting test wells for production. At the Olkaria area, geothermal energy has been realized where at present 45 megawatts of electric power are produced. He recommended that further investigations be carried out in the area lying south of Olkaria geothermal field. He termed the southern extent of the Olkaria geothermal field as 'open' and apart from the few observations made by Torfason (1987), no previous geophysical work has been carried out on the geothermal potential of the areas south of Suswa volcano. However, the Ministry of Energy and Regional Development (M.O.E.R.D.) carried out a few soundings mainly for training purposes. They had previously been working on a project in the area between Longonot and Suswa volcanoes. Ndombi (1981) re-interpreted the resistivity and gravity data of the Olkaria region obtained by E.A.P.L.Co. Ltd/U.N.D.P between 1968 and 1975. He suggested a three-layered horizontal volcanic sequence overlying the basement. Mwangi (1981) carried out electrical resistivity soundings in Olkaria with a view to establishing the boundaries of the Olkaria geothermal fields. He, however, did not achieve the intended goals.

In 1987, Geotermica Italiana s.r.l. of Italy, contracted by U.N.D.P. to the Kenya Power and Lighting Company Limited (K.P.L. Co. Ltd) and the Ministry of Energy and Regional Development (M.O.E.R.D.), carried out resistivity soundings in Suswa - Longonot areas and most parts of Kedong Valley. The Geotermica Italiana team carried out the soundings in the areas between Longonot and Suswa with a maximum current electrode separation of up to 8000 metres (AB/2=4000 metres). The M.O.E.R.D. team carried out a few soundings in the areas south of Suswa volcano with a maximum current electrode separation of 8000 metres. The purpose of the resistivity survey by the M.O.E.R.D. team was to train them on how to operate the Geo-Resistivity Meter GR 3000 and how to carry out a field survey with it. Their data have, however, yet to be interpreted.

The present work was also compared with related work that has been done elsewhere around the world, especially in known geothermal fields. Notable examples are works by Cataldi et al. (1978) who did some assessment of the geothermal potential of central and southern Tuscany, Italy; Isherwood and Mabey (1978) who evaluated the Battazor geothermal resources in Nevada, U.S.A; Razzo et al. (1989) who carried out resistivity studies of Cerro Prieto geothermal fields, Mexico; Zohdy et al. (1980) who outlined the application of surface geophysics to groundwater investigations and so is Meidav (1960).

1.7   Objectives of the study

The basic aim of this study was to investigate the subsurface geoelectric structure in the area south of Suswa and use the results to assess the groundwater and geothermal energy potential of the area. The vertical electrical sounding method employed to do this makes use of the electrical properties of rocks and minerals (i.e., their ability to conduct electric currents) by introducing an artificial source of current into the ground through point electrodes. The potential associated with this current is measured and used to study the subsurface structure.

The main objectives of this study are, therefore, to use the electrical sounding method to

(a) determine the geoelectric structure beneath the area south of Suswa volcano by studying the conductivity of the formations and delineating zones showing similar electrical properties, and

(b) interpret the resulting geoelectric structure in terms of the groundwater and geothermal energy potential of the area.

These objectives are aimed at delineating the lateral and vertical boundaries of the conductive and resistive subsurface zones and relating them to those two important natural resources. In trying to accomplish them, two important facts, which make the study much more interesting, should be borne in mind: (i) that the geological setting of the areas north and south of Suswa volcano are almost comparatively similar and so are other characteristic features such as fault trends and physiography (Baker, 1958; Thompson and Dodson, 1963; Randel and Johnson, 1970; Baker et al., 1987) and (ii) that the southern extent of the Olkaria geothermal field, which is situated a short distance to the north, appears 'open' (Bhogal, 1978). This is interesting because the groundwater system beneath these regions may be connected.

Chapter 2

THEORY

2.1 General

This chapter deals with the theory of the electrical resistivity method and a brief description of the inversion algorithm used in the program employed to analyse the data. The theory of current propagation and the potentials associated with this current in a homogeneous and isotropic medium is outlined in various geophysical texts such as Dobrin (1978), Grant and West (1965), Keller and Frischknecht (1966), Telford et al. (1990), among others. Therefore, only a short outline of the basic principles will suffice.

A program code-named SCHINV (SCHlumberger INVersion) was used in the computer analysis of data. It employs a number of subroutines that are invoked during the computations. It had been coded by Barongo (1989) and it makes use of the least squares inverse theory as presented by Jackson (1972). The inverse problem is formulated as a matrix equation (Jackson, 1972) from which a generalized inverse matrix is constructed. The solution to the problem is then defined in terms of this matrix which is used to optimize it.

In inversion of electrical resistivity data, an attempt is made to obtain information concerning the thicknesses and resistivities of the subsurface layers. Greater success of obtaining solution parameters that are as close to the true values as possible depends on the stability of the algorithm used but, most usually, on the geologic conditions of the subsurface. The geologic control of the area under investigation is, therefore, necessary for one to obtain more reliable results. Limited but useful geologic and hydrogeologic

information of the study area was available in the literature (Baker, 1958; Thompson and Dodson, 1963; Randel and Johnson, 1970; and Torfason, 1987) and from a few boreholes in the vicinity of the area, respectively.

2.2 The vertical electrical sounding method

2.2.1 The forward problem

The vertical electrical sounding method is used to study the changes of the electrical properties of the subsurface with depth. Because of the large contrast in electrical resistivity between dry resistive formations, cold groundwater and hot saline geothermal fluids (Bibby et al., 1984), the electrical sounding method is the most effective tool used in subsurface exploration. The Schlumberger array (Fig. 2.1) was used during the field work. The subsurface targets were mainly the conductive zones, which are associated with low resistivities, and the resistive substratum. The theory of the electrical resistivity method is normally based on several assumptions:

    (a) the subsurface consists of layers separated from each other by horizontal planes;

    (b) each of the layers is homogeneous and isotropic;

    (c) vertical interfaces and lateral variations in resistivity are non-existent; and

    (d) the current delivered into the ground is Direct Current (D.C.) or low frequency Alternating Current (A.C.).

However, the real earth on which the resistivity sounding measurements are carried out is usually complicated and may deviate from one or more of these assumptions. When the subsurface is not homogeneous and isotropic and the electrode spacing is varied, then the measured resistivity is not constant. The measured resistivity is, therefore, known as 'apparent resistivity' (ρ_a). It varies with the electrode separation since it depends on the electrical conductivity of the different subsurface zones in which the current and the potential are variously distributed. This distribution depends on the composition of the rock types, their porosity, fluid content, temperature and degree of hydrothermal alteration.

16
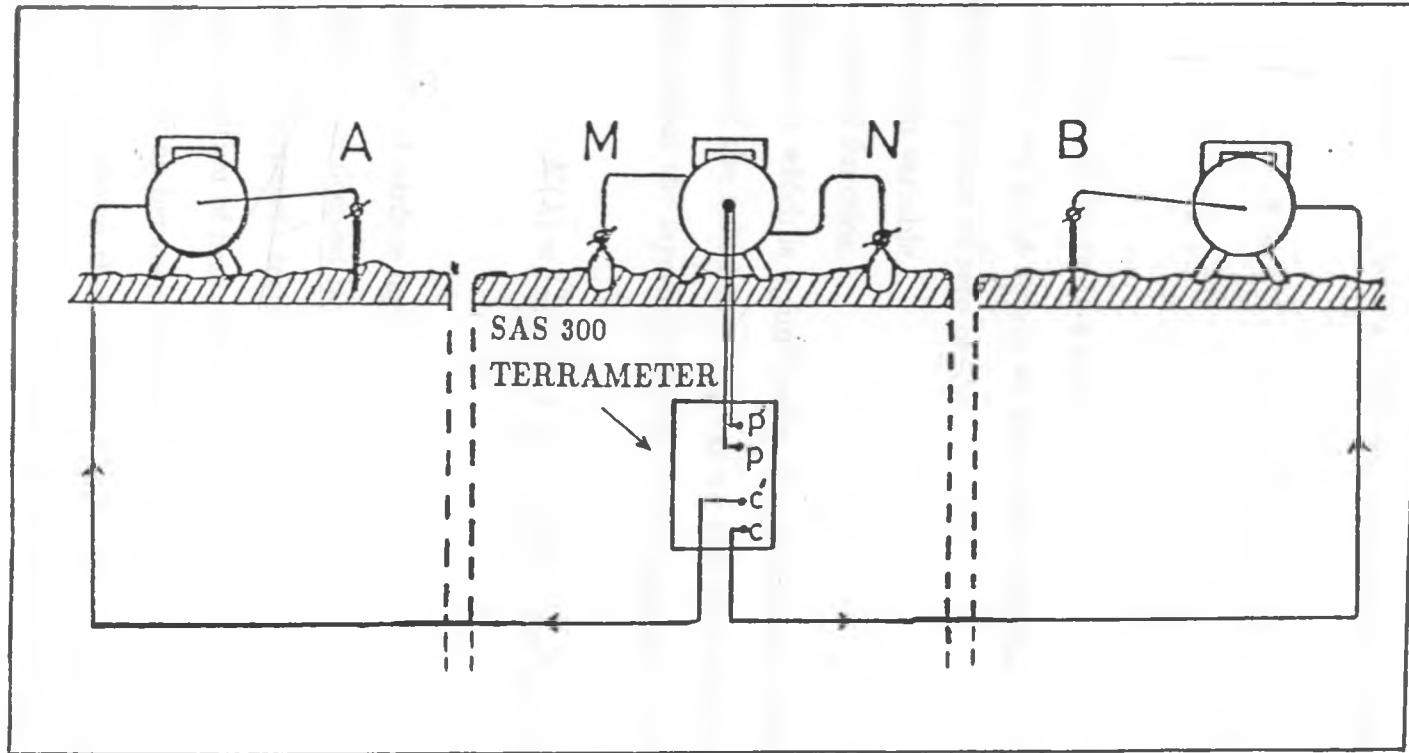
Figure 2.1   The Schlumberger array of resistivity sounding with A and B as the current electrodes, and M and N as the potential electrodes, where AB ≫ MN.

Consider a single current electrode at the surface of a stratified, infinitely extended, homogeneous and isotropic medium delivering a current I into the medium (Fig. 2.2). The return current electrode is considered to be at a great distance from the source. The electric potential around the point source is given by (Koefoed, 1968)

$$V = \frac{\rho_1 I}{2\pi} \{ 1/r + 2 \int_0^\infty K(\lambda) \cdot J_0(\lambda r) \cdot d\lambda \}, \tag{2.1}$$

where

ρ_1 = resistivity of the surface layer,

r = distance from point source at which the potential is considered,

J_0 = Bessel function of zero order,

λ = integration variable,

$K(\lambda)$ = Kernel function.

The kernel function which is a function of the reflection coefficients and depths to the boundary planes of the subsurface layering as well the integration variable λ contains all information about the layering. For two point sources of current, it is expressed as

$$K(\lambda) = \frac{\rho_n - \rho_1}{2\rho_1} + \int_0^\infty \frac{\rho_a - \rho_n}{2\rho_1 s} \cdot J_1(\lambda s) \cdot ds, \tag{2.2}$$

where

ρ_1 = resistivity of surface layer,

ρ_n = resistivity of deepest layer,

ρ_a = measured apparent resistivity

J_1 = Bessel function of first order,

s = half the spacing between current electrodes.

It has been, however, shown that (Vosoff, 1958) the apparent resistivity curve can be used to derive what is known as the 'resistivity transform'. Thus, from (2.2)

$$\rho_a = s^2 \int_0^\infty T(\lambda) \cdot J_1(\lambda s) \cdot \lambda d\lambda, \tag{2.3}$$

from which

18
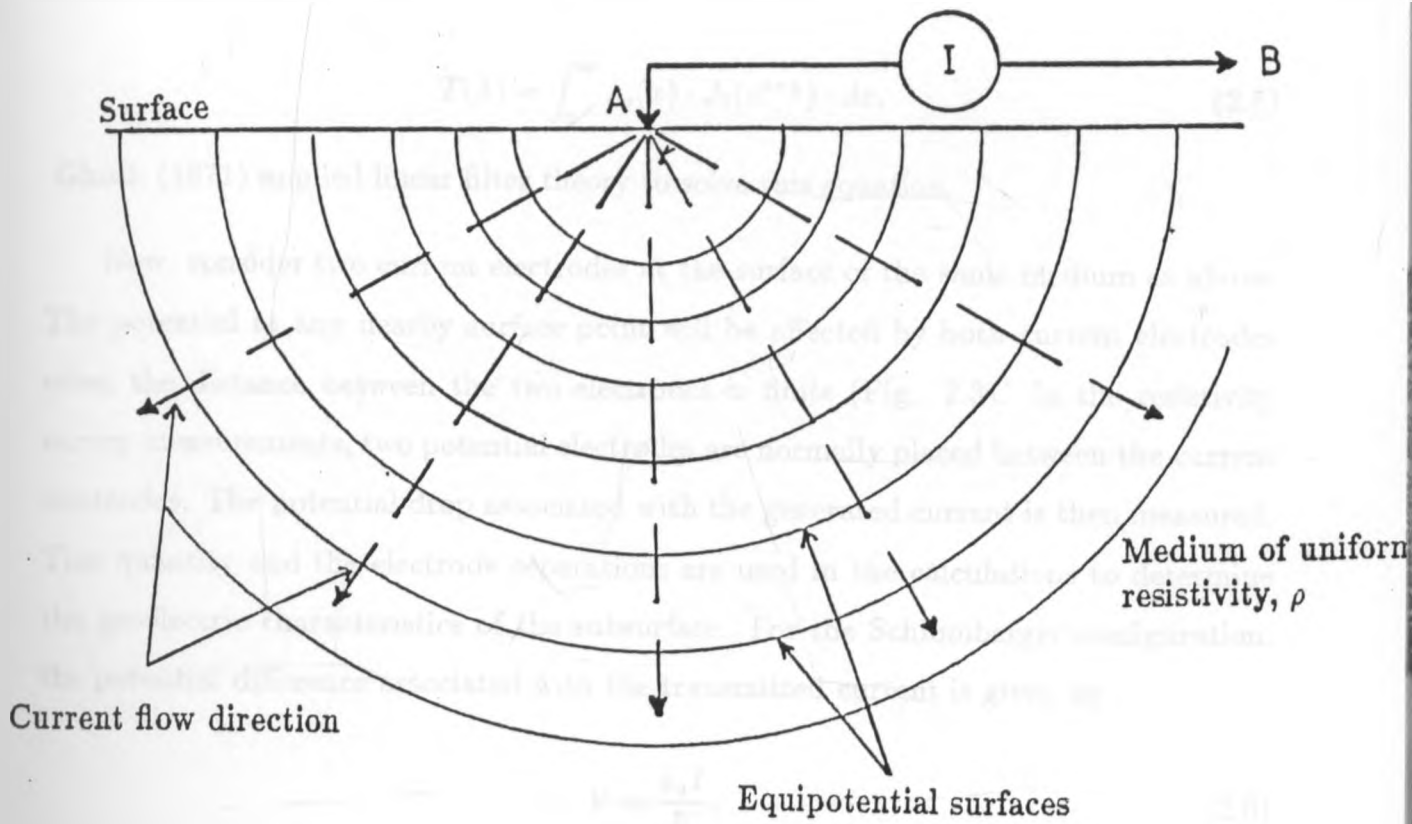
Figure 2.2   Point source of current at the surface of homogeneous, isotropic medium (Telford et al, 1990).

$$T(\lambda) = \int_0^\infty \{\rho_a(s) \cdot J_1(\lambda s)/s\} \cdot ds \qquad (2.4)$$

$$= \text{resistivity transform.}$$

Substituting $x = \log s$ and $y = \log (1/s)$, the resistivity transform becomes

$$T(\lambda) = \int_0^\infty \rho_a(x) \cdot J_1(e^{x-y}) \cdot dx. \qquad (2.5)$$

Ghosh (1971) applied linear filter theory to solve this equation.

Now, consider two current electrodes at the surface of the same medium as above. The potential at any nearby surface point will be affected by both current electrodes when the distance between the two electrodes is finite (Fig. 2.3). In the resistivity survey measurements, two potential electrodes are normally placed between the current electrodes. The potential drop associated with the generated current is then measured. This quantity and the electrode separations are used in the calculations to determine the geoelectric characteristics of the subsurface. For the Schlumberger configuration, the potential difference associated with the transmitted current is given by

$$V = \frac{\rho_a I}{K}, \qquad (2.6)$$

where

I = current delivered into the medium,

ρ_a = apparent resistivity of the medium,

and K is a geometric factor involving current and potential electrode separations and is given by

$$K = \{\frac{(AB/2)^2 - (MN/2)^2}{MN}\}\pi, \qquad (2.7)$$

where

AB/2, MN/2 and MN are defined in Figure 2.1 and $AB \gg MN$.

With some resistivity equipment such as the one used in this investigation, the measured parameter is the apparent resistance which, from (2.6), is given by
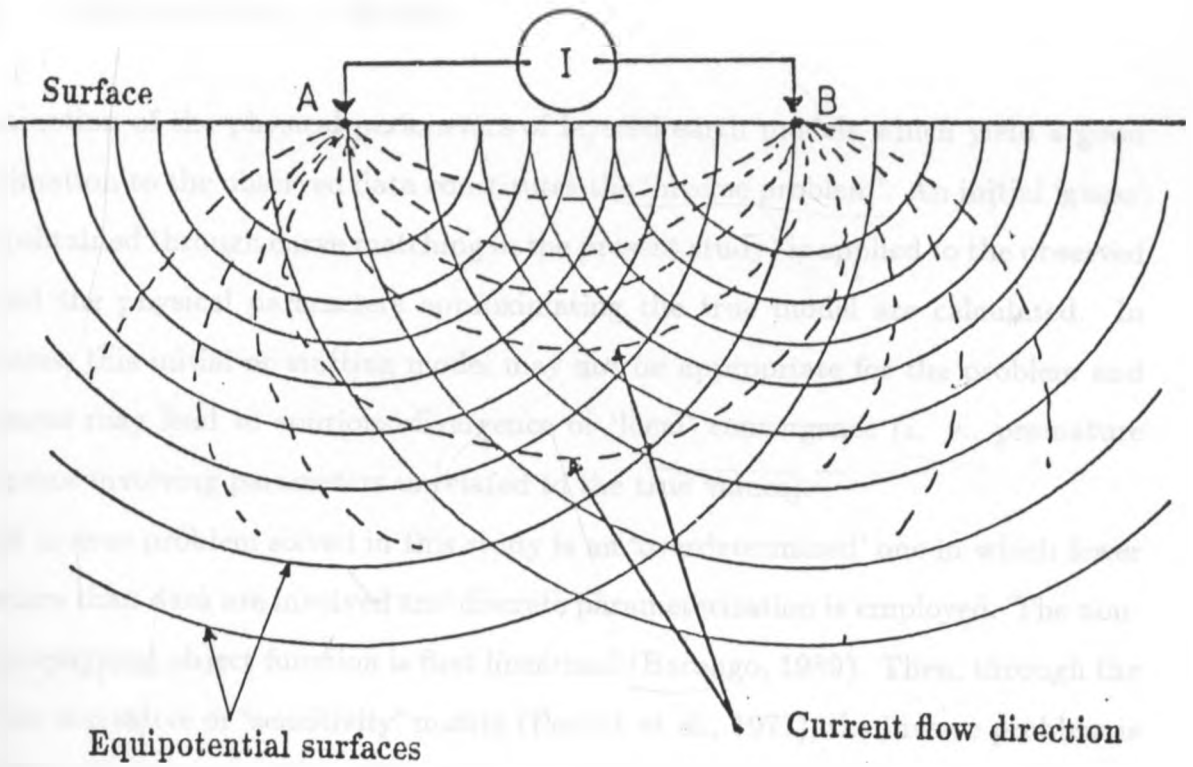
Figure 2.3   Two current electrode sources at the surface of homogeneous, isotropic medium (Telford et al, 1990).

$$R = V/I = \rho_a/K \qquad (2.8)$$

This resistance is multiplied by K to obtain the apparent resistivity ρ_a.

2.2.2 The inverse problem

Determination of the physical parameters of layered earth models which yield a good approximation to the observed data constitutes the 'inverse problem'. An initial 'guess' model (obtained through curve matching in the present study) is applied to the observed data and the physical parameters approximating the true model are calculated. In some cases, this initial or starting model may not be appropriate for the problem and the process may lead to spurious divergence or 'local' convergence (i. e., premature convergence involving parameters unrelated to the true values).

The inverse problem solved in this study is an 'overdetermined' one in which fewer parameters than data are involved and discrete parameterization is employed. The non-linear geophysical object function is first linearized (Barongo, 1989). Then, through the use of the derivative or 'sensitivity' matrix (Petrick et al., 1977), the inverse problem is solved in the least squares sense. In other words, the solution is obtained by minimizing the square error between the calculated and the observed data. The SCHINV program (Barongo, 1989) was used. In this program, the 'sensitivity' matrix is decomposed into a parameter eigenvector matrix, a data eigenvector matrix and an eigenvalue matrix all of which are used to construct the generalised inverse matrix of Lanczos (1961). This technique is kown as Singular Value Decomposition (Wiggins, 1972; Jackson, 1972). To stabilize this matrix, a small positive constant known as 'damping constant' or 'Marquardt parameter' (Marquardt, 1963) is added to small eigenvalues. If the general noise level in the observed data is known or assumed, it can be used to weight the matrix in order to stabilize it further.

The square error between the calculated and the observed data is compared through the Chi-square (χ^2) test

$$\chi^2 = \sum_{i=1}^{n} \frac{(D_0 - D_c)^2}{\sigma^2}, \tag{2.9}$$

where

$D_0 = $ observed data,

$D_c = $ calculated data,

$\sigma^2 = $ data variance,

or through the percentage **Root Mean Square** (**%RMS**) error given by

$$\%RMS = \{\frac{1}{n} \sum_{i=1}^{n} (\frac{D_0 - D_c}{D_0})^2\}^{1/2} \times 100. \tag{2.10}$$

But, before this comparison is carried out, the theoretical data are interpolated to the points at which the observed data had originally been recorded in the field. If, during the iteration process, the χ^2 value falls below a prior chosen tolerance value, the parameter estimates are accepted as the solution to the problem. Since the electrical sounding problem is nonlinear, several iterations are required to obtain a satisfactory solution for the given initial 'guess' parameters (Petrick et al., 1977). As long as the χ^2 value has not fallen below the tolerance value or a certain chosen maximum number of iterations has not been reached, the partial derivatives of the model data with respect to the model parameters are recalculated via the forward difference method (Barongo, 1989). The new calculated parameters are then used as the input model parameters for the second iteration. A second χ^2 value is then calculated. Before the process continues to the next step, the new χ^2 value is compared with the previous immediate χ^2 value. If it is smaller, the Marquardt parameter (Barongo, 1989) is reduced by a factor of 10; if it is larger, it is raised by the same factor and the process proceeds through the subsequent iterations. If, at some stage during the iterations, the χ^2 value remains constant, an instruction in the program stops the iteration process after six consecutive constant χ^2 values and the results are passed on to the part of the program which deals with solution appraisal. Accepted solutions are then printed out. If, on the other hand, the problem continuously converges, there is an instruction in the program that stops the process after the χ^2 has fallen below a prior chosen tolerance value or after some pre-assigned

maximum number of iterations has been reached. In the present study, a maximum of 15 iterations was found appropriate for all the sounding data.

Once a model which best fits the observed data has been produced, the final parameters and data are statistically appraised to determine if the solution reflects the values of the true parameters. In this case, the parameter covariance matrix is examined and the standard deviation for each parameter is calculated as the square root of the diagonal elements of the covariance matrix. The parameter correlation coefficients are obtained by normalizing the parameter covariance matrix (Jackson, 1972, 1979). Also given in the final solution are the longitudinal conductance (thicknes/resistivity and the transverse resistance (thickness × resistivity), data errors, resolution values for each layer parameters and the information values for the data.

The flow chart of the SCHINV program is illustrated in Figure 2.4

2.3 Limitations of the resistivity method

The main limitation of the electrical resistivity method is its large sensitivity to minor variations in near-surface conductivity. A near-surface conductive layer causes a screening effect and, hence, prevents current from penetrating deeper. Few soundings carried out in the study area indicated the presence of conductive upper layers.

This method also suffers a limitation of the resolving power. If the area approaches conditions that are dry and arid, the electrical contact problems at the electrode points are great since the ground is generally resistive. This usually leads to distortion of the equipotential surfaces in the ground. The method also suffers the problems of equivalence (two layers with completely different physical parameters appear electrically the same) and suppression (two different layers appear electrically as one layer, i.e., the presence of the other is suppressed or hidden). In practice, different resistivity distributions in the subsurface may show the same apparent resistivity curve and, hence, mislead the interpretation. This is the problem of equivalence. Suppression, on the other hand, leads to the masking of thin layers which are sandwiched between layers of contrasting resistivities. This leads to ambiguous interpretation of observed data.
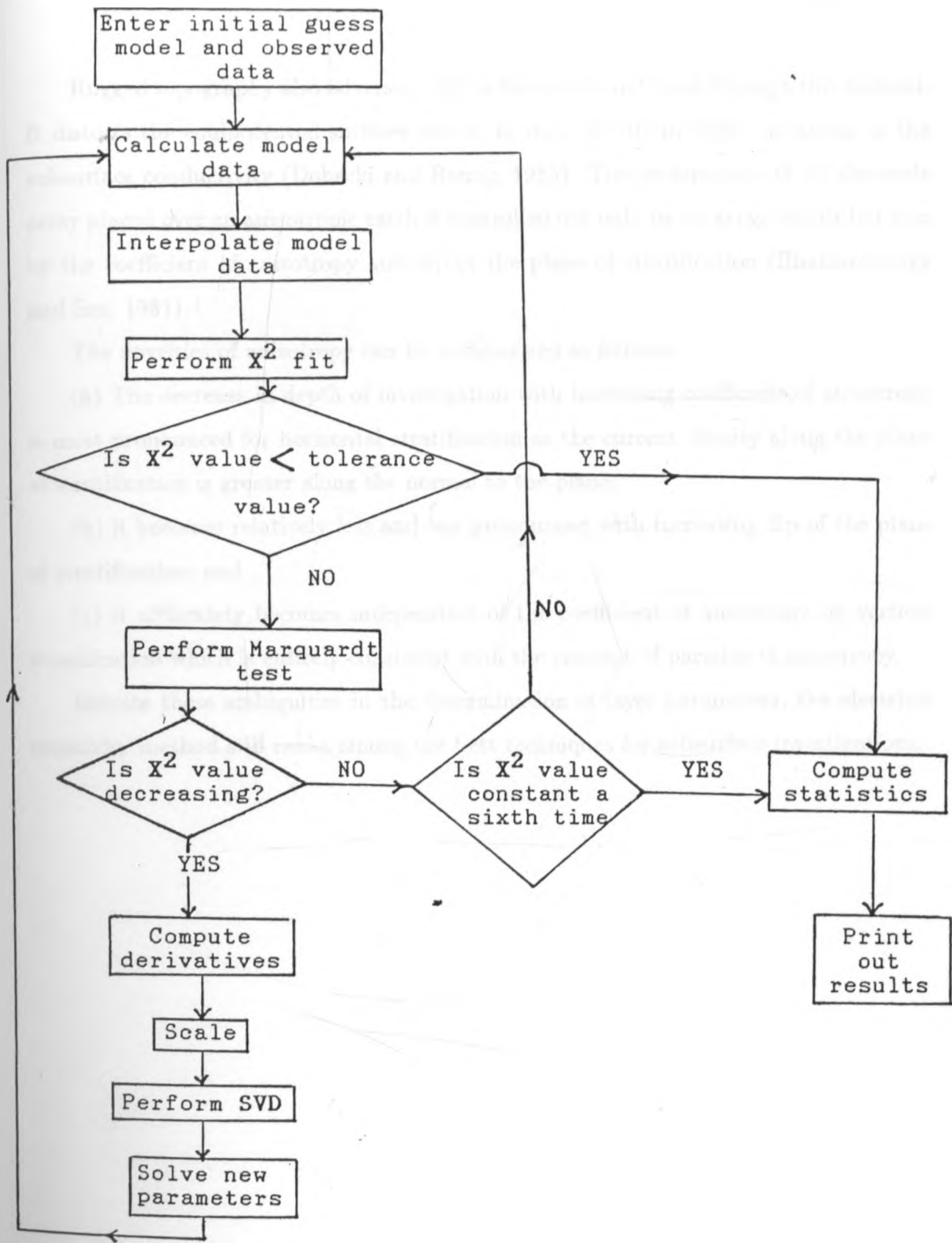
Figure 2.4   Flow chart illustrating the iteration process of the SCHINV program.

Rugged topography also adversely affects the results obtained through this method. It distorts the equipotential surfaces which, in turn, results in slight variations of the subsurface conductivity (Dobecki and Romig, 1985). The performance of an electrode array placed over an anisotropic earth is controlled not only by its array length but also by the coefficient of anisotropy and dip of the plane of stratification (Bhattacharhya and Sen, 1981).

The novelties of anisotropy can be summarized as follows:

(a) The decrease in depth of investigation with increasing coefficient of anisotropy is most pronounced for horizontal stratification as the current density along the plane of stratification is greater along the normal to the plane;

(b) it becomes relatively less and less pronounced with increasing dip of the plane of stratification; and

(c) it ultimately becomes independent of the coefficient of anisotropy by vertical stratification which is entirely consistent with the concept of paradox of anisotropy.

Despite these ambiguities in the determination of layer parameters, the electrical resistivity method still ranks among the best techniques for subsurface investigations.

Chapter 3

FIELDWORK

3.1   General

The fieldwork was carried out during the month of March 1990 for a period of three weeks. Ewaso Kedong shopping centre, which is about 8 kilometres from the area of study, was selected as the main camping site. Narok and Ngong towns, which are both about 20 kilometres from the area, were occasionally used as camping sites as well.

Two field assistants were engaged to help with the fieldwork. A four-wheel drive vehicle was used to transport the field equipment to selected sites. The driver of the vehicle also assisted in this work besides his normal duties as a driver. The local people of the area were also helpful in that they assisted in the general field oparations such as locating motorable tracks and providing useful logistic information about the area (see Plate 3).

3.2   Field equipment

The data used in the analysis and interpretation consisted of two sets acquired at different times by different workers. The first set of data had been acquired by the Ministry of Energy and Regional Development (M.O.E.R.D.) geophysical crew in 1987. They used an Italian-made Geo-Resistivity Meter (GRM) 3000 which is designed for deep electrical sounding and allows fast and accurate measurements to be taken even when the field conditions are unfavourable. It's main disadvantages are:

(a) the increased effect of disturbing potentials when the current electrode separa-

tion is more than 6000 metres,

(b) the risk of taking readings in the wrong scale, and

(c) the increased error in the higher scale.

The first disadvantage was not of much concern in the present work since the maximum current electrode separation used was 2000 metres. The other disadvantages could be avoided by taking great care in conducting the soundings. This set of data was from 17 best quality soundings of the M.O.E.R.D. It formed a larger fraction of all the data used in this investigation. The author found it also useful in assessing situations where execution of adjacent soundings was necessary. Sounding ST17 carried out by M.O.E.R.D. compares well with sounding ST22 carried out by the author. The second set of data was acquired by the author using a Swedish-made ABEM Terrameter SAS 300 and Terrameter SAS 2000 Booster (SAS stands for Signal Averaging System).

3.2.1 Terrameter SAS 300

The Terrameter SAS 300 comprises a battery powered, deep-penetration resistivity meter with an output sufficient for a current electrode separation of 2000 metres under good surveying conditions. Discriminatory circuitry and programming separates D.C. voltages, self potentials and noise from the incoming signal. The resistance (V/I) is calculated automatically and displayed on a liquid crystal display in ohms or milliohms (Fig. 3.1). The instrument is generally designed for both shallow and deep resistivity soundings.

It consists of three main units - the transmitter, the receiver and the microprocessor - all housed in a single casing.

(i) Transmitter

The electrically isolated transmitter sends out well defined and regulated signal currents which are commutated in a time pattern suitable for resistivity surveying. The transmitted signal (plus SP and ground noise) is measured by the receiver at discrete time intervals when the eddy currents, the IP and the cable transients have decayed to low levels.

(ii) Receiver
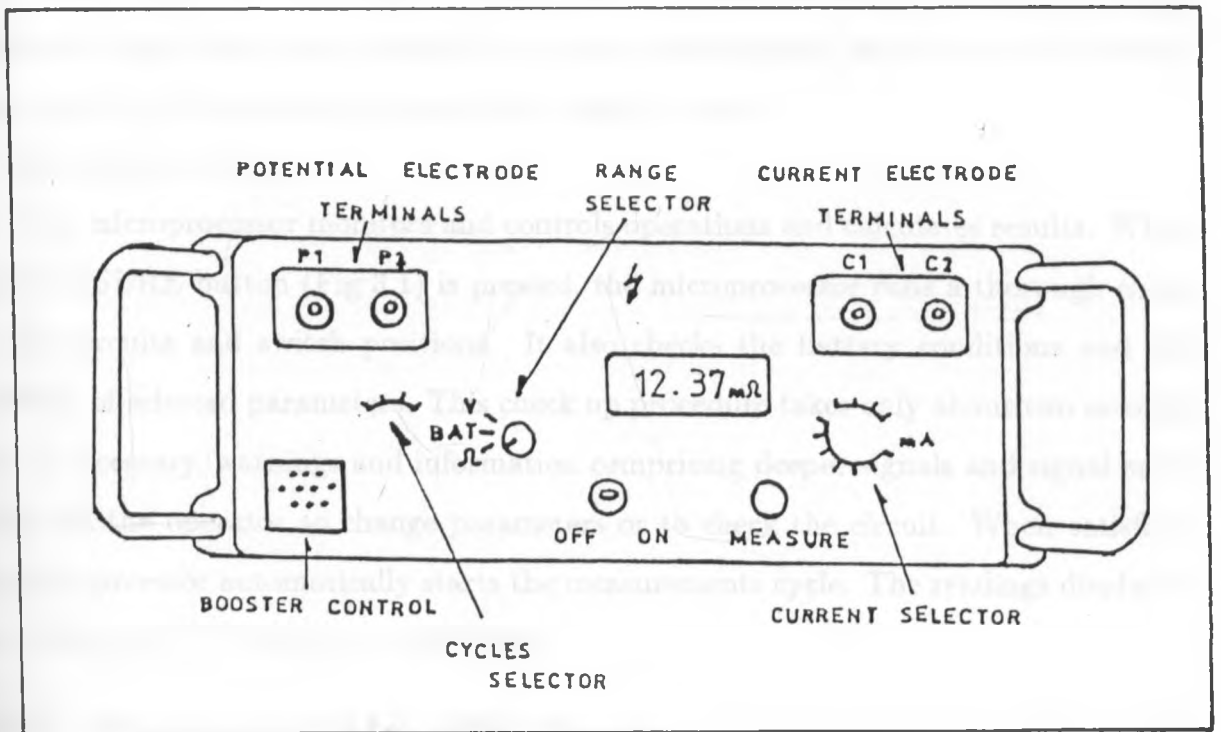
Figure 3.1   The operating panel of SAS 300 Terrameter.

The receiver discriminates noise and measures voltages correlated with transmitted signal current. It is designed for signal extraction only. Penetration and accurancy limits are imposed mainly by noise caused by telluric currents, power tansmission lines and electrochemical variations at the potential electrodes.

A unique integrator combined with an ingenuous measurement strategy permits the Terrameter SAS 300 Receiver to extract the signal from man-made and natural noise, even when using low safe signal voltage levels. This measurement strategy includes signal stacking, logical and analog filtering, rejection of induced polarization (IP) effects and rejection of the transient phase of the signal current.

(iii) Microprocessor

The microprocessor monitors and controls operations and calculates results. When the MEASURE button (Fig 3.1) is pressed, the microprocessor runs a thorough check on the circuits and switch positions. It also checks the battery conditions and the usability of selected parameters. This check up procedure takes only about two seconds and, if necessary, warnings and information comprising deeper signals and signal error codes tell the operator to change parameters or to check the circuit. When satisfied, the microprcessor automatically starts the measurements cycle. The readings displayed are resistance (V/I) in ohms or milliohms.

3.2.2   Terrameter SAS 2000 Booster

The current used for resistivity surveying is increased by means of the Terrameter SAS 2000 Booster to obtain greater depths of penetration. In the field, the Booster is also used when the readings are seen to fluctuate and this usually happens at current electrode separations of more than 500 metres. It is also used where difficulties of driving the current electrodes into the resistive ground are encountered. It is directly attached (or 'slaved') to the Terrameter SAS 300 during field operation.

3.2.3   Other components

The other components of the resistivity equipment include the current and the potential electrodes and shielded electrical cables mounted on reels. The current electrodes are

made of non-polarisable steel rods whereas the potential electrodes are made of porous pots. The cables are mounted on reels so that it is easier to wind, unwind and transport around in the field. Each reel is capable of holding up to 500 metres of cable.

3.3   Field measurements

The author's resistivity soundings were carried out on sites where no soundings had previously been conducted by the M.O.E.R.D. However, one sounding, ST22, was carried out at a location closer to where a resistivity sounding (ST17 by M.O.E.R.D.) had been conducted. This was done in order to compare the two data sets with a view to checking how well they agreed. With the use of the Terrameter SAS 300, the readings were seen to be fluctuating slightly after reaching current electrode separations greater than 500 metres. However, a total of 7 electrical soundings were carried out using the Schlumberger configuration in which the maximum current electrode separation was 4000 metres (i.e., $AB/2 = 2000$ metres). This resulted in the execution of only one sounding per day. Geologic and topographic features at and around each sounding station were also studied and noted down. There were, in total, 24 soundings used in this investigation including the M.O.E.R.D.'s 17 soundings.

In conducting the soundings, the electrode spread was oriented either in an E-W or N-S direction. The direction was selected depending on how open the terrain was to allow for large $AB/2$ spread. However, the E-W direction was found to be more appropriate because it is perpendicular to the principal structures in the area, thus allowing for greater amount of subsurface information to be obtained (Razzo et al., 1980).

The field sounding locations were first marked on topographic maps (scale 1:50 000) of the area (Fig 4.1). Field features such as geology, geography, elevation, ground conditions, etc., at and around the sounding stations were noted down before the electrode spread was layed out. The electrodes were placed on a straight line and the point midway between the current and the potential electrodes was taken as the location of the sounding station (Fig. 2.1 and Plate 5). The potential electrodes (M and N)
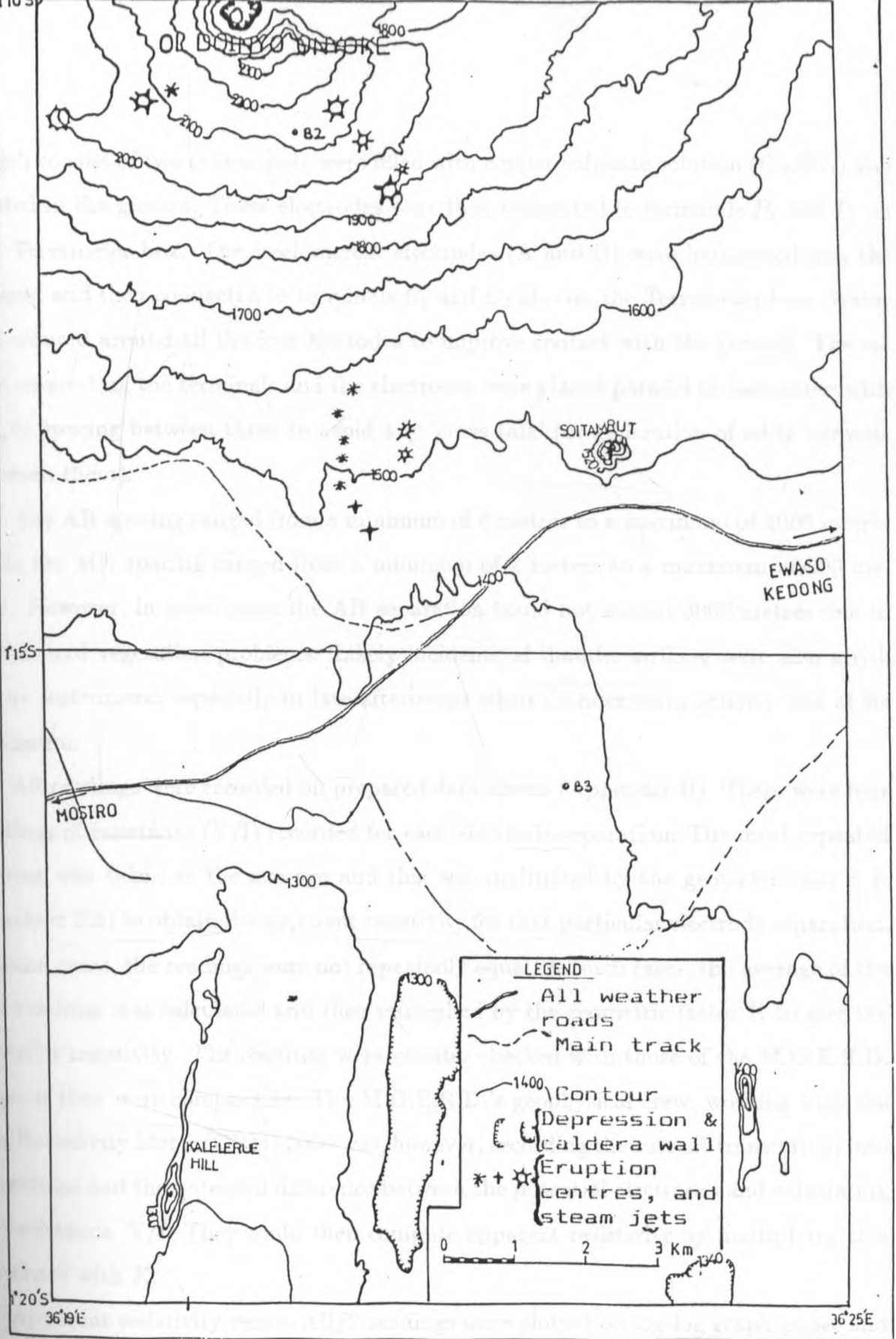
Figure 3.2 The topographic map of the area south of Suswa volcano and the locations of geothermal manifestations represented by steaming jets.

which consist of two porous pots were filled with copper sulphate solution ($CuSO_4$) and buried in the ground. These electrodes were then connected to terminals P_1 and P_2 on the Terrameter box. The steel current electrodes (A and B) were hammered into the ground and then connected to terminals C_1 and C_2 also on the Terrameter box. Water was poured around all the four electodes to improve contact with the ground. The cables connecting the terminals and the electrodes were placed parallel to each other with ample spacing between them to avoid any 'cross talk' (or generation of eddy currents between them).

The AB spacing ranged from a minimum of 6 metres to a maximum of 4000 metres while the MN spacing ranged from a minimum of 2 metres to a maximum of 200 metres. However, in some cases the AB separation could not exceed 3000 metres due to terrain and vegetation problems. Likely incidents of thunder striking were also a risk to the instrument, especially in late afternoons when thunderstorm activity was at its maximum.

All readings were recorded on prepared data sheets (Appendix II). There were four readings of resistance (V/I) recorded for each electrode separation. The most repeated reading was taken as the average and this was multiplied by the geometric factor K (equation 2.8) to obtain the apparent resistivity for that particular electrode separation. In some cases, the readings were not repeatedly equal. In such cases, the average of the four readings was calculated and then multiplied by the geometric factor K to give the apparent resistivity. The readings were counter-checked with those of the M.O.E.R.D. to see if they were comparable. The M.O.E.R.D.'s geophysical crew, working with the Geo-Resistivity Meter (GRM) 3000 was, however, recording the current transmitted into the ground and the potential difference between the potential electrodes and calculating the resistance, V/I. They could then compute apparent resistivity by multiplying this resistance with K.

Apparent resistivity versus AB/2 readings were plotted on log-log graph paper and qualitatively inspected. This was done the same day the sounding was conducted so that a repeat sounding could be recommended if necessary. However, none of the stations called for any repeat sounding.

Chapter 4

DATA ANALYSIS

4.1   General

Apparent resistivity data from a total of 24 sounding stations were analysed to determine resistivities and thicknesses that could give a geologically meaningful subsurface structure. To meet this goal, analytical results from the sounding stations along preferable directions were used to construct two-dimensional vertical sections of the subsurface geoelectric structure. It was then possible to infer from this structure the possible geological information relating to it.

There were two kinds of analysis carried out. The first involved qualitative and the second quantitative analysis. Qualitative analysis involved visual inspection of the field data and the corresponding sounding curves. This was mainly done in the field so that, if need arose, then additional soundings could be carried out.

Quantitative analysis involved the manual technique of partial curve matching using the auxiliary point method (Compagnie General de Geophysique, 1963; Zohdy, 1965; Orellana and Mooney, 1966) and the computer-based least squares inversion method. The layer parameters obtained through the partial curve matching technique were used as the initial 'guess' model parameters in the inversion. These analyses were carried out at the Department of Geology, University of Nairobi using a personal computer, IBM PS/2.

4.2 Qualitative analysis

Qualitative analysis was mainly done in the field to check whether a particular sounding station required a repeat sounding or further investigation. It was done by visual inspection and comparison with sounding data from adjacent stations and, where necessary, with data collected previously in the area by M. O. E. R. D. The previously collected data include both geophysical and hydrogeological. Qualitative analysis also involved taking note of the general characteristics of the sounding curves with a view to grouping and interpreting similar curves together. The locations and numbering of all the sounding stations involved in this study are shown in Figure 4.1.

4.2.1 General characteristics of the sounding curves

At least five different types of sounding curves were recognized in the study area. These curves, referred to as Types I, II, III, IV and V curves, are illustrated in Figures 4.2 (a) and 4.2 (b).

(i) Type I curves

This type of curves indicates the presence of two conductive layers each sandwiched between two resistive layers (Fig. 4.3). The first descending and ascending limbs of the curves correspond to the first conductive layer sandwiched between a resistive top layer and an underlying resistive layer. The latter is underlain by a main conductive layer which overlies a resistive substratum. The second set of descending and ascending limbs correspond to the latter situation. The conductive layer is encountered at a depth of slightly more than 500 metres and has an apparent resistivity of less than 15 ohm-metres. The resistive substratum (electric basement) is encountered at a depth of about 1000 to 2000 metres. Its resistivity is, in most cases, more than 50 ohm-metres. This type of curves is a combination of H and K type curves (Fig. 4.4) which results into an H-K-H type curve (Fig. 4.2(a)).

35
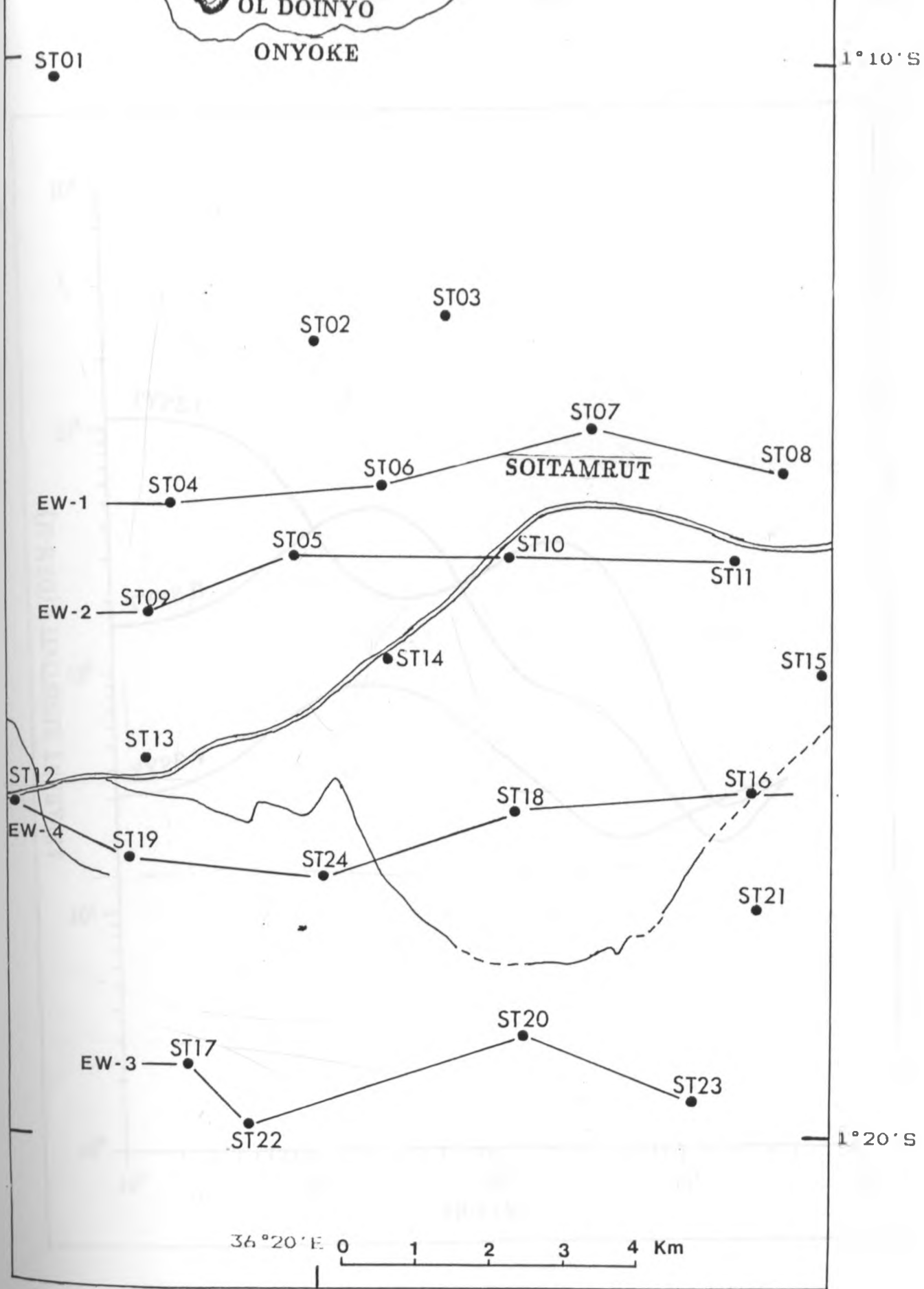
Figure 4.1   Resistivity sounding stations and the locations of East-West (E-W)
geoelectric profiles.
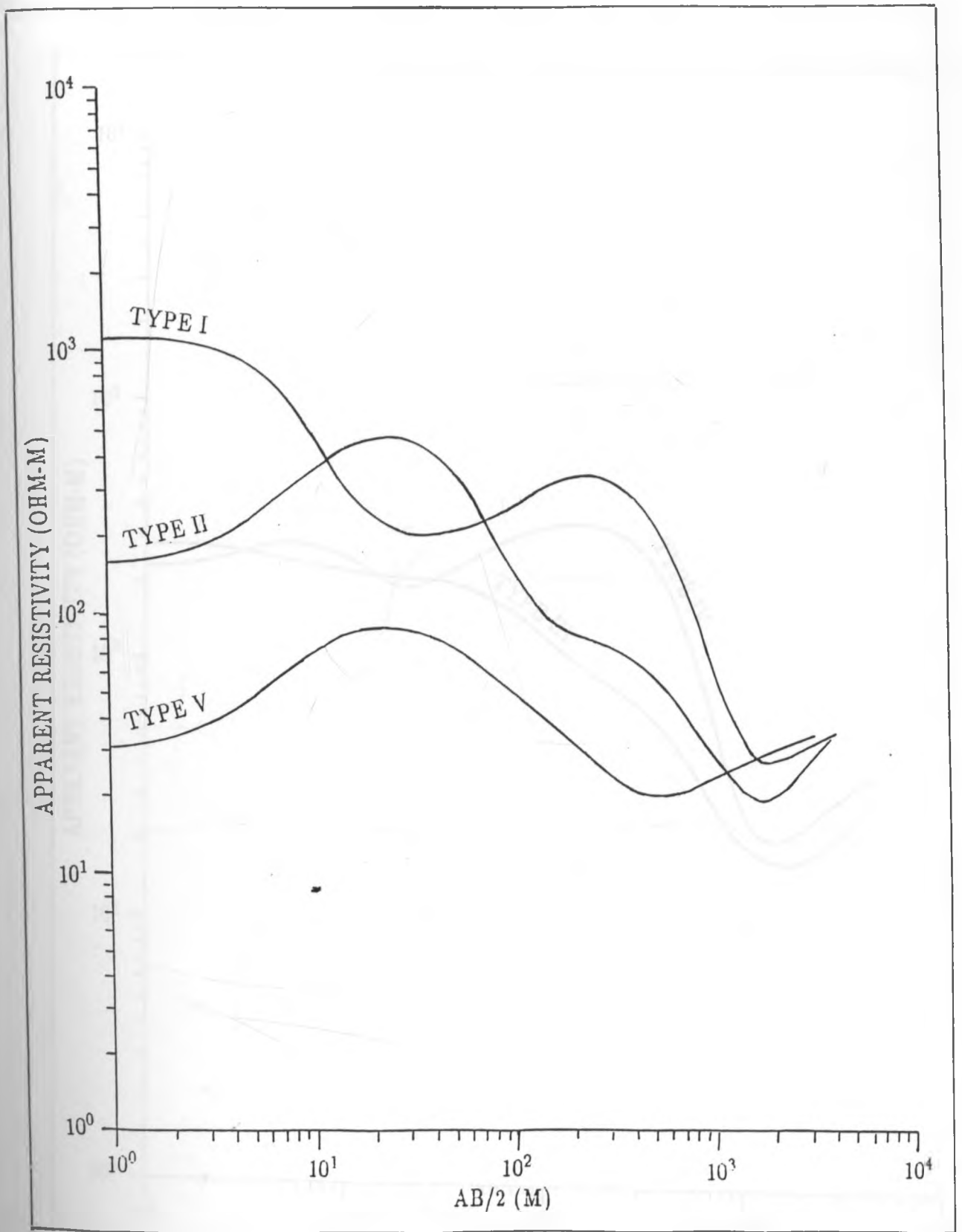
Figure 4.2 (a)   Types I, II and V apparent resistivity curves.
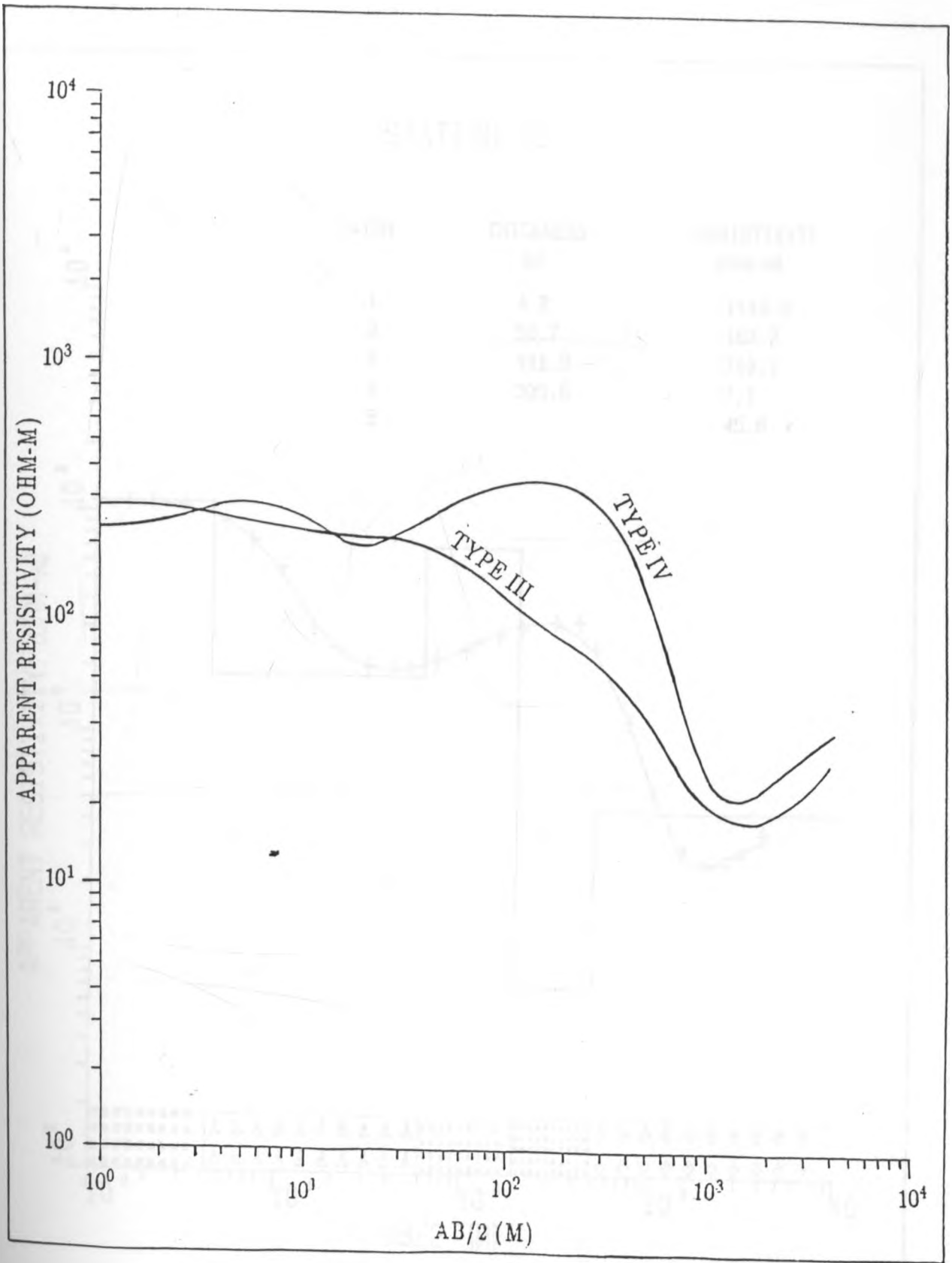
Figure 4.2 (b)   Types III and IV apparent resistivity curves.

STATION 15

LAYER	THICKNESS (M)	RESISTIVITY (OHM-M)
1	4.2	1113.0
2	55.7	183.2
3	131.9	710.1
4	305.6	7.1
5		45.6

APPARENT RESISTIVITY (OHM-M)

AB/2 (M)
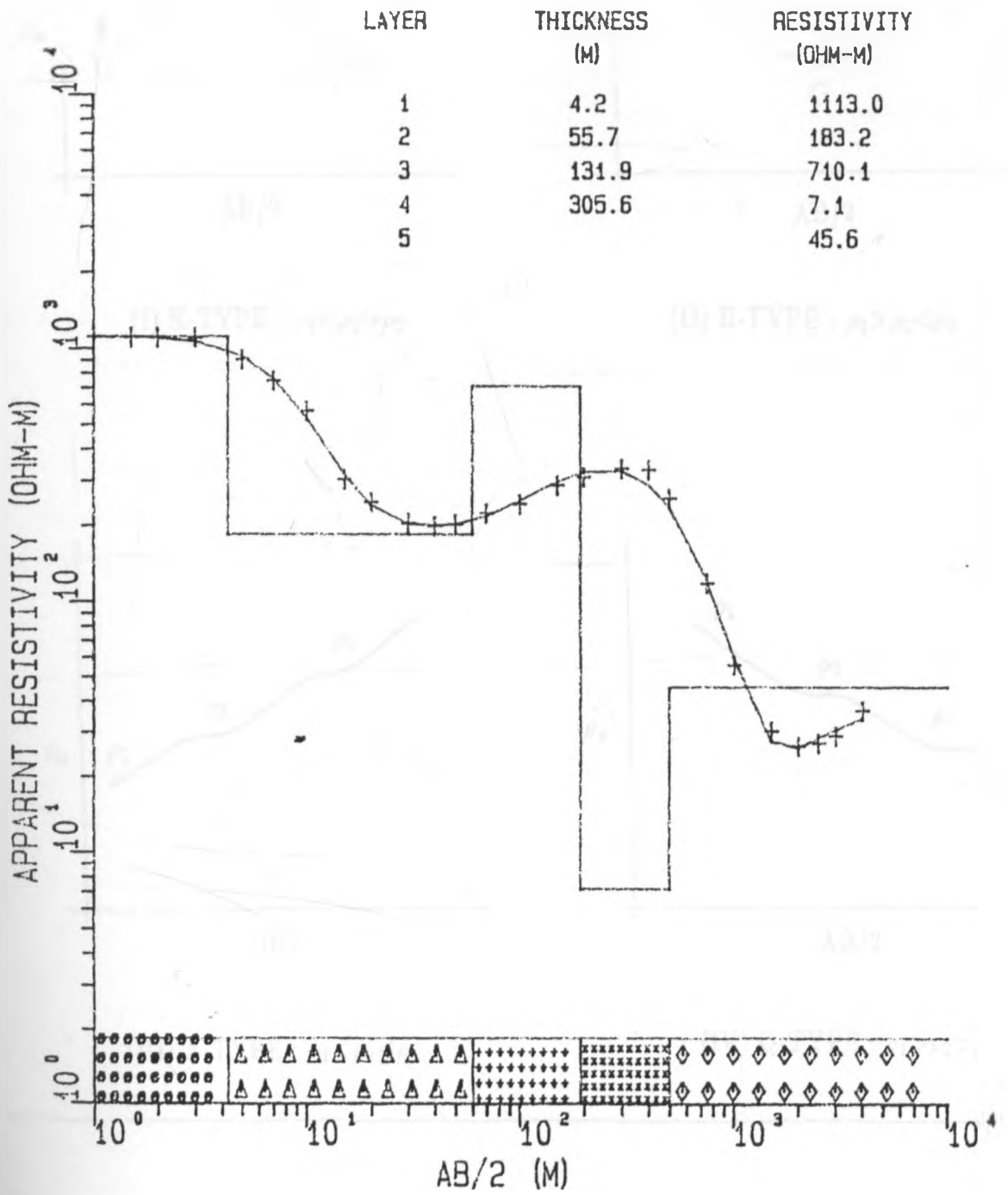
Figure 4.3   Fitted sounding curve and estimated profile for field results of ST15.
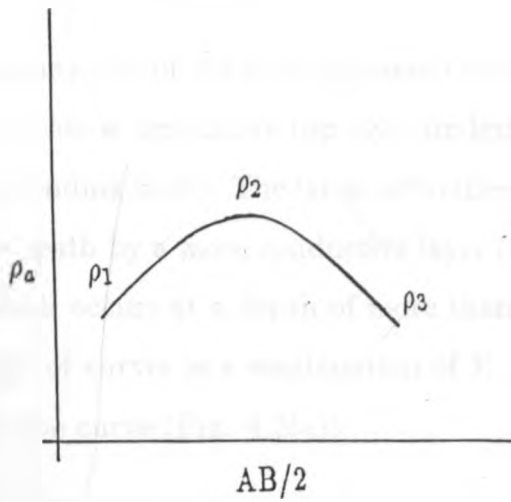
(I) K-TYPE : $\rho_1 < \rho_2 > \rho_3$
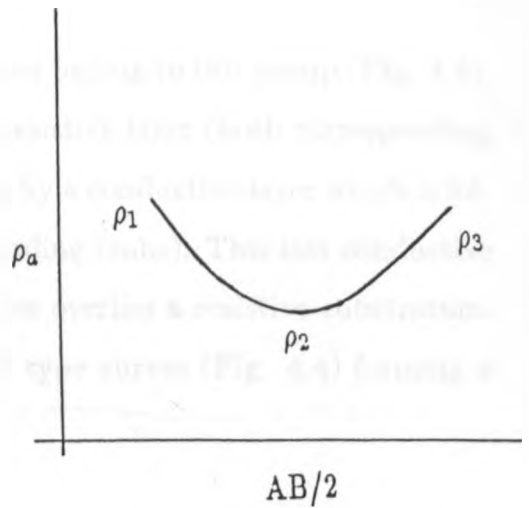
(II) H-TYPE : $\rho_1 > \rho_2 < \rho_3$
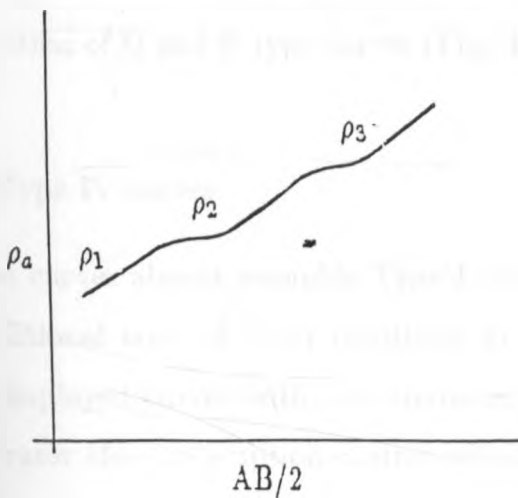
(III) A-TYPE : $\rho_1 < \rho_2 < \rho_3$
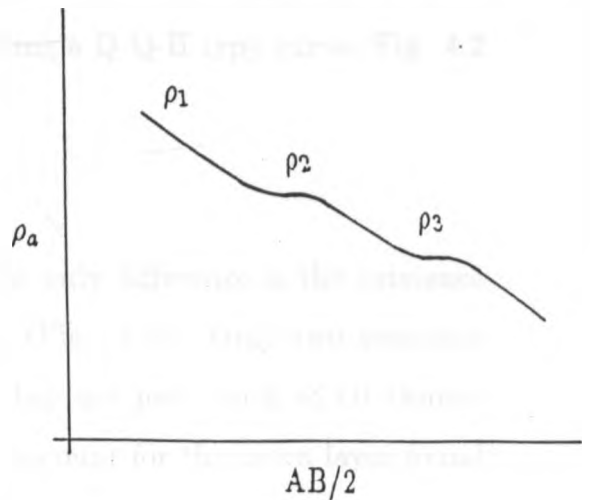
(IV) Q-TYPE : $\rho_1 > \rho_2 > \rho_3$

Figure 4.4   Type curves of three-layered earth model.

(ii) Type II curves

The majority of the field apparent resistivity curves belong to this group (Fig. 4.5). They indicate a conductive top layer underlain by a resistive layer (both corresponding to the ascending limb). The latter is further underlain by a conductive layer which is followed beneath by a more conductive layer (two descending limbs). This last conductive layer which occurs at a depth of more than 400 metres overlies a resistive substratum. This type of curves is a combination of K, Q, and H type curves (Fig. 4.4) forming a K-Q-H type curve (Fig. 4.2(a)).

(iii) Type III curves.

This type of curves indicates a general descending curve corresponding to a gradual decrease of resistivity with depth up to depths of over 1500 metres after which the resistivity rises (Fig. 4.6). This characteristic is displayed by three descending limbs and a last ascending limb of the curve. This type of curves can be considered to be the same as Type II curves minus the top conductive layer (Fig. 4.5). Type III curves are a combination of Q and H type curves (Fig. 4.4) forming a Q-Q-H type curve (Fig. 4.2 (b)).

(iv) Type IV curves.

These curves almost resemble Type I curves. The only difference is the existence of an additional layer of lower resistivity at the top (Fig. 4.7). Only two sounding stations displayed curves with this characteristic. They are just south of Ol Doinyo Onyoke crater close to eruption centres which might account for the extra layer found on top due to volcanic material having flowed to limited distances. Type IV curves are a combination of K and H type curves (Fig. 4.4) forming a K-H-K-H type curve (Fig. 4.2(b)).

(v) Type V curves.

These curves resemble Type II curves but show the absence of the step-like descending limb displayed in Type II curves. They display, from top to bottom, a conductive

STATION 14

LAYER	THICKNESS (M)	RESISTIVITY (OHM-M)
1	2.2	195.0
2	17.2	756.4
3	352.6	39.4
4	699.7	11.9
5		55.1
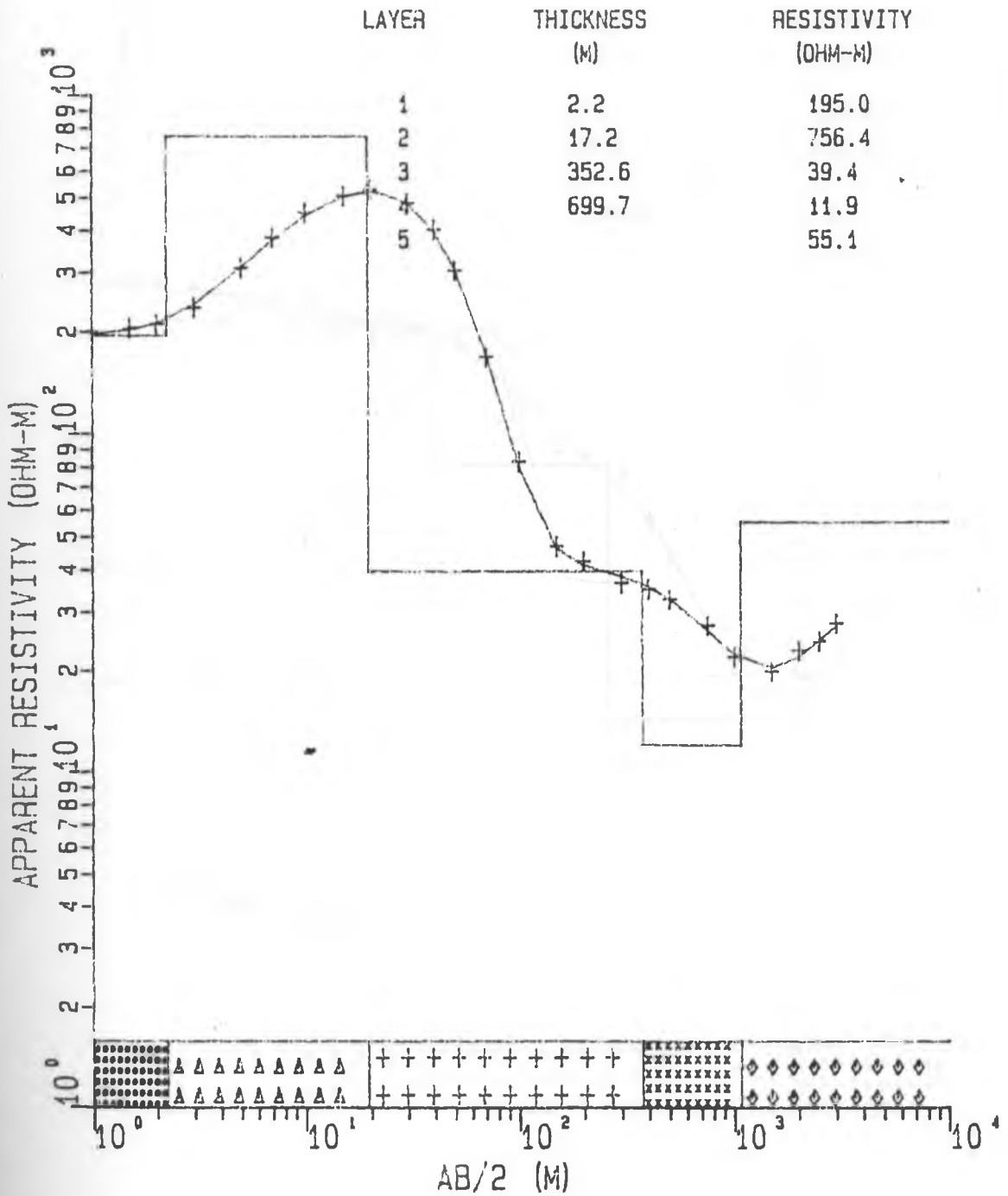
Figure 4.5   Fitted sounding curve and estimated profile for field results of ST14.
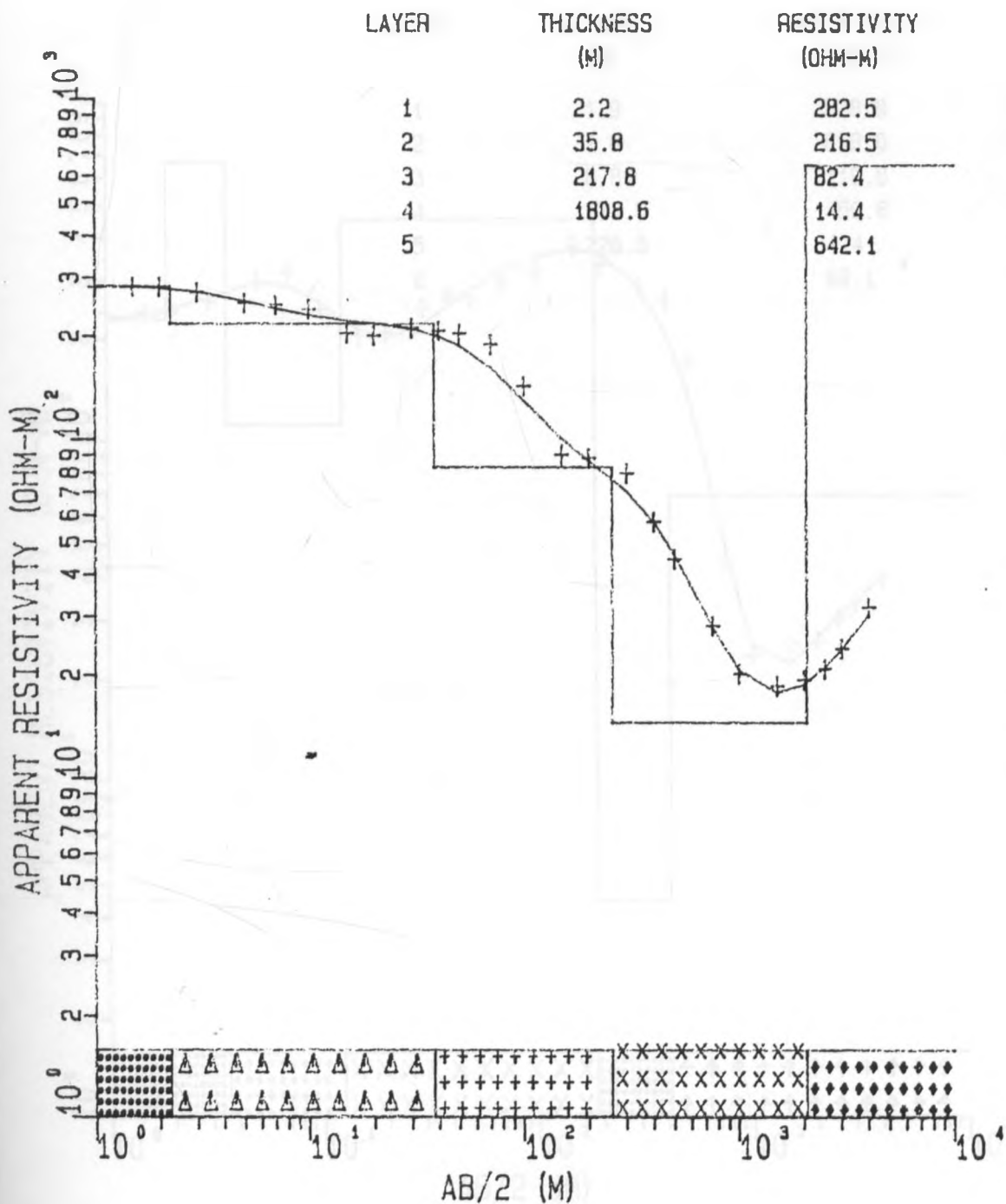
Figure 4.6   Fitted sounding curve and estimated profile for field results of ST13.

STATION 4

LAYER	THICKNESS (M)	RESISTIVITY (OHM-M)
1	1.9	228.8
2	1.6	668.0
3	8.8	110.6
4	174.0	450.6
5	226.3	4.4
6		68.1

APPARENT RESISTIVITY (OHM-M)

AB/2 (M)
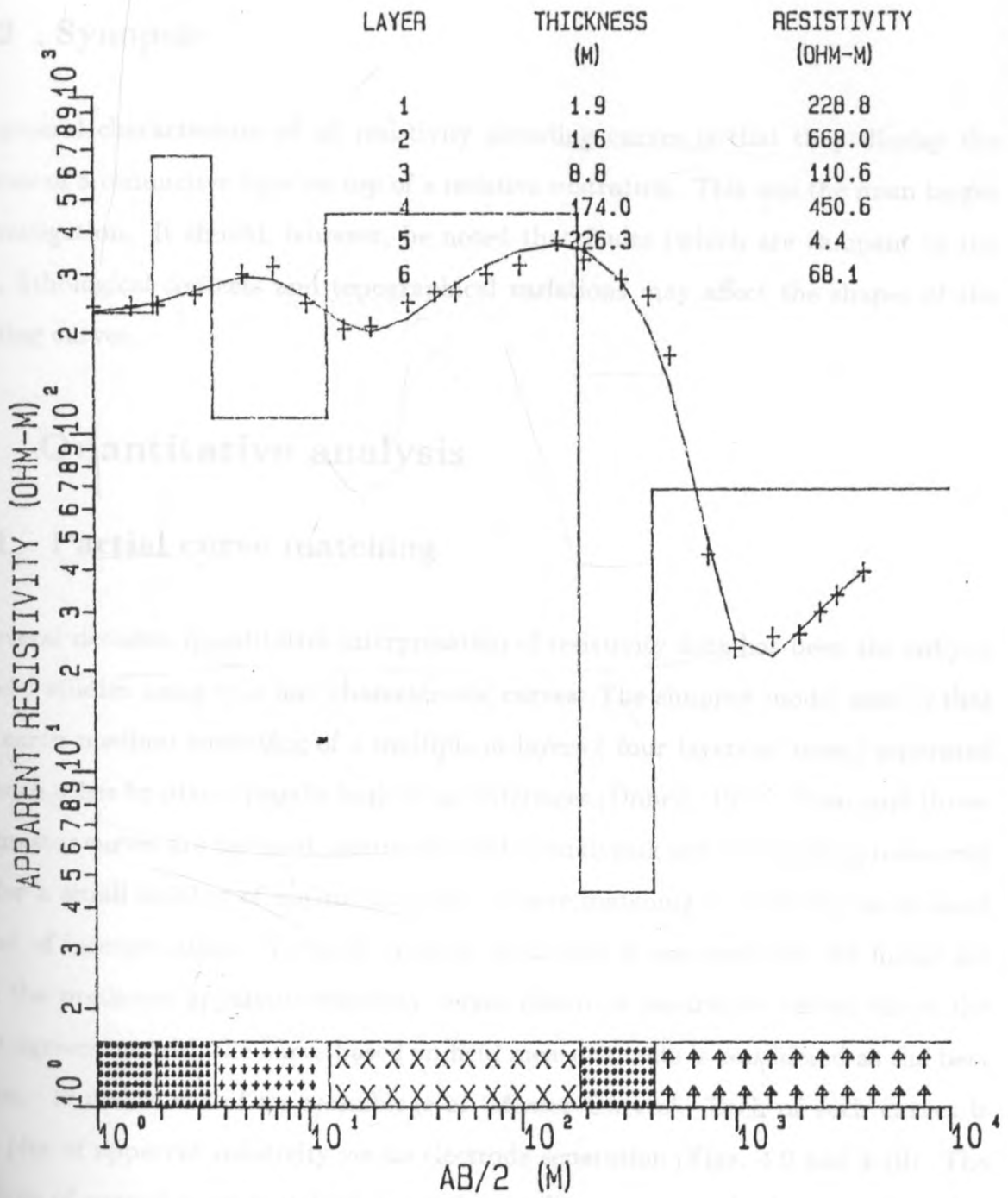
Figure 4.7   Fitted sounding curve and estimated profile for field results of ST04.

44

layer, a resistive layer, a conductive layer, a main conductive layer and a resistive substratum. This characteristic is displayed by an ascending, a descending and an ascending limb (Fig. 4.8). Type V curves are a combination of K and H type curves (Fig. 4.4) forming a K-H curve (Fig. 4.2 (a)).

4.2.2 Synopsis

The general characteristcs of all resistivity sounding curves is that they display the presence of a conductive layer on top of a resistive sustratum. This was the main target of investigation. It should, however, be noted that faults (which are rampant in the area), lithological contacts and topographical variations may affect the shapes of the sounding curves.

4.3 Quantitative analysis

4.3.1 Partial curve matching

For several decades, quantitative interpretation of resistivity data has been the subject of model studies using type and characteristic curves. The simplest model used is that of an earth medium consisting of a multiple of layers (four layers at most) separated from each other by plane (usually horizontal) interfaces (Dobrin, 1978). Two- and three-layer master curves are the most commonly used in analysing and interpreting resistivity data for a small number of horizontal layers. Curve matching is generally an indirect method of interpretation. Normally, a series of models is assumed and the model for which the predicted apparent resistivity versus electrode separation curves shows the closest agreement with the curve based on field measurements is considered as the best solution. It makes use of an assemblage of 'Master Curves'. Each of such curves is also a plot of apparent resistivity versus electrode separation (Figs. 4.9 and 4.10). The technique of partial curve matching using the auxiliary point method was used in this part of the analysis to obtain parameter estimates of the subsurface geoelectric structure
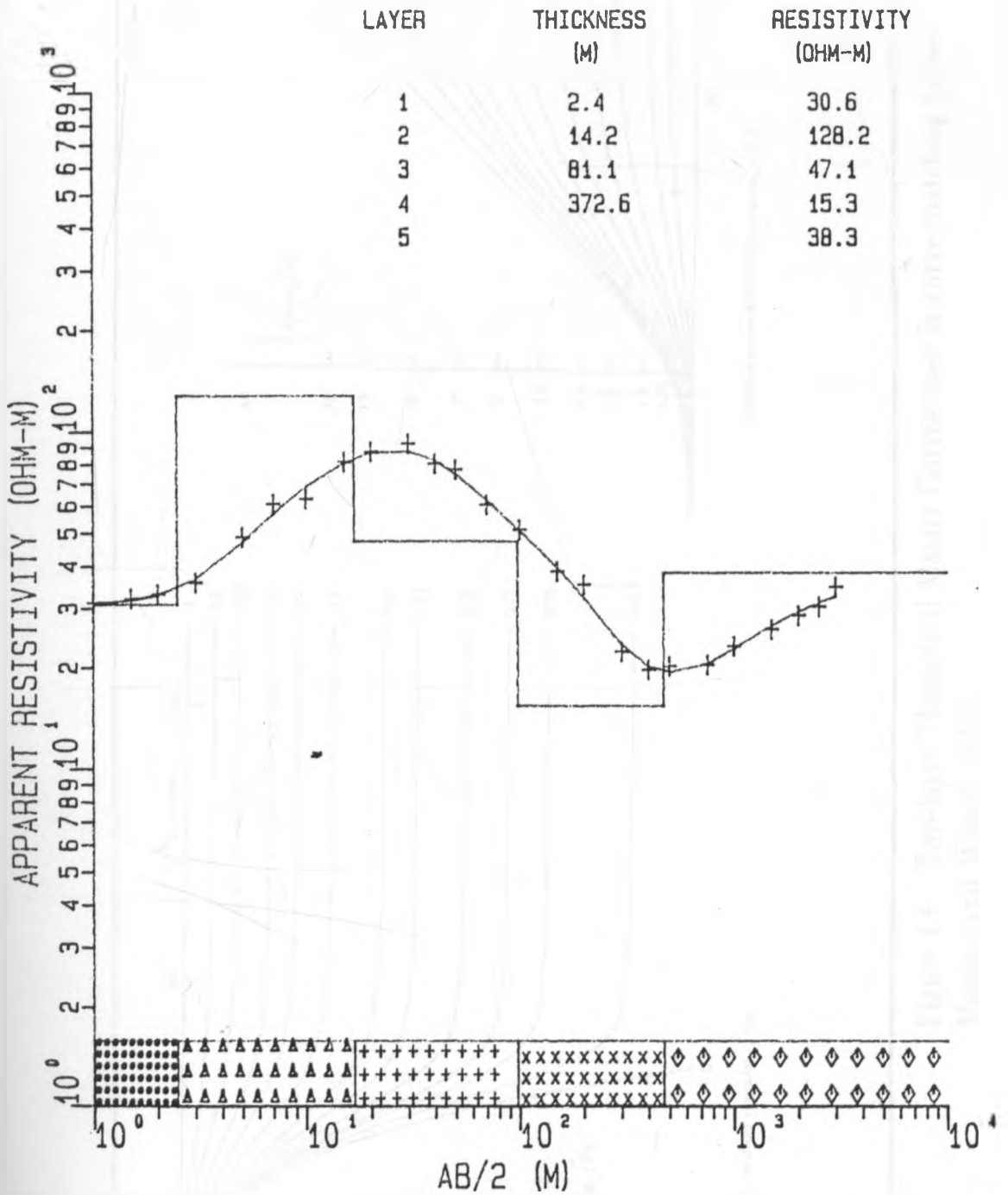
Figure 4.8 Fitted sounding curve and estimated profile for field results of ST06.

$s/t_1 \longrightarrow$

10   100

ρ app./ρ_1

1
0.8
0.65
0.5
0.4
0.3
0.2
0.15
0.10
0.07
0.05
0.025
0

Two-layer apparent resistivity curves for $\rho_2 < \rho_1$.

ρ app./ρ_1

∞

40
20
15
10
7
5
3.5
2.5
2.0
1.5
1.25
1

$s/t_1 \longrightarrow$

10   100

Two-layer apparent resistivity curves for $\rho_2 > \rho_1$.
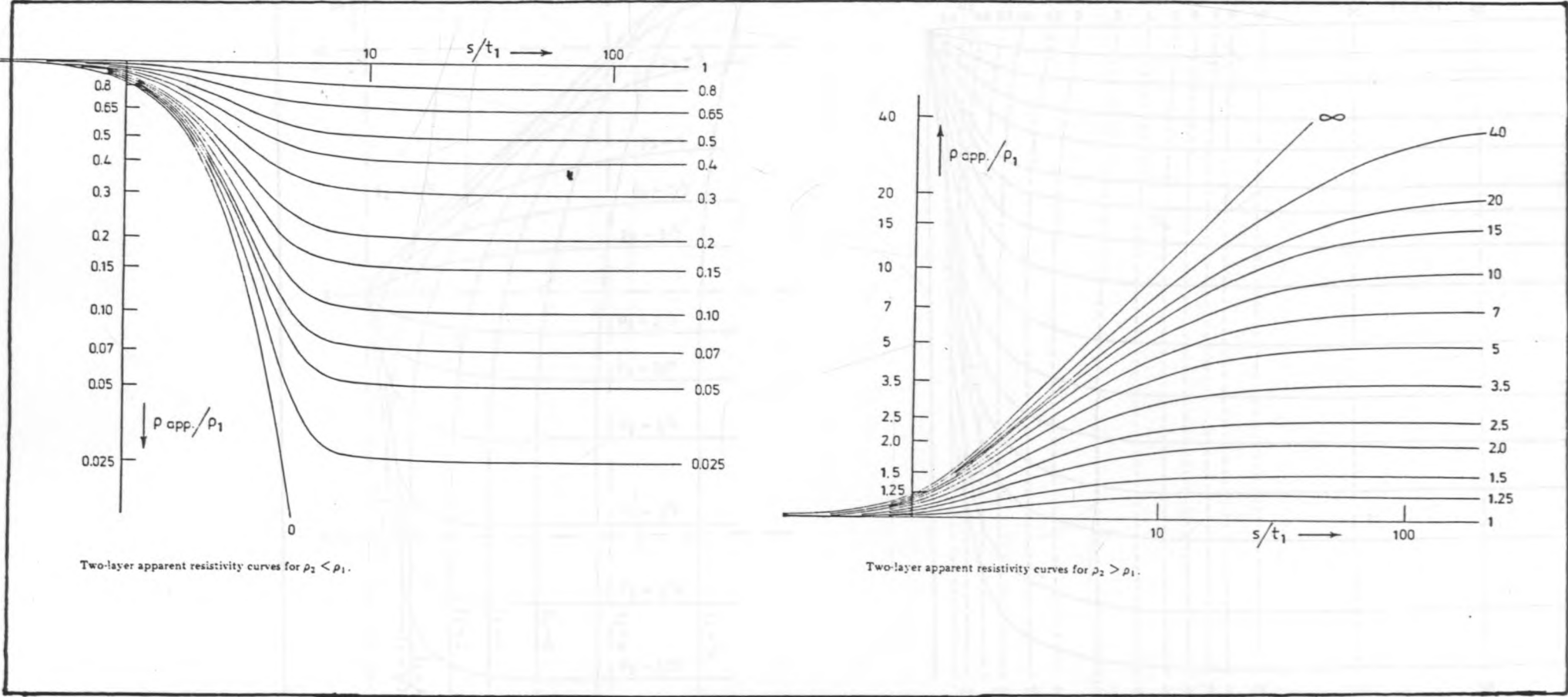
Figure 4.9   Two-layer Theoratical Master Curves used in curve matching (After Mooney and Wetzel, 1956).
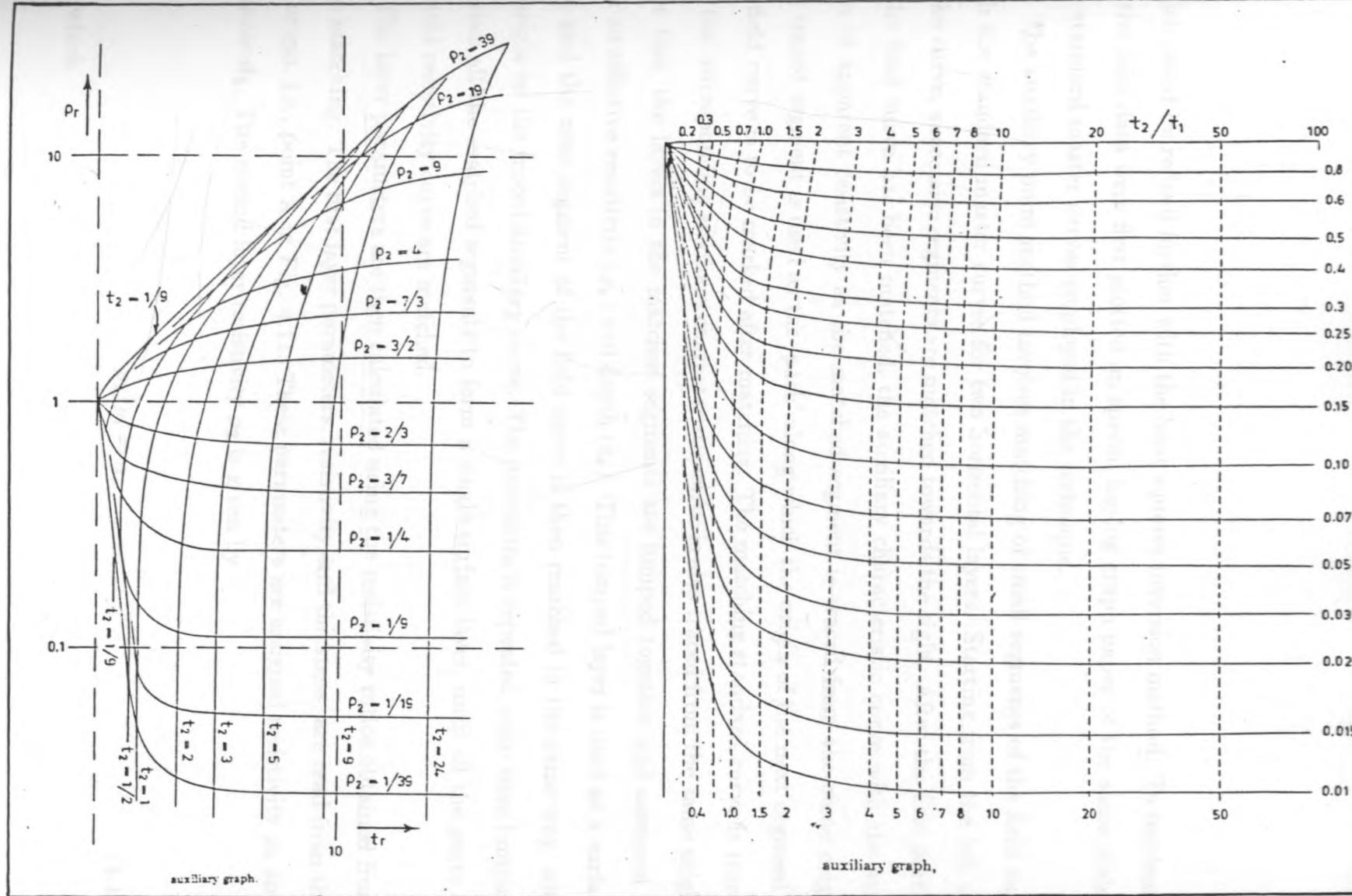
Figure 4.10 Auxiliary Point Charts used in conjuction with the Two-layer Master
Curves (After Orellana and Mooney, 1966).

which could be refined further with the least squares inversion method. To implement it, the field data were first plotted on special log-log graph paper of the same scale as the standard master curves employed in the technique.

The auxiliary point method involves matching of small segments of the field curve with the standard master curves for two horizontal layers. Starting from the left side of the curve, successive segments are matched towards the right. After the first portion of the field curve has been matched, the auxiliary characteristic curve with the same ratio of apparent resistivity as the matched segment is traced from the same origin. The traced segment is used as the 'path' along which the origin of the next segment of the field curve is to be marked after matching. The matching standard curve is traced and the corresponding auxiliary characteristic curve is also traced from the same origin. After this, the layers in the matched segments are lumped together and assumed to have an effective resistivity (ρ_e) and depth (z_e). This lumped layer is used as a surface layer and the next segment of the field curve is then matched in the same way, with the origin on the traced auxiliary curve. The procedure is repeated, each time lumping together all the matched segments to form a single surface layer, until all the parts of the field resistivity curve are matched.

The layer parameters are then calculated using the resistivity ratios obtained from curve matching. The first layer parameters, resistivity and thickness, are read from the first origin, i.e., point A in Fig. 4.11. These parameters are assigned resistivity ρ_1 and thickness d_1. The second layer resistivity ρ_2 is given by

$$\rho_2/\rho_1 = n, \qquad (4.1)$$

from which

$$\rho_2 = n \cdot \rho_1, \qquad (4.2)$$

where n is the resistivity ratio given by the matching standard curve of the first segment. The second layer thickness d_2 is given by

49
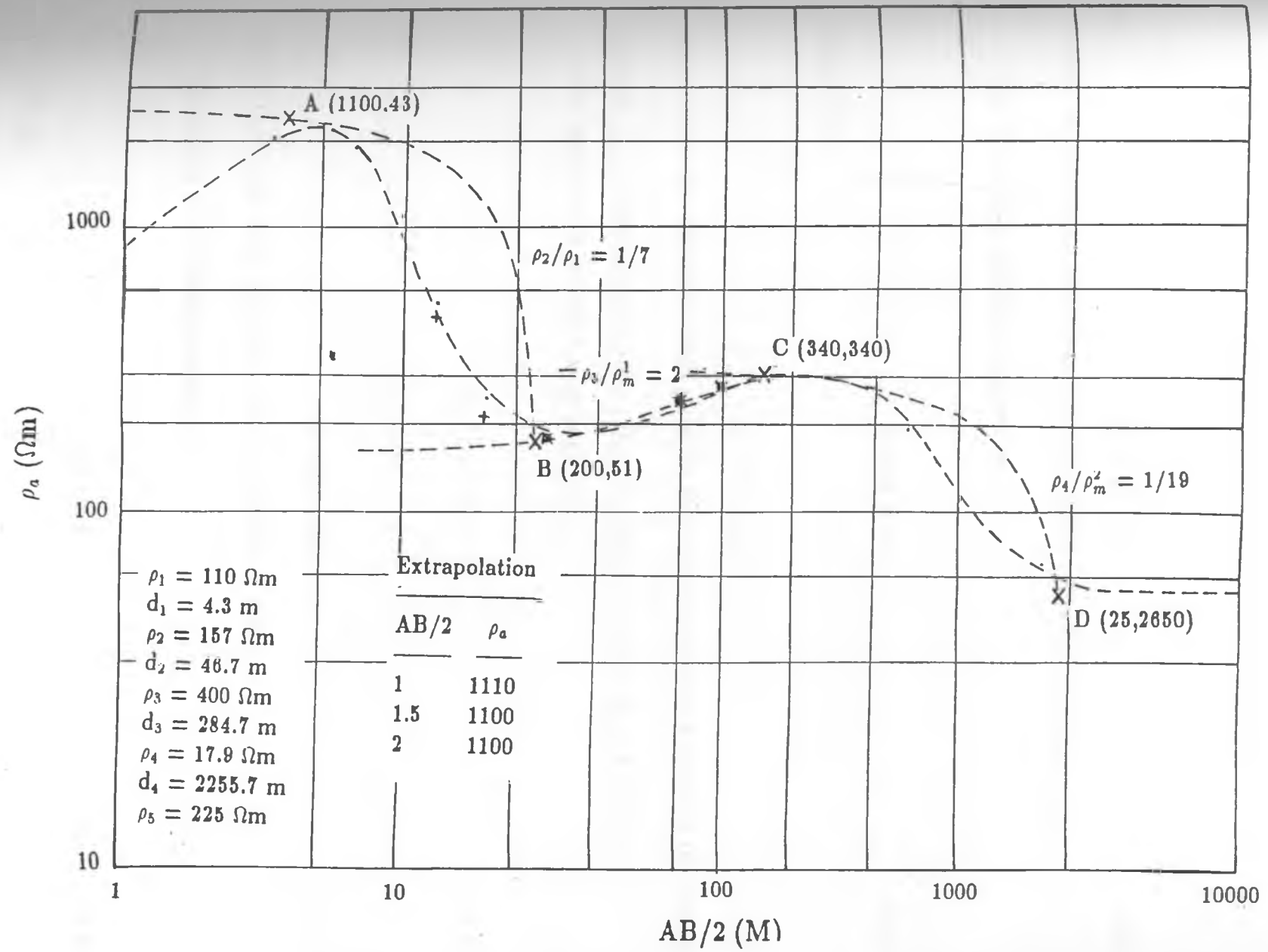
Figure 4.11   Fitted sounding data by partial curve matching method for ST15.

$$d_2 = B_x - d_1, \tag{4.3}$$

where $\mathbf{B_x}$ is the value read from the x-coordinate of point $\mathbf{B}$ in Figure 4.11

The third layer resistivity is given by

$$\rho_3/\rho_{m1} = n_2, \tag{4.4}$$

from which

$$\rho_3 = n_2 \cdot \rho_{m1}. \tag{4.5}$$

where $\mathbf{n_2}$ is the resistivity ratio given by the matching standard curve of the second segment. ρ_{m1} is the value read from the y-coordinate of point $\mathbf{B}$ in Figure 4.11.

The thickness of the third layer is given by

$$d_3 = C_x - (d_1 + d_2), \tag{4.6}$$

or

$$d_3 = C_x - B_x, \tag{4.7}$$

where $\mathbf{C_x}$ is the value read from the x-coordinate of point $\mathbf{C}$.

The fourth layer resisivity is given by

$$\rho_4/\rho_{m2} = n_3, \tag{4.8}$$

from which

$$\rho_4 = n_3 \cdot \rho_{m2}, \tag{4.9}$$

where $\mathbf{n_3}$ is the resistivity ratio given by the matching standard curve of the third

51

segment. ρ_{m2} is the value read from the y-coordinate of point **C**.

The thickness of the fourth layer is given by

$$d_4 = D_x - (d_1 + d_2 + d_3),\qquad(4.10)$$

from which

$$d_4 = D_x - C_x,\qquad(4.11)$$

where D_x is the value read from the x-coordinate of point **D**. The procedure is repeated for curves with more than four layers. The last layer has a resistivity value but the thickness is assumed to be at infinity.

This technique was used to analyse all the apparent resistivity data involved in this study. The layer parameters determined were then used as the initial 'guess' parameters in the least squares inversion program. The technique, like other geophysical interpretation techniques, has the ambiguity that the same data might equally fit a number of other theoretical curves representing a wide range of solutions. Unique solutions can be only possible if some independent geologic control is incorporated in the analysis. Usually, the resemblance to geology might be crude (Grant and West, 1963), but the number of the interpretated layers very often gives useful information about the subsurface geology although it is difficult to identify the formation from the conductivity values alone.

4.3.2 Least squares inversion

Least squares inversion formed the main part of the analysis of data in this study. It involved determining more accurate and reliable layer parameters and statistically assessing their viability. The computer program used was that written by Barongo (1989) based on the inversion theory. A brief outline of the algorithm it uses has already been presented in Chapter 2. Known as SCHINV (SCHlumberger INVersion), the program is designed to run through a pre-assigned number of iterations and stops if convergence has not been reached. The layer parameters obtained from partial curve matching using auxiliary point method were used as the initial 'guess' model parameters

52

in the program. However, sounding stations ST10 and ST21 (Figs. 4.12 and 4.13) were subjected to O'Neil curve matching (O'Neil, 1975; O'Neil and Merrick, 1984) to obtain the required starting model for SCHINV program. The guess model obtained by partial curve matching for these two stations were not 'behaving' well when used in the SCHINV program, but the model obtained by computation of O'Neil curves 'behaved' well. The model parameters from O'Neil curve matching were then successfully modified automatically by the SCHINV program and there was convergence.

Computation of O'Neil curves is based on Ghosh's convolution method using O'Neil filter coefficients (O'Neil, 1975). The layer parameters were obtained by adjusting the parameters of the initial input model until the calculated apparent resistivities fitted the field data. The advantage of O'Neil curve matching over partial curve matching is that it has more standard curves and has good resolution when there are appreciable contrasts in layer parameters. Furthermore, partial curve matching results in overestimation of thickness while resistivities are well resolved. However, a 'good fit' to the field data does not necessarily indicate an accurate determination of the layer parameters, and therefore the need for the SCHINV program.

Table 4.1 shows an example of the inversion results for sounding station ST03. In the table are columns showing the iteration number, the corresponding χ^2 value and the %RMS (per cent Root Mean Square) values. The estimated and the calculated problem variances are also indicated. Below these are the initial and the final model parameters. Two columns on the right show the longitudinal conductance (thickness/resistivity) and the transverse resistance (thickness $\times$ resistivity) calculated for each layer. The appraisal statistics of the final model parameters and the parameter correlation coefficients are also given. The weights applied are given for every data point and the amount of information for each of the data points is listed.

The SCHINV program has the criterion that a solution is acceptable if the minimum χ^2 value at convergence is equal or close to the number of data points, N. The %RMS value is expected to be zero or close to zero at convergence if the inverse problem was linear and well-behaved and the data were noise-free. However, in practice, no field data are free from noise. Therefore, the %RMS value was also calculated and recorded at
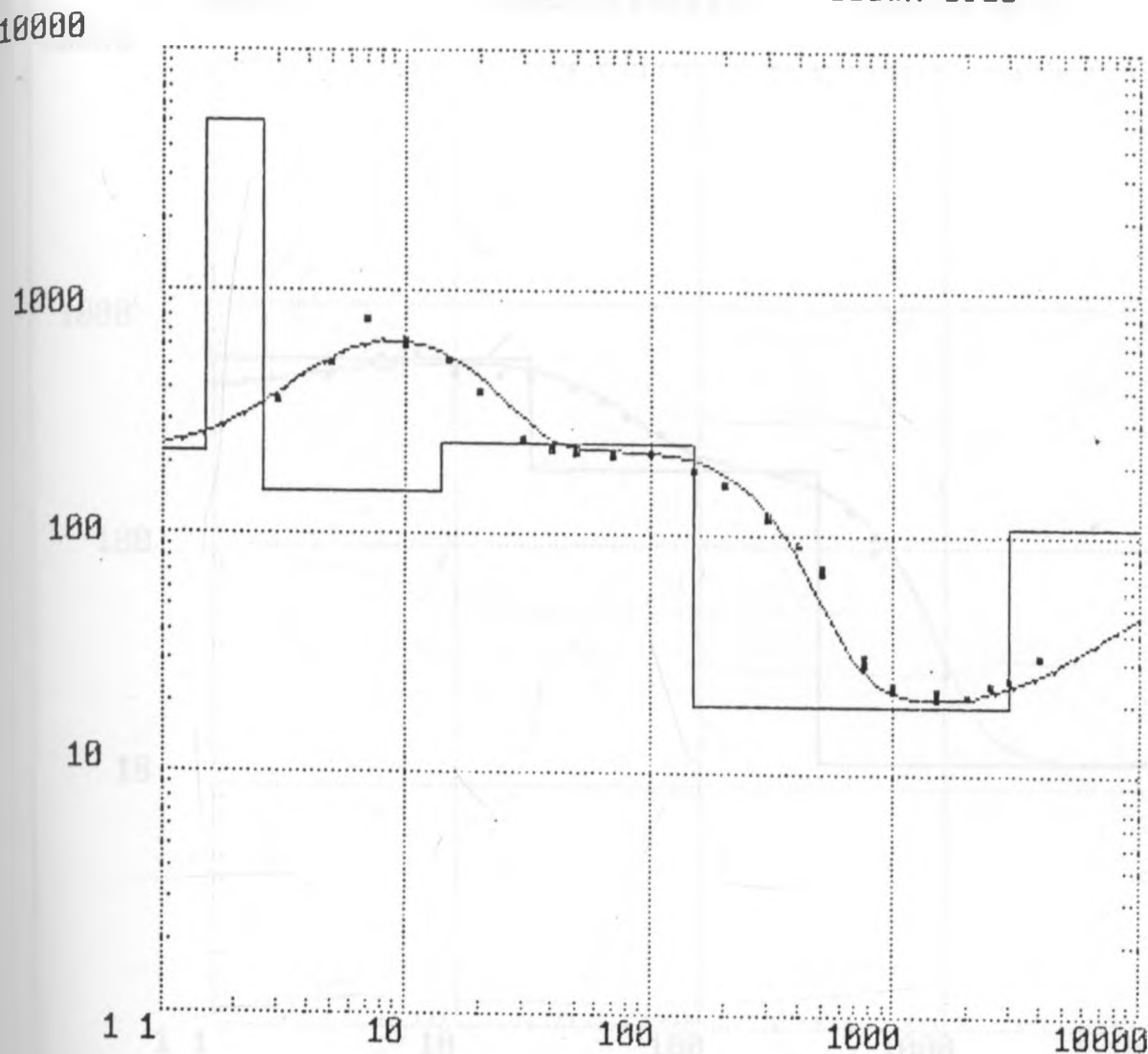
File number 1: SUSWA ST10

Resistivity model(s).

Nr.	Depth(m)	Res.(ohmm)	Modelnr.
1.	1.5	217.9	begin 1
2.	2.6	5000.0	
3.	14.0	150.0	
4.	150.0	240.0	
5.	3000.0	19.7	
6.	9999.0	110.0	end of 1

Figure 4.12   Fitted sounding curve and resistivity model for ST10 by computation of O'Neill curves.

MODEL 1   Press <ENTER>   SUSWA ST21

File number 2: SUSWA ST21

Resistivity model(s).

Nr. Depth(m) Res.(ohmm) Modelnr.
 1.   1.0   440.0   begin 1
 2.   20.0   600.0
 3. 300.0   208.0
 4. 9999.0   13.0   end of 1
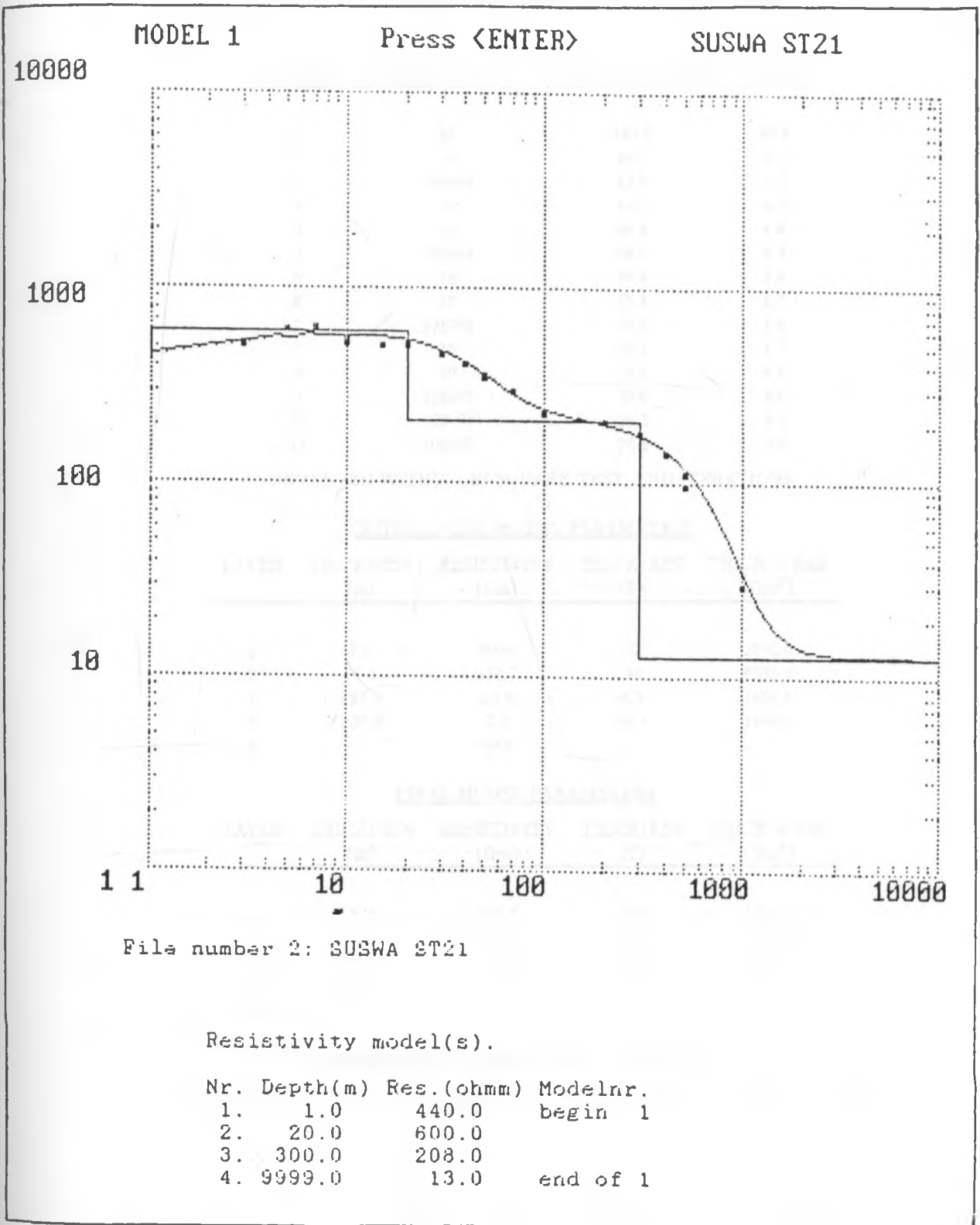
Figure 4.13   Fitted sounding curve and resistivity model for ST21 by computation of O'Neill curves.

Table 4.1 Inversion results for ST03 field data.

ITERATION	MARQT CONST.	CHI-SQUARE VALUE	%RMS
1	.10	183.6	10.8
2	.10	40.3	5.1
3	.10E-01	42.6	5.2
3	10	40.3	5.1
4	.10	36.8	4.9
5	.10E-01	38.6	5.0
5	.10	36.8	4.9
6	.10	35.1	4.7
7	.10E-01	35.6	4.8
7	.10	35.1	4.7
8	10	33.6	4.6
9	.10E-01	33.0	4.6
10	10E-01	25.3	4.0
11	.10E-02	24.4	3.9

CONVERGED WITHIN CHI-SQUARE TEST, END ITERATIONS

INITIAL GUESS MODEL PARAMETERS

LAYER	THICKNESS (m)	RESISTIVITY (Ωm)	THICK/RES (S)	THICK × RES (Ωm^2)
1	7.0	350.0	.02	2450.0
2	56.0	116.7	.48	6535.2
3	147.0	23.5	6.3	3454.5
4	220.0	7.5	29.3	1650.0
5		50.8		

FINAL MODEL PARAMETERS

LAYER	THICKNESS (m)	RESISTIVITY (Ωm)	THICK/RES (S)	THICK × RES (Ωm^2)
1	5.2	335.7	.02	1736.1
2	35.5	156.1	.23	5545.9
3	88.1	61.9	1.42	5454.9
4	349.6	9.9	35.1	3477.2
5		55.4		

FINAL MODEL PARAMETERS AND STATISTICS

PARAMETER	FINAL SOLUTION	STANDARD DEVIATION	RESOLUTION
1	5.1	2.3	1.00
2	35.5	8.3	.97
3	88.1	14.9	96
4	349.6	43.3	.67
5	335.7	1.5	1.00
6	156.1	2.9	99
7	61.9	12.5	.95
8	9.9	44.8	65
9	55.4	3.4	99

PARAMETER CORRELATION MATRIX, LOWER LEFT HALF

	1	2	3	4	5	6	7	8	9
1	1.00								
2	.47	1.00							
3	.21	.72	1.00						
4	-.19	-.63	-.97	1.00					
5	-.48	-.12	-.05	.05	1.00				
6	-.77	-.72	-.34	.31	.23	1.00			
7	-.37	-.95	-.88	.78	.10	.57	1.00		
8	-.19	-.64	-.97	1.00	.05	.31	.78	1.00	
9	-.08	-.28	-.52	.65	.02	.12	.35	.60	1.00
	1	2	3	4	5	6	7	8	9

FINAL MODEL DATA AND STATISTICS

SPACING (m)	OBSERVED DATA (Ωm)	CALCULATED DATA (Ωm)	ERROR (Ωm)	WEIGHTS	INFORMATION
1.0	340.0	335.4	4.6	185.0	.46
1.5	338.0	335.0	3.0	182.8	.46
2.0	335.0	334.0	1.0	179.6	.45
3.0	315.0	330.6	-15.6	158.8	.45
5.0	315.0	316.5	-1.5	158.8	.38
7.0	307.0	295.1	11.9	150.8	.41
10.0	259.3	259.7	-0.4	107.6	.58
15.0	216.1	213.8	2.3	74.7	.61
20.0	188.6	187.5	1.1	56.9	.51
30.0	148.3	163.1	-14.8	35.2	.62
40.0	157.9	150.0	7.9	39.9	.54
50.0	147.4	139.0	8.4	34.8	.49
70.0	125.8	118.1	7.7	25.3	.56
100.0	86.6	91.8	-5.2	12.0	.77
150.0	64.0	63.3	0.7	6.6	.68
200.0	48.4	45.8	2.6	3.8	.75
300.0	27.2	26.5	0.7	1.2	.78
400.0	17.8	18.4	-0.6	0.5	.76
500.0	16.3	15.8	0.5	0.4	.84
750.0	17.2	16.9	0.3	0.5	.65
1000.0	18.9	19.9	-1.0	0.6	.69
1500.0	25.4	25.6	-0.2	1.0	.51
2000.0	28.8	30.1	-1.3	1.3	.47
2500.0	34.6	33.6	1.0	1.9	.54
3000.0	36.6	36.5	0.1	2.1	.72

FINAL SOLUTION EIGENVALUES

1.85   1.52   1.30   .93   .63   .43   .33   .12   .02

each iteration to keep track of the noise level.

The program was first run with resistivity data being weighted with a noise level of one per cent (**1%**) of the data values. There was no convergence after an assigned maximum number of 15 iterations. Due to the presence of higher noise level in the data, most of the parameters were not well resolved. The smallest constant value in the %**RMS** column was the actual noise level in the data. In Table 4.1, the noise level in this case is seen to be 4% of the data values. The program was then re-run using this value for weighting. This time, the problem converged at the eleventh iteration. The solutions in the table indicate that the value of χ^2 at convergence is approximately equal to 24, which is the number of data points in this particular sounding.

High resolution values, almost equal to 1, indicate good results which are almost fully resolved. The parameters with the smallest standard deviations are the best resolved. The coefficients in the correlation matrix mean that when a coefficient value is equal or close to +1.0, the ratio of the two corresponding parameters (thickness/resistivity=longitudinal conductance) is the best determined combination of parameters. Conversely, if the coefficient value is equal or close to -1.0, then the product of the parameters (thickness × resistivity = transverse resistance) is the best determined. Correlation coefficients equal or nearly equal to zero indicate that the parameters involved are not correlated The 4th layer parameters in Table 4.1 are the most positively correlated. Therefore, this implies that the conductivity-thickness product (=thickness/resistivity) of the layer is the better determined parameter combination than the individual parameters themselves. Note the high standard deviations of the 4th and 8th parameters which correspond to the 4th layer parameters. The other covariance values are relatively low while others have high negative values such as those for the third layer. The high negative correlation coefficients imply that the thickness-conductivity (= thickness × resistivity) ratio is the best resolved parameter combination. The differences between the observed and the calculated data are small as is indicated by the error column.

The information about the last two layers is high as is indicated by the high information values for data points corresponding to **AB/2** = 1000 m and above. These

data points relate to the bottom layers. Maximum information also exists for the first two top layers. Generally, the surface and the bottom layers are well resolved. The bottom layer is resistive and is overlain by a very conductive layer. Figure 4.14 shows the apparent resistivity curve for the solution obtained for station ST03 and shown in Table 4.1. The curve fits the field data quite well.

Table 4.2 for ST07 indicates that parameters 2 and 7 are negatively correlated (-1.0). These parameters are those of the 2nd layer. The implication here is that their product is better determined than the individual parameters themselves. Conversely, parameters 5 and 10 are positively correlated (+1.0). These parameters are those of the 5th layer. This implies that their ratio is better determined than the individual parameters. High information values corresponding to the best resolved values mean that most information is provided about the geoelectric characteristics of the subsurface. Thus, the first and last two layers have best resolved parameters and show most information.

4.4 Summary

The accepted solutions in the least squares inversion are those that converged within the Chi-square test. The 'guess' model parameters were re-adjusted (reparameterized) accordingly so that all the sounding field data converged. Most of the solutions indicate that the surface layers were best resolved except for a few cases (Stations ST05 and ST13).

There was a general disagreement between the layer parameters obtained through the SCHINV program and those obtained through the partial curve matching. This can be attributed to the general tendency of overestimated parameter solutions in curve matching, especially thickness. The overestimation is due to the fact that, in curve matching, a probing depth equal to AB/2 spacing is assumed. In practice, however, there is a decrease in current penetration to deeper layers as the AB/2 values increase so that the apparent resistivities measured at large current electrode separations do not represent response from deeper subsurface regions. This probing depth is also a function of the rock type being investigated. On the other hand, there is a 'probing depth to
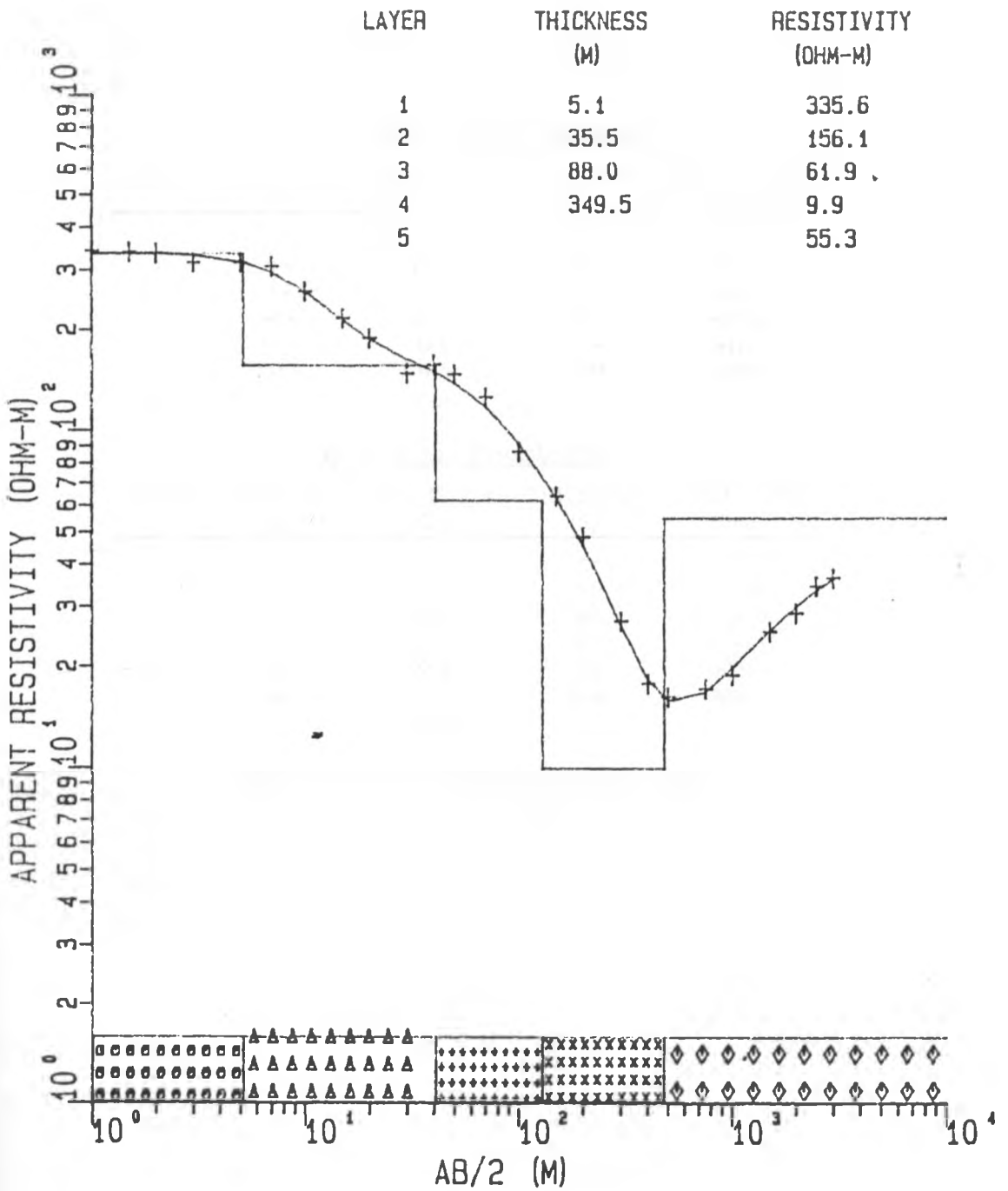
Figure 4.14   Fitted sounding curve and estimated profile for field results of ST03.

60

Table 4.2 Inversion results for ST07 field data.

ITERATION	MARQT CONST.	CHI-SQUARE VALUE	%RMS
1	10	1156.6	27.2
2	10	104.6	8.1
3	.10E-01	58.0	6.1
4	.10E-01	29.0	4.3
5	.10E-02	813.7	22.8
5	.10E-01	29.0	4.3
6	.10E-01	22.4	3.8

CONVERGED WITHIN CHI-SQUARE TEST, END ITERATIONS

INITIAL GUESS MODEL PARAMETERS

LAYER	THICKNESS (m)	RESISTIVITY (Ωm)	THICK/RES (S)	THICK × RES (Ωm²)
1	2.8	160.0	.02	448.0
2	5.8	800.0	.01	4640.0
3	83.6	106.7	.78	8920.1
4	351.6	41.0	8.58	14415.6
4	555.6	16.0	34.73	8889.6
6		42.0		

FINAL MODEL PARAMETERS

LAYER	THICKNESS (m)	RESISTIVITY (Ωm)	THICK/RES (S)	THICK × RES (Ωm²)
1	2.1	150.3	.01	311.4
2	2.4	754.3	.00	1781.0
3	82.5	115.7	.71	9540.7
4	366.8	51.1	7.2	18738.0
5	828.1	11.7	70.8	9690.0
6		209.5		

FINAL MODEL PARAMETERS AND STATISTICS

PARAMETER	FINAL SOLUTION	STANDARD DEVIATION	RESOLUTION
1	2.1	10.2	.95
2	2.4	50.6	.56
3	82.5	4.4	.93
4	366.8	14.3	.91
5	828.1	67.7	.41
6	150.3	2.5	.97
7	754.3	51.2	.51
8	115.7	2.8	.97
9	51.1	6.4	.90
10	11.7	57.3	.52
11	09.5	17.4	.76

PARAMETER CORRELATION MATRIX, LOWER LEFT HALF

	1	2	3	4	5	6	7	8	9	10	11
1	1.00										
2	-.98	1.00									
3	-.19	.25	1.00								
4	-.09	.10	.60	1.00							
5	.07	-.08	-.48	-.95	1.00						
6	.68	-.57	-.07	-.04	.03	1.00					
7	.98	-1.00	-.23	-.10	.08	.56	1.00				
8	.47	-.56	-.66	-.24	.20	.21	.54	1.00			
9	.17	-.21	-.90	-.80	.65	.07	.20	.46	1.00		
10	.08	-.09	-.51	-.98	.99	.03	.09	.21	.70	1.00	
11	.04	-.05	-.32	-.77	.92	.02	.05	.12	.45	.86	1.00
	1	2	3	4	5	6	7	8	9	10	11

FINAL MODEL DATA AND STATISTICS

SPACING (m)	OBSERVED DATA (Ωm)	CALCULATED DATA (Ωm)	ERROR (Ωm)	WEIGHTS	INFORMATION
1.0	158.0	152.8	5.2	39.9	.75
1.5	160.0	158.1	1.9	41.0	.57
2.0	163.0	166.5	-3.5	42.5	.53
3.0	178.2	189.9	-11.7	50.8	.77
5.0	240.0	236.8	3.2	92.2	.60
7.0	274.2	263.3	10.9	120.3	.61
10.0	277.3	269.1	8.2	123.0	.60
15.0	245.9	239.1	6.8	96.8	.56
20.0	199.8	202.4	-2.6	63.9	.64
30.0	150.8	154.4	-3.6	36.4	.59
40.0	132.0	133.3	-1.3	27.9	.51
50.0	126.2	124.2	2.0	25.5	.53
70.0	116.5	115.5	1.0	21.7	.57
100.0	106.8	106.6	0.2	18.3	.51
150.0	94.5	92.2	2.3	14.3	.60
200.0	81.2	79.6	1.6	10.6	.66
300.0	57.9	63.0	-5.1	5.4	.64
400.0	58.7	53.8	4.9	5.5	.61
500.0	48.1	47.8	0.3	3.7	.54
750.0	35.7	34.8	0.9	2.0	.75
1000.0	29.5	29.2	0.3	1.4	.75
1500.0	23.8	23.6	0.2	0.9	.89
2000.0	26.2	24.9	1.3	1.1	.76
2500.0	27.6	28.7	-1.1	1.2	.74
3000.0	35.6	33.2	2.4	2.0	.95

FINAL SOLUTION EIGENVALUES

1.84   1.60   1.45   1.29   .86   .55   .44   .24   .12   .02   .01

AB/2 spacing' ratio of 'one to one' (1:1) for shallower depth probes conducted with smaller electrode separations. However, the perfomance of an electrode array placed over an anisotropic earth is controlled not only by its array length but also by the coefficient of anisotropy and dip of the plane of stratification (Bhattacharya and Sen, 1981) There is, therefore, enough reason to contend that parameter solutions obtained through the inversion program are reliable and cannot be equated to those obtained through partial curve matching technique.

Chapter 5

INTERPRETATION

5.1   General

The geoelectric structure beneath the study area has been interpreted in terms of a one-dimensional (1-D) layered earth model. Normally, parameters determined through inversion are not necessarily unique. Other geologically viable model parameters could as well fit the observed data perfectly. Due to this known problem, any available geological and hydrogeological information in the study area was very useful in providing some necessary control in the inversion. Thus, the goal was to determine models that relate as closely as possible to the real field situation in the area. Geological information of the area was obtained from works by Baker (1958), Thompson and Dodson (1963), Randel and Johnson (1970), Kagasi (1983) and Baker et al. (1987). Hydrogeological information was found in Torfasson (1987). The following are the geophysical and hydrogeological results obtained, their descriptions and interpretations.

5.2   Iso-resistivity maps

Contours through points of equal apparent resistivity for different current electrode separations were drawn. Iso-resistivity maps at a scale of 1:50 000 were obtained for current electrode separations, AB/2, equal to 100, 200, 500, 1000 and 2000 metres. These maps are shown in Figures 5.1 to 5.5.

The iso-resistivity maps for AB/2=100 and AB/2=200 metres shown in Figures 5.1 and 5.2, respectively, appear to be characterized by high resistivities. Two prominent
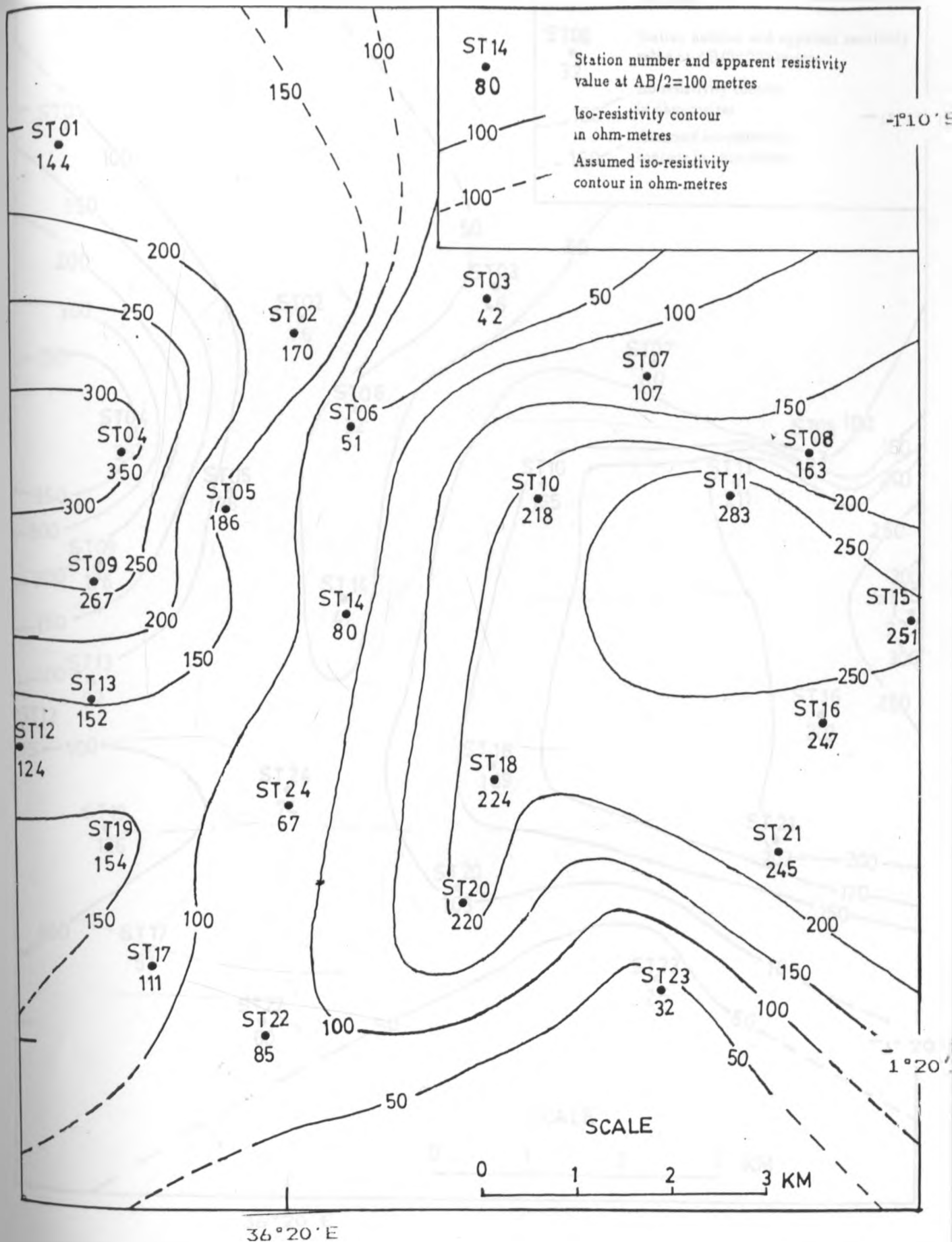
Figure 5.1   Iso-Resistivity contour map for AB/2=100 m.
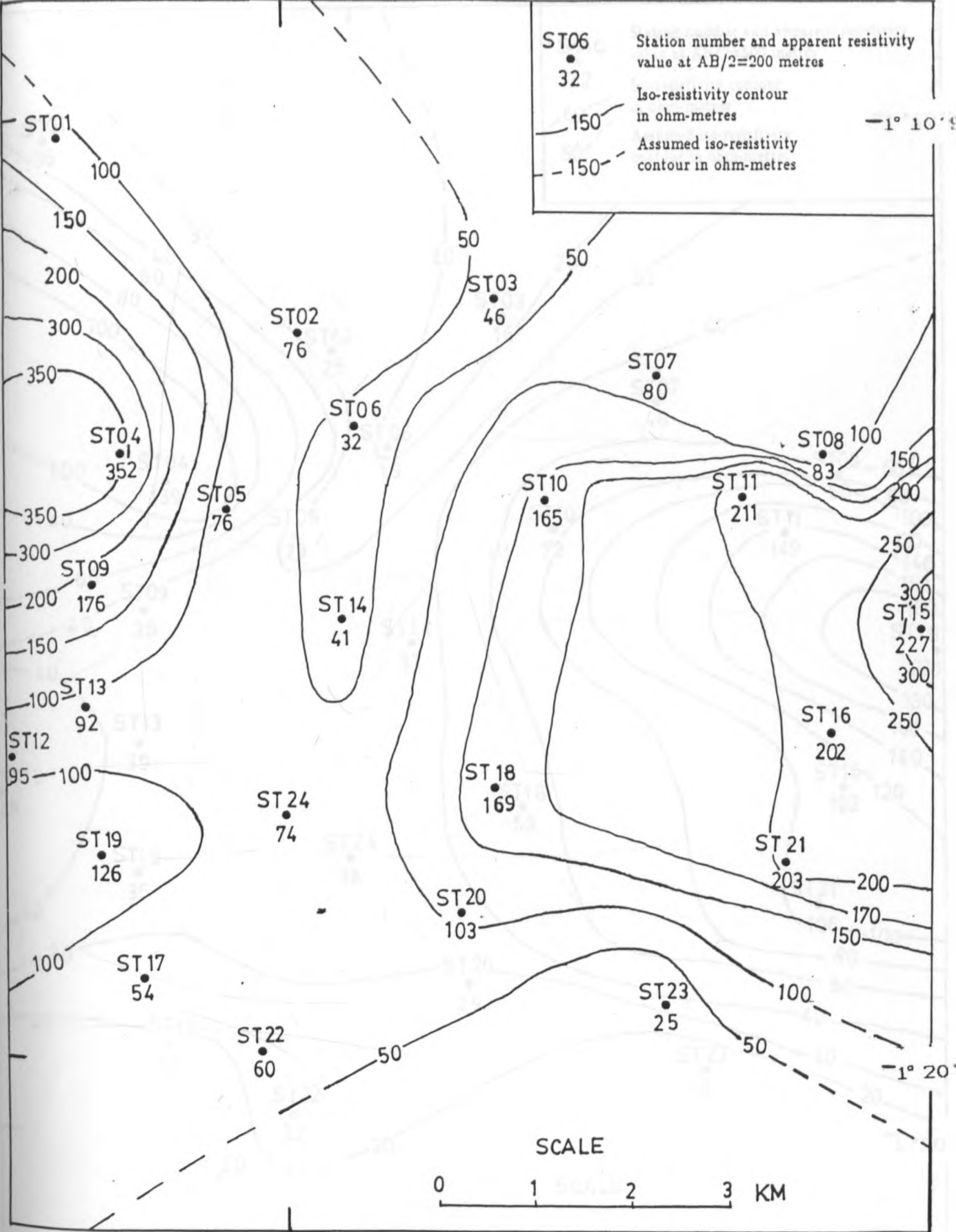
Figure 5.2   Iso-Resistivity contour map for AB/2=200 m.

66
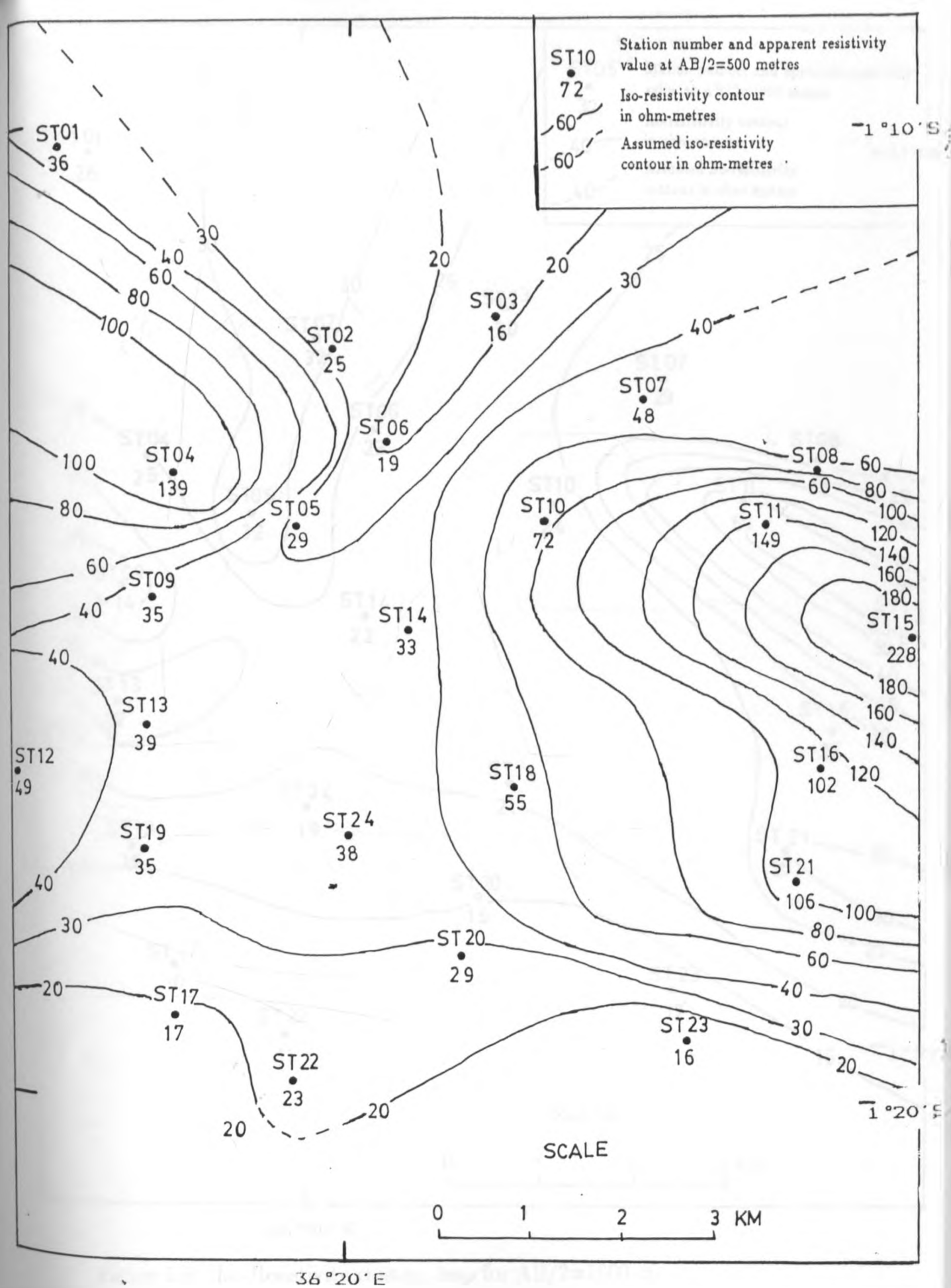
Figure 5.3   Iso-Resistivity contour map for AB/2=500 m.
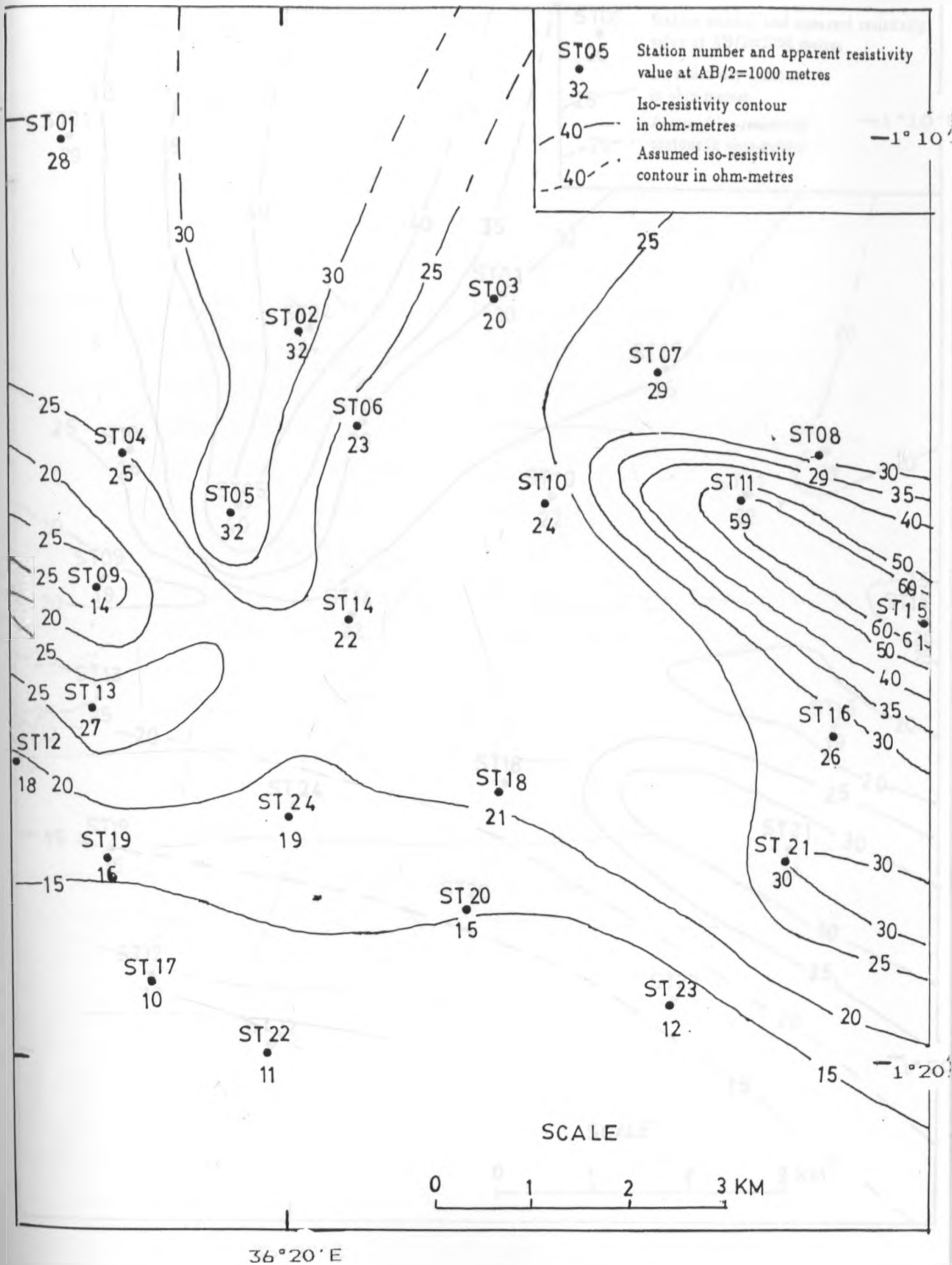
Figure 5.4   Iso-Resistivity contour map for AB/2=1000 m.
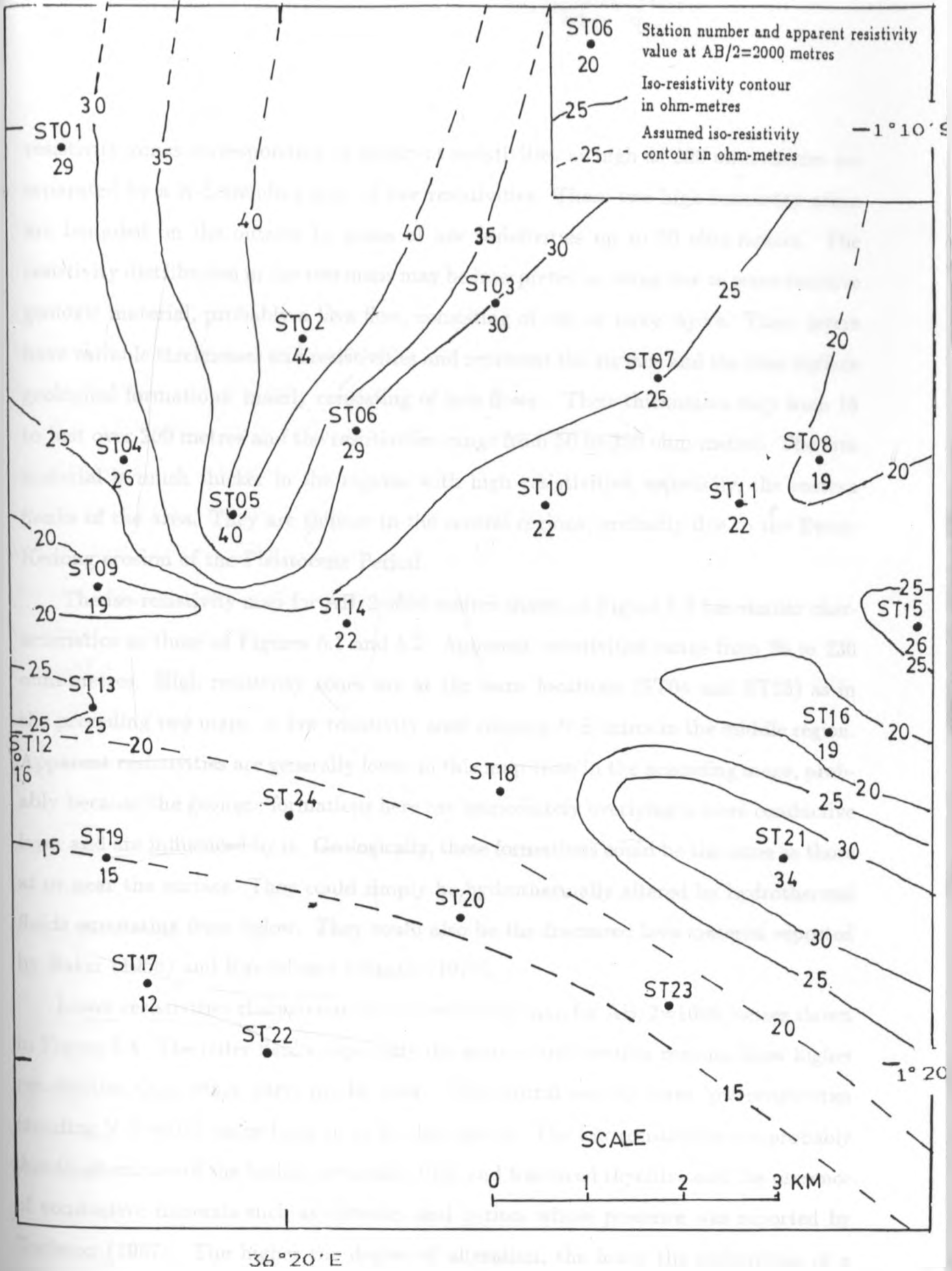
Figure 5.5   Iso-Resistivity contour map for AB/2=2000 m.

ST06 — Station number and apparent resistivity value at AB/2=2000 metres
20

25 — Iso-resistivity contour in ohm-metres

25 — Assumed iso-resistivity contour in ohm-metres

SCALE
0   1   2   3 KM

36°20'E

−1°10'S

−1°20'

resistivity zones corresponding to apparent resistivities as high as 200 ohm-metres are separated by a N-S trending zone of low resistivities. These two high resistivity zones are bounded on the outside by zones of low resistivities up to 50 ohm-metres. The resistivity distribution in the two maps may be interpreted as being due to some resistive geologic material, probably a lava flow, consisting of one or more layers. These layers have variable thicknesses and resistivities and represent the surface and the near-surface geological formations, mainly consisting of lava flows . Their thicknesses vary from 15 to just over 200 metres and the resistivities range from 50 to 350 ohm-metres. The lava material is much thicker in the regions with high resistivities, especially, the eastern flanks of the area. They are thinner in the central regions, probably due to the Ewaso Kedong erosion of the Pleistocene Period.

The iso-resistivity map for AB/2=500 metres shown in Figure 5.3 has similar characteristics as those of Figures 5.1 and 5.2. Apparent resistivities range from 20 to 230 ohm-metres. High resistivity zones are at the same locations (ST04 and ST15) as in the preceding two maps. A low resistivity zone running N-S exists in the middle region. Apparent resistivities are generally lower in this map than in the preceding maps, probably because the geologic formations here are immediately overlying a more conductive layer and are influenced by it. Geologically, these formations could be the same as those at or near the surface. They could simply be hydrothermally altered by hydrothermal fluids emanating from below. They could also be the fractured lava material reported by Baker (1958) and Randel and Johnson (1970).

Lower resistivities characterize the iso-resistivity map for AB/2=1000 metres shown in Figure 5.4. The outer flanks, especially the eastern and western regions. show higher resistivities than other parts of the area. The central regions have low resistivities trending N-S which range from 10 to 24 ohm-metres. The low resistivities are probably due to alteration of the highly permeable tuffs and fractured rhyolites and the presence of conductive minerals such as chlorites and pyrites whose presence was reported by Torfason (1987). The higher the degree of alteration, the lower the resistivities of a particular formation. The formation resistivity could also be due to increase in temperature, porosity of the rocks or salinity of the fluids. The highest apparent resistivity

70

for this AB/2 value is 61 ohm-metres (ST15), but the average resistivity is about 20 ohm-metres. The two resistive zones probably correspond to resistive lenses of limited size enclosed within a conductive zone. Such lenses have previously been encountered in Olkaria geothermal field where drilling results have proved them to be due to geothermal reservoirs (Geotermica Italiana, 1988). This iso-resistivity map corresponds to a conductive zone that is generally homogeneous but somewhat rendered heterogeneous by the fractured and weathered trachytes and tuffs.

For AB/2=2000 metres, the iso-resistivity map shown in Figure 5.5 reveals the same pattern as the preceding map. However, the apparent resistivites for this AB/2 separation are comparatively higher. High apparent resistivities are noted on the eastern and western outer flanks of the area. This map could correspond partly to the lower parts of the conductive layer and partly to the top parts of the substratum ('electric basement'). Resistive lava material lying on top of the basement might also be the cause of the high resistivity. The resistive substratum is also manifested at several locations (e.g., ST12 and ST13) on the edges of the area.

5.3   Geoelectric sections

Vertical geoelectric sections representing the subsurface geoelectric structure were constructed along selected directions using final model parameters determined through the inversion method. These sections are useful as they enable an interpreter to see how the determined parameters correlate from one sounding station to another. More importantly, they are greatly helpful in extracting useful new geologic information from the subsurface. Such problems as equivalence, suppresion and situations where sounding stations are far from each other (e.g., profiles NS 4 and EW 3 in Figs. 5.6 and 5.7, respectively) may mislead the interpretations. This is, therefore, where extra information to control the interpretations is found useful. It is, therefore, stressed here that a geologic section interpreted from a geoelectric section may not provide all information concerning the true geologic section. For example, fewer layers than the true number may be inferred.
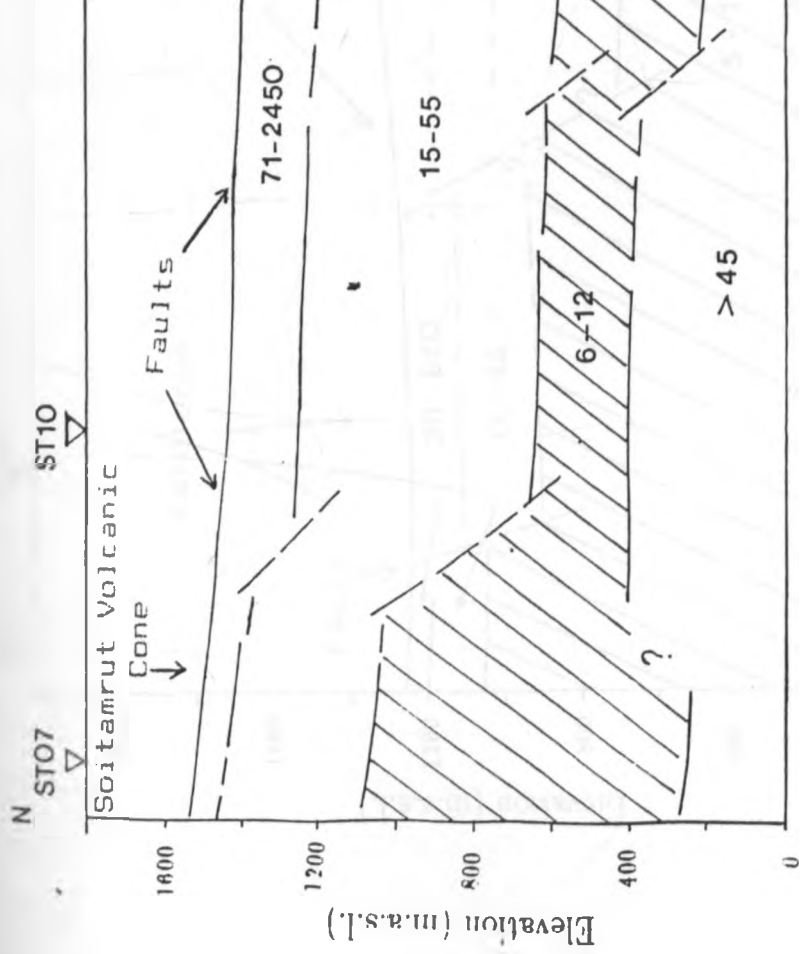
Figure 5.6   Geoelectric profile NS-4.

ST07   ST10

Soitamrut Volcanic Cone

Faults

71-2450

15-55

6-12

>45

?

Elevation (m.a.s.l.)

1600   1200   800   400   0

72
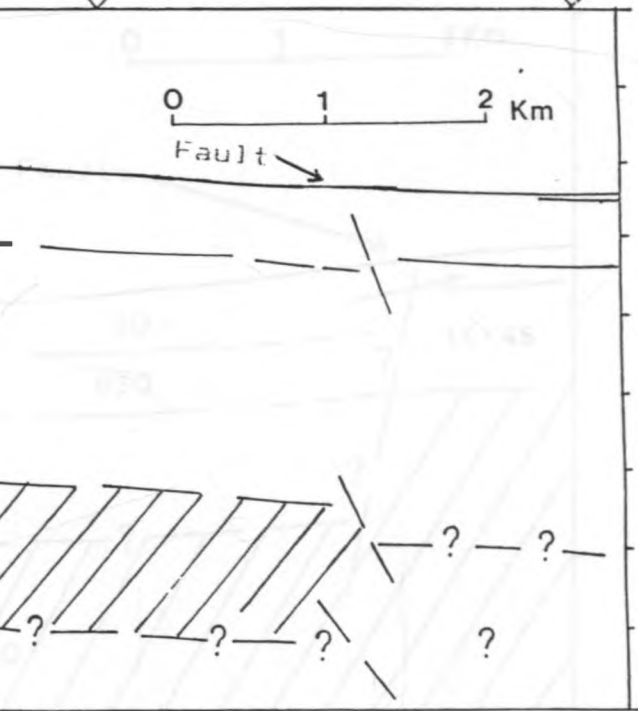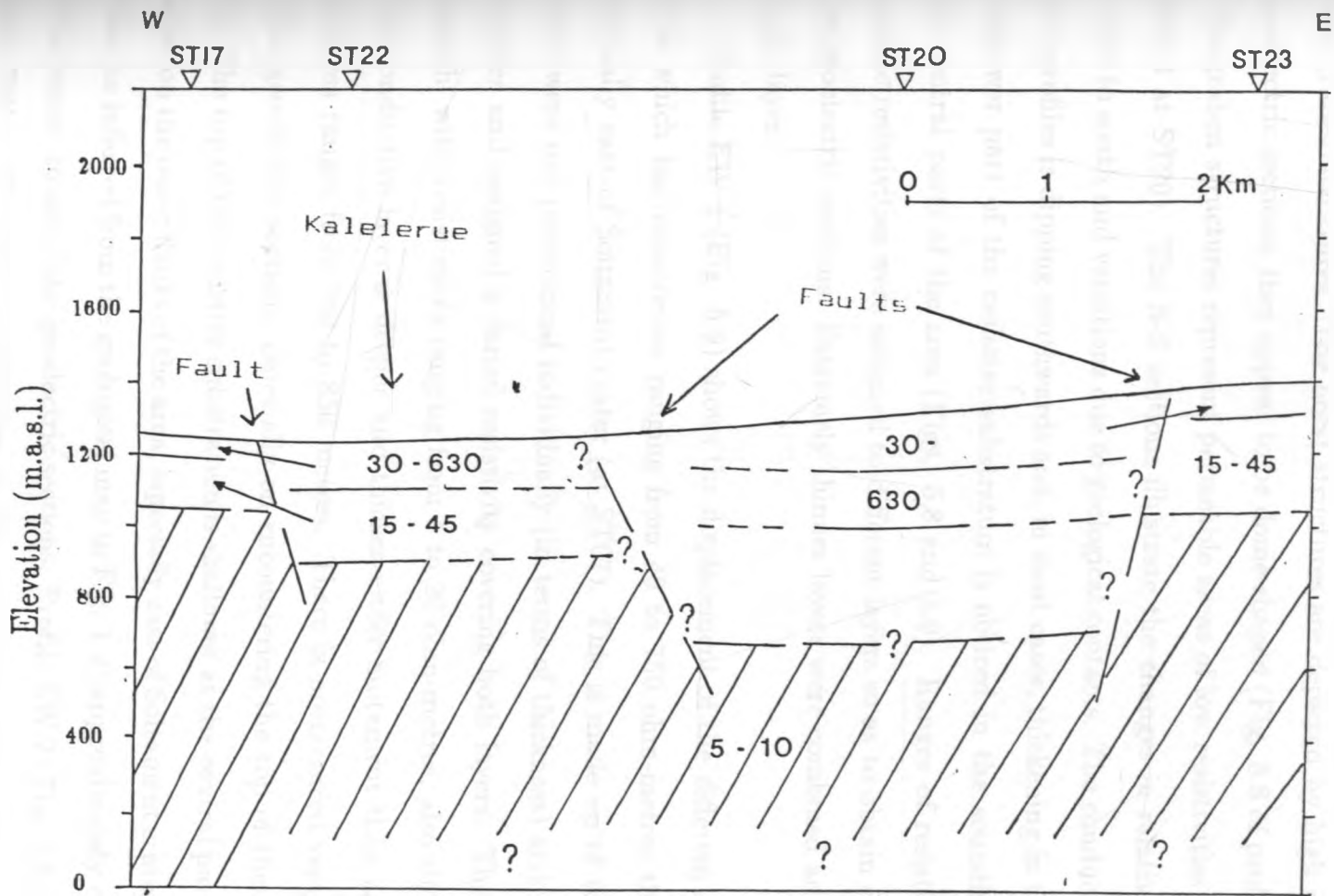
Figure 5.7   Geoelectric profile EW-3.

The geoelectric sections drawn across and along the geological strike, in E-W and N-S directions, respectively, are shown in Figures 5.6 to 5.13. The E-W profiles illustrate the effects of the lateral variations across the strike. These variations give an indication of fault zones. These profiles can also be interpreted as representing a series of horst and graben structures. The horst structures are depicted by high resistivities and, in geoelectric sections, they appear to be dome-shaped (Fig. 5.8 of profile EW 2 at ST05). The graben structures represent permeable areas of low resistivities (Fig. 5.7 of profile EW 3 at ST20). The N-S sections illustrate the changes in relative thicknesses from north to south and variations due to geological contacts. The conductive layer in all the N-S profiles is dipping southwards and, in most cases, thickening in that direction. The shallower part of the resistive substratum is noticed in the sounding stations within the central parts of the area (Figs. 5.8 and 5.9). Ranges of resistivities rather than specific resistivities were assigned to different layers so as to obtain continuity between the geoelectric sections. Extremely thinner layers were combined and interpreted as a single layer.

Profile EW 1 (Fig. 5.9) shows the displacement of the different layers. The upper layer which has resistivities ranging from 40 to 750 ohm-metres thickens eastwards, especially east of Soitamrut crater (at ST07). This is made up of two resistive layers which were not pronounced individually (in terms of thickness) and so were combined together and assigned a varied resistivity covering both layers. The conductive layer beneath, with resistivities ranging from 4 to 20 ohm-metres, also shows displacement. This conductive layer is deeper and thicker under Soitamrut than anywhere else. Its thickness ranges from 200 to 850 metres. There is pronounced vertical displacement of the geoelectric sections, especially on encountering the top of the substratum (Fig. 5.9). The top of the resistive substratum is shallower at the central parts of the area and deeper on the outer flanks of the area, especially east of Soitamrut crater. The location of faults (as inferred from the geological map in Fig. 1.2) approximately coincides with the displacement zones of the geoelectric sections. Profile EW 2 (Fig. 5.8) closely resembles profile EW 1. The layers are thicker on the outer flanks of the area and thinner at the central regions of the area. The first two layers are resistive and could be a continuous
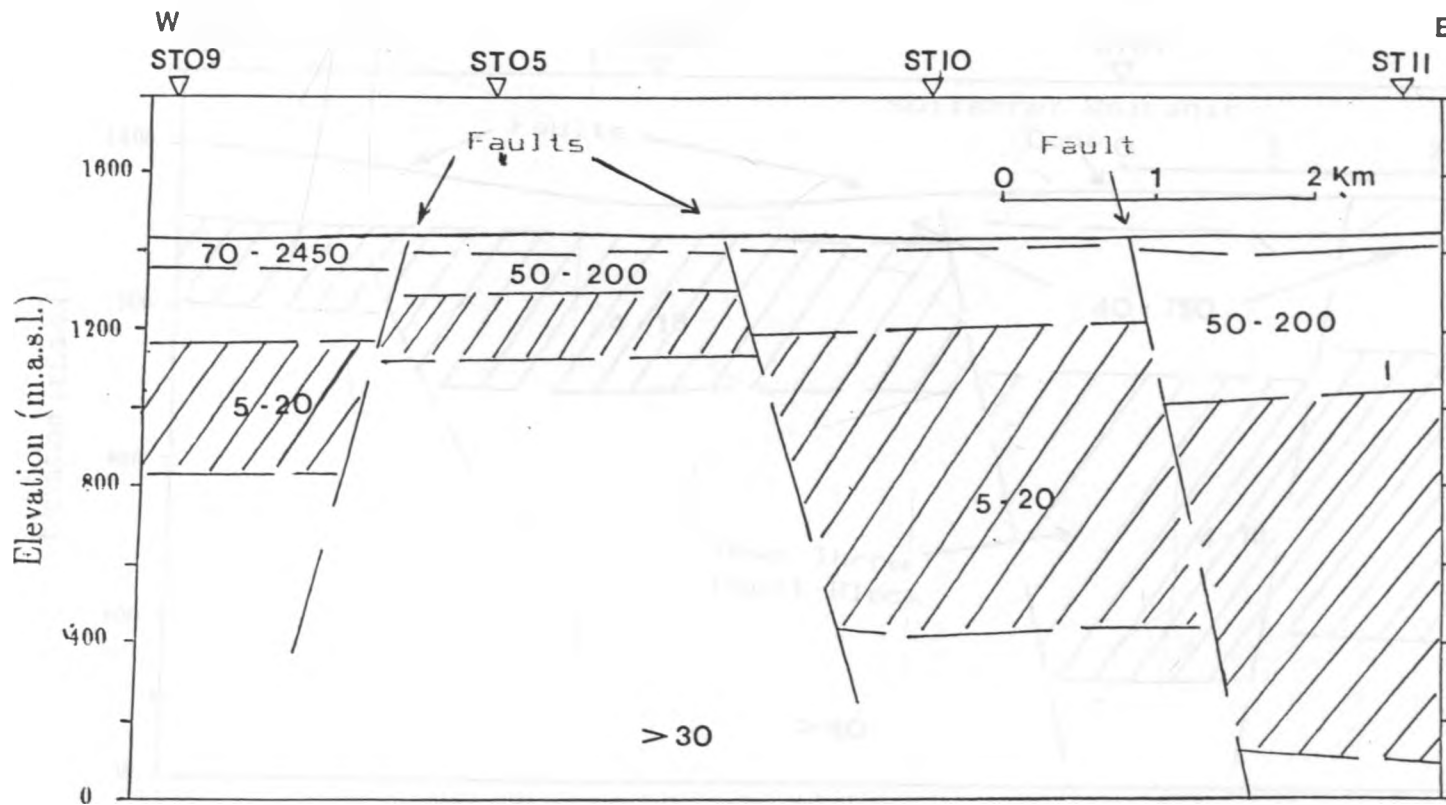
Figure 5.8   Geoelectric profile EW-2.
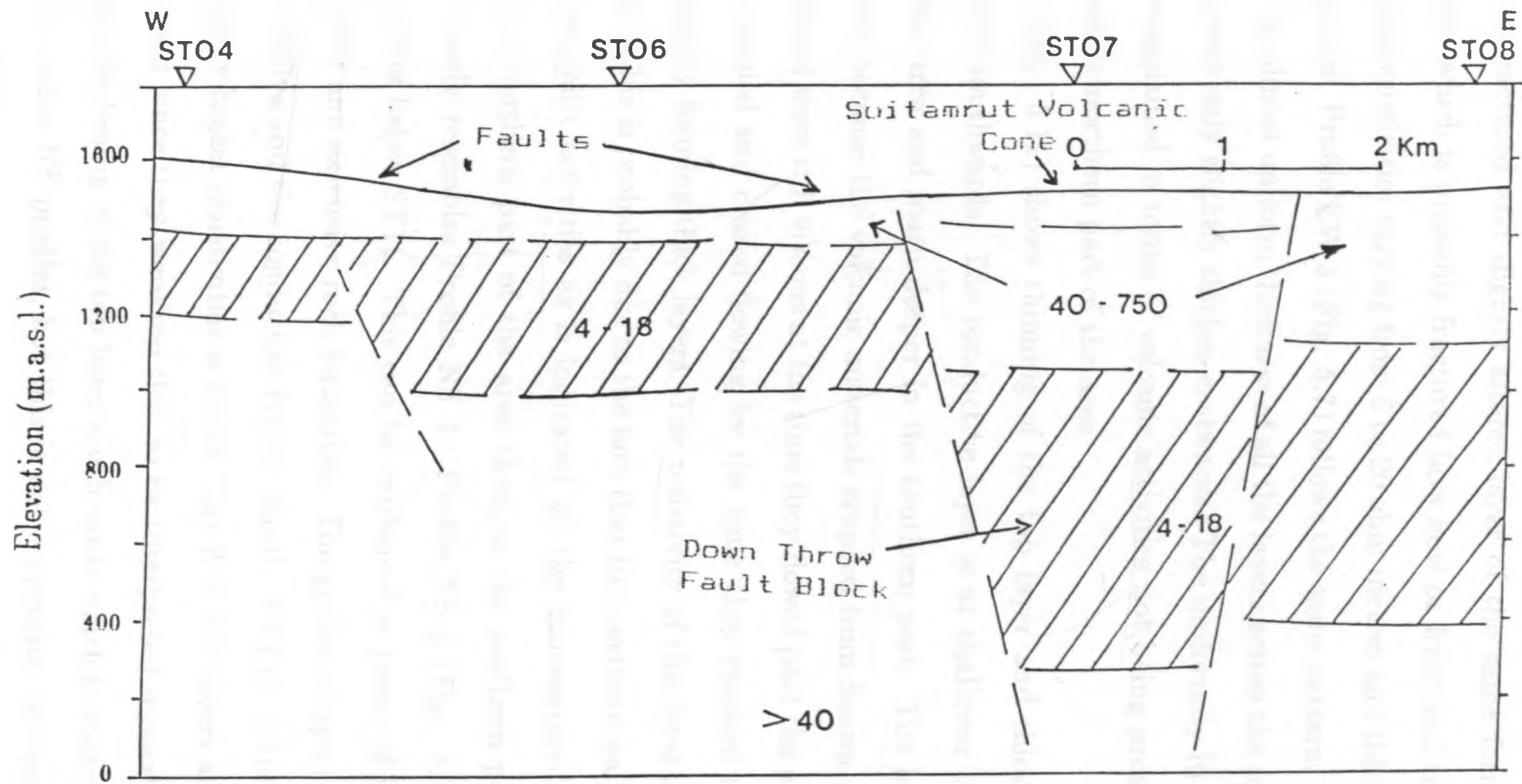
Figure 5.9   Geoelectric profile EW-1.

layer with little or no significant difference in their conductivities. The lower resistive layer is probably a fractured and slightly altered layer of the same formation as the upper resistive layer which is probably fractured lava flow or fractured trachytes. The conductive layer has resistivities varying from 5 to 20 ohm-metres and thickness ranging from 170 to 950 metres. Profile EW 3 (Fig. 5.7) follows the same pattern. Profile EW 4 (Fig. 5.10) shows an almost uniform thickness of all the layers across the southern parts of the area. The layers only slightly thicken eastwards. The uniformity in thickness for this profile can be explained in terms of volcanic activities not being prominent in the southern part as in the northern part of the area.

Profile NS 1 (Fig. 5.11) shows thinning of the top layer and thickening of the second resistive layer southwards. The conductive layer is at shallower depths at the northern part of the area and much deeper in the southern part. The layers thicken southwards probably because the volcanic materials erupted from Suswa volcano were flowing southwards and were still viscous at the time they flowed past the northern part of the area. They cooled and ceased flowing by the time they reached the southern part of the area, thereby forming thick layers. The resistivity of this layer also tends to increase southwards. This is probably due to the fact that the northern part of the area is associated with volcanic activities as is indicated by the concentrated geothermal manifestations in the northern part of the area than in the southern part. Profile NS 2 (Fig. 5.12) closely resembles Profile NS 1. Profile NS 3 (Fig. 5.13) shows a graben-shaped structure below ST11. This can be explained in terms of faulting and downwarping of a large and extensive rock formation. The graben-shaped structure is noted in both the resistive and the conductive layers. South of ST11, a horst structure characterized by slightly higher resistivities is noted. The first two layers at ST23 were combined into one layer since they were too thin to be interpreted separately. Profile NS 4 (Fig. 5.6) shows thickening of the top layer southwards which is contrary to what has been noted in the other NS profiles, but this is not surprising. Soitamrut crater, at ST07 (Fig. 5.6), is a volcanic centre and, therefore, there was probably a combined flow of volcanic material from Suswa and Soitamrut southwards. The second layer also thickens southwards. The conductive layer is thicker under Soitamrut crater, ST07 (Fig.
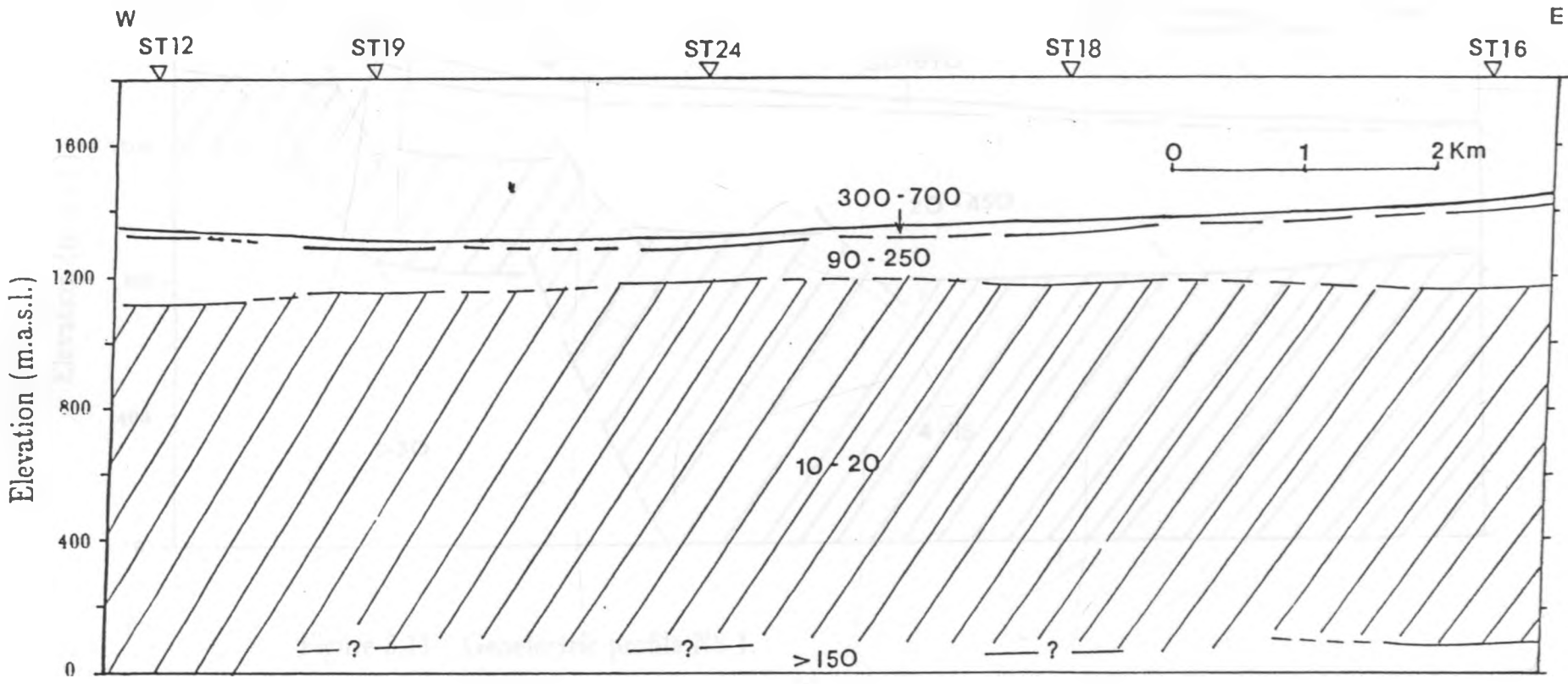
Figure 5.10   Geoelectric profile EW-4.
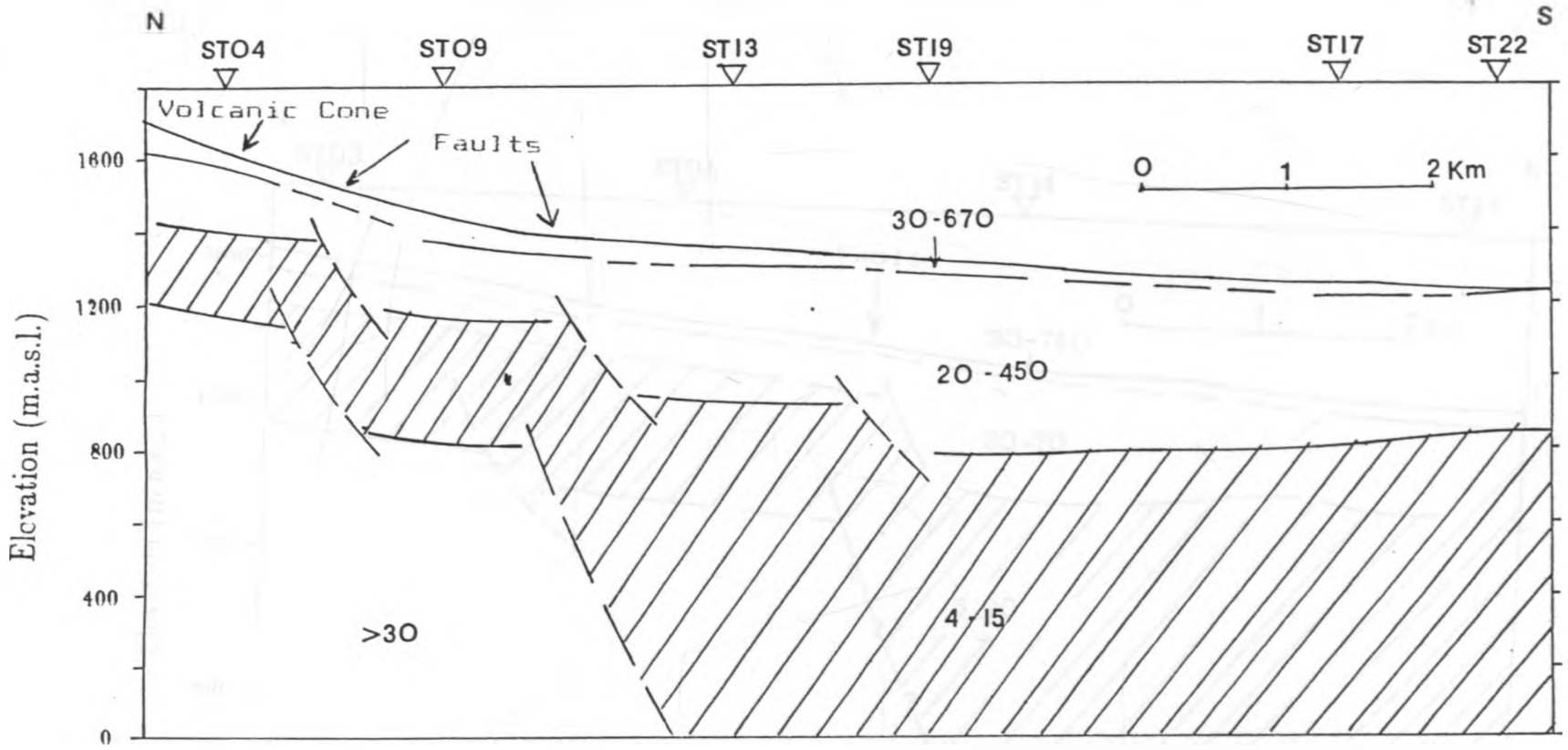
Figure 5.11 Geoelectric profile NS-1.
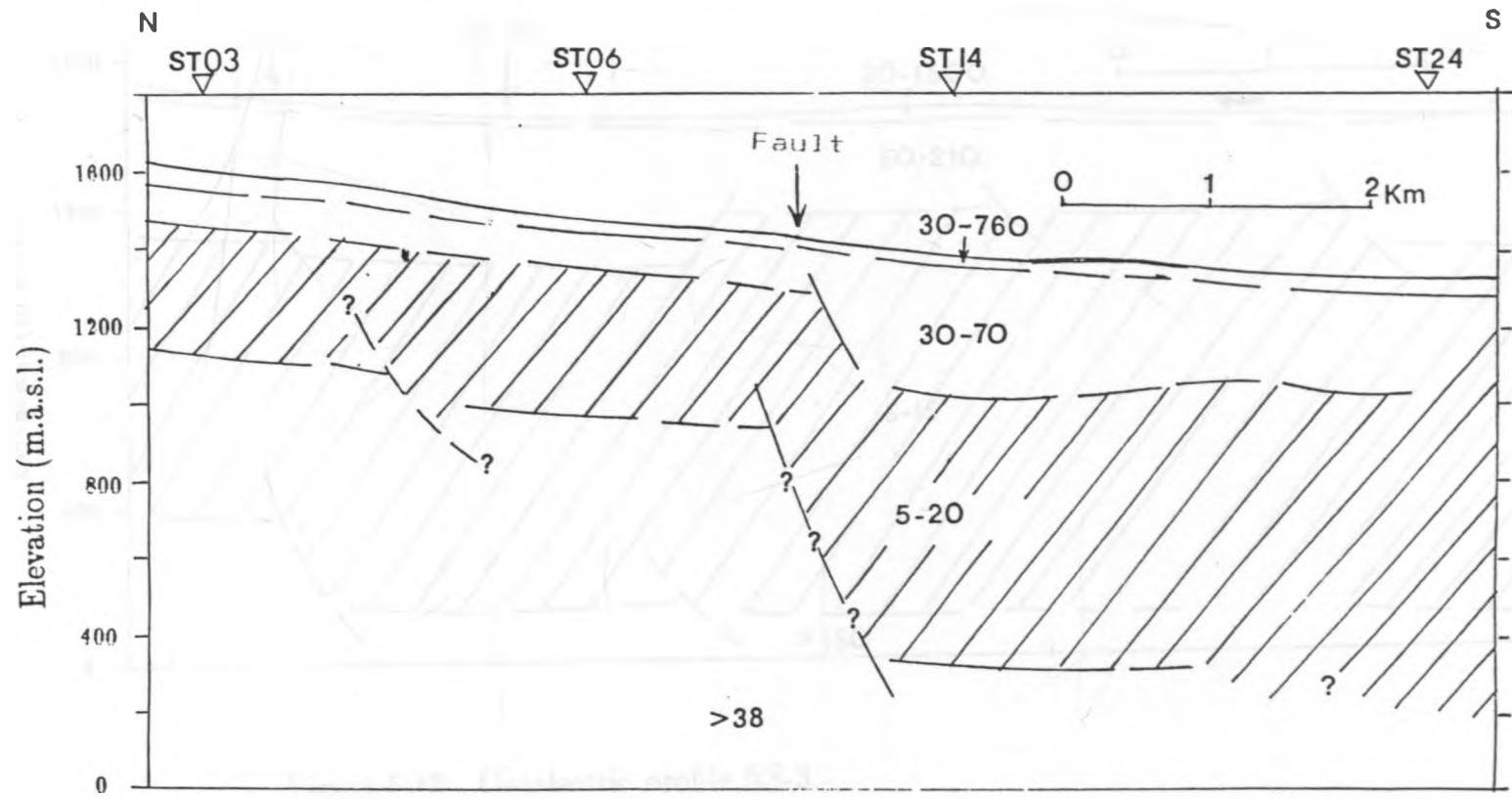
Figure 5.12   Geoelectric profile NS-2.
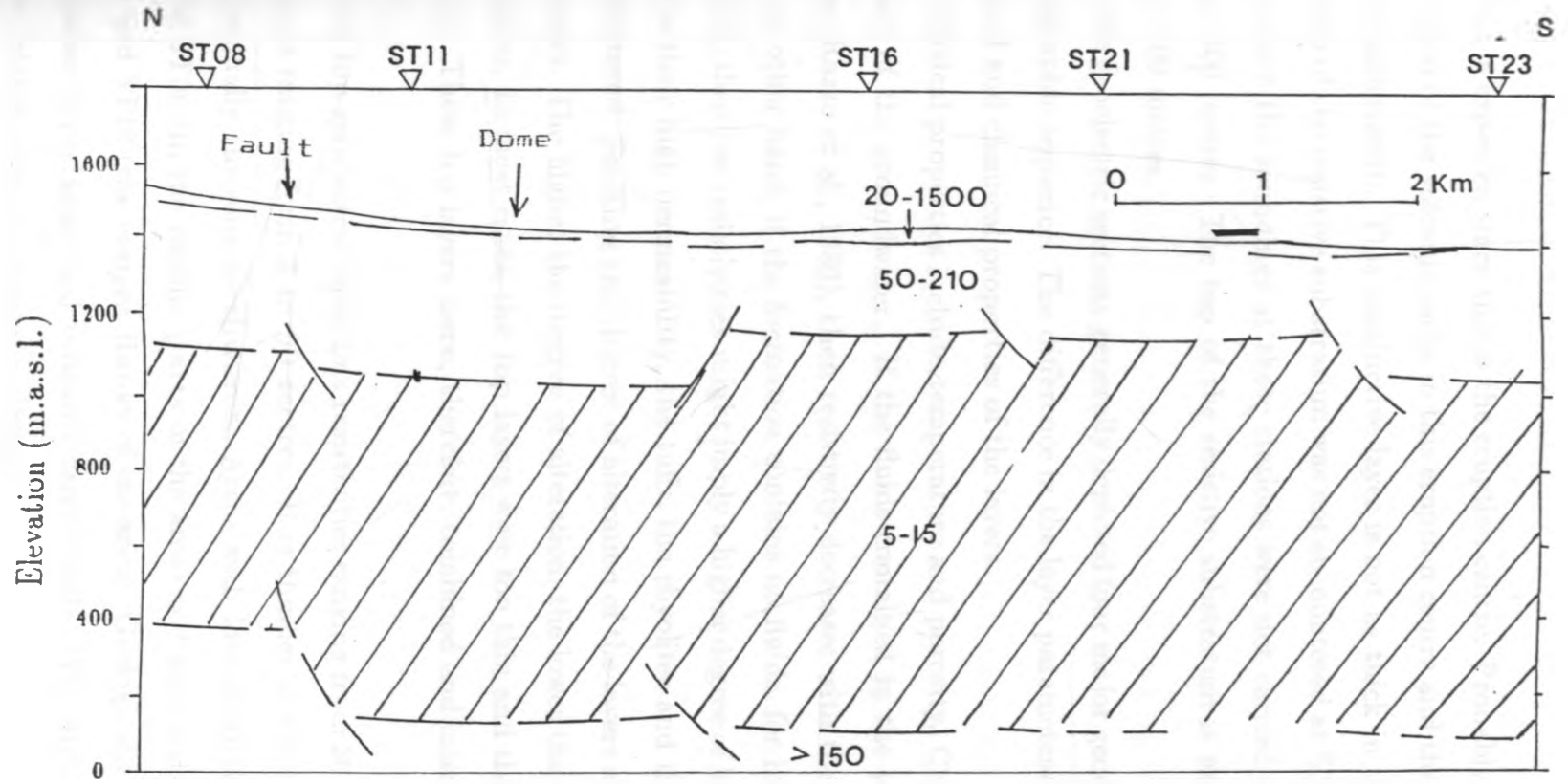
Figure 5.13   Geoelectric profile NS-3.

5.6), as is expected since this is the eruption centre. Probably there was fracturing and alteration of the volcanic rocks in this eruption centre and these materials formed thick layers underneath. This conductive layer is not as thick in the south as in the north. The top of the resistive substratum was not encountered at ST18, ST19 and ST24 (Fig. 5.10) since the soundings at these stations were not carried out to AB/2 values more than 1500 metres. The top of the resistive substratum is expected at depths greater than 1100 metres.

The geoelectric sections generally depicted four major geoelectric layers with similar stratigraphic sequence. The difference in the layer parameters is attributed to effects of physical and chemical properties of the layers.

Physical properties include temperature and porosity. Chemical properties include salinity of the groundwater. If the fluids contained in the permeable formations are saline (Razzo et al., 1980), then resistivity decreases with the increase in temperature. On the other hand, if the formation contains no fluids, for instance, the resistive substratum, then low resistivities might imply a higher degree of hydrothermal alteration. Due to their high permeability, the tuffs, the rhyolites and the pyroclastics are extensively altered. Faulting and degree of alteration of the layers affect the conductivities of the layers. The higher the degree of alteration, the lower the resistivity of a particular formation. In most cases, the top layers were too thin and their resistivities were overlapping. These top layers were, therefore, combined and interpreted as one geoelectric layer.

The top geoelectric layer has resistivities ranging from 30 to 2450 ohm-metres, and thickness ranging from 2 to 90 metres. It is thinner in the northern part of the area and gradually thickens southwards. Areas with low resistivities within this layer are around ST06 (in the middle parts of the area) and high resistivities are noted around ST15 and ST16 (the eastern flanks of the area). Geologically, this layer may represent the surface pyroclastics and volcanic derived soils. Very high resistivities are probably due to thicker zones of volcanic glasses.

The second layer has high resistivities but not as high as the first one. This layer has been interpreted as the resistive 'cap' rock and has resistivities ranging from 30 to 750 ohm-metres. There is probably a gradual decrease of porosity with depth of the

volcanics. Its thickness varies from 80 to 400 metres. The layer is thinner along the N-S trending middle regions of the area and thicker on the eastern flanks, especially east of Soitamrut crater, and in areas around Mount Kalelerue on the southern part of the area. Low resistivities are noted in the central regions of the area and high resistivities on the western and eastern flanks of the area. Geologically, this layer is probably made up of intercalations of trachytes, rhyolites and tuffs. Areas with higher resistivities than 100 ohm-metres within this layer are probably covered by Ol Doinyo Onyoke lava and areas with resistivities between 30 and 80 ohm-metres are probably of fractured lava materials.

The third layer is conductive with resistivities ranging from 4 to 26 ohm-metres. Low resistivity regions are noted in the northern part of the area (just south of Ol Doinyo Onyoke crater). These are areas with concentrated eruption centres and volcanic craters. Temperatures measured in boreholes drilled some decades ago were between 40^0 C and 100^0 C (Torfason, 1987). Geologically, this layer is composed of trachytes, ignimbrites, rhyolites, tuffs - all hydrothermally altered. Their conductivities are increased by the presence of clays, chlorites and oxides. The resistivities are lower when the rocks are more weathered and have an increased amount of the conductive minerals. Electrical resistivities less than 10 ohm-metres are typical of porous volcanic material saturated with highly conductive 'geothermal' waters. At the Broadlands geothermal areas (Risk et al., 1970), typical electrical resistivities are between 2 and 3 ohm-metres. The geothermal fluid has a chloride concentration of about 1200 ppm. Resistivities higher than 18 ohm-metres are too high to be caused by the presence of conductive alteration products such as clays. The thickness of this layer ranges from 50 to 500 metres. Notable areas with low resistivities are mainly along the N-S trending central regions, especially areas closer to what were previously eruption centres (Fig. 1.3).

The fourth and last layer is part of the resistive substratum. It is probably the top of the 'electric basement' since it has resistivities not as high as those expected of the 'true' resistive substratum. This layer has resistivities between 50 and 100 ohm-metres. These areas have lower resistivities probably due to thermal alteration of the basement rocks. Higher resistivities were noted on the outer flanks of the area. The

top of the resistive substratum was not encountered in some resistivity soundings that were not carried out to AB/2 spacing of more than 1200 metres. Geologically, this layer represents compact trachytes, basalts, phonolites and welded tuffs with a low degree of mineral alteration. Generally, the resistive substratum is constituted by volcanic rocks of older age. This layer is expected to be at depths of from 1100 to 2000 m. The shallower part of the resistive substratum is at ST10 where it was encountered at 1100 metres.

5.4 Other geophysical models

Several models have been proposed from the various geophysical surveys carried out in the eastern rift valley. Notable models are those from gravity, seismic, electromagnetic and magnetotelluric surveys.

Most gravity models have indicated an intrusive zone reaching within 2 kilometres of the surface in several places (Baker and Wohlenberg, 1971). The intrusive body is described as the source of heat in several places where steaming jets and other geothermal manifestations are noted. Fairhead (1976) interpreted the gravity high noted as being caused by partial infill of the rift by dense lavas overlain by an interbedded mixture of trachytes, phonolites and basalts. On the other extreme, the gravity high is thought as being caused by a linear dyke injection zone intruding the rift volcanics. A combination of these two models is more appealing as it is known to hold in several places within the rift, especially in geothermally active places. Such a model would fit quite well in the northern part of the study area. The rift shoulders which are associated with negative Bouguer anomalies have been interpreted as large thicknesses of low density lavas.

Seismic studies have revealed the existence of an anomalously low density, low velocity zone within the upper mantle region where the seismic S_n waves are attenuated, P_n waves are slowed and teleseismic travel-time delays are positive and correlate well with the low gradient of the regional Bouguer anomaly (Fairhead, 1976). The model assumed in seismic studies is the thinning of the lithosphere into the lower part (upper mantle) of the lithosphere. Such a model with a large volume of low density material

replacing the upper mantle readily explains the travel time delays associated with the rifting (Fairhead and Girdler, 1972). Aftab et al. (1986) have further suggested the existence of considerable basement topographic relief beneath an infill of sediments and volcanics. Beneath this layer, the crust appears to have relatively normal seismic velocities. At this level, it was suggested that there may be a 10 kilometre thick lens of low velocity material at the base of the crust.

Magnetotelluric models have been explained in terms of high temperatures and water saturation of the crust under the rift (Rooney and Hutton, 1977). Measurements have indicated a concentration of currents below the rift valley and apparent resistivities lie between 2 and 20 Ωm in several places. Very low resistivities have been explained in terms of high temperatures of subsurface fluids. The conductor was further interpreted to be at shallow depths below the rift.

Such models tie quite well with the resistivity models and they are important in correlating with the various models proposed from the varied geophysical methods. Certain parameters cannot be detected by a particular geophysical method, but another method can detect it. Therefore, to achieve a suitable model, an integrated geophysical survey is suggested in future work.

5.5 Hydrogeology

The study area has only a few boreholes which are widely spaced and were drilled more than two decades ago. Boreholes with comprehensive completion records which should include water struck levels, water rest levels, aquifer properties (transmissivity, actual yields and recovery periods) and lithological logs are the basis for understanding the hydrogeology of the area. These parameters are in most cases missing or are poorly recorded in the study area.

Hydrogeological studies on a regional scale in the rift valley from Lake Nakuru to Lake Magadi (within which the study area falls) has been conducted by the British Geological Survey and the Kenya Ministry of Energy and Regional Development. They noted that the area exhibits the hydrogeological features expected of a rift valley -

interflure system with lateral groundwater flows from the rift escarpment to discharge areas in the rift floor (i.e., Lake Naivasha), and axial groundwater flow away from the rift floor southwards. This model is modified by the presence of major faults which act as barriers to lateral flow, leading to longer deeper flow paths (Clark et al, 1990) and by the grid faulting in the rift floor which tends to align flow paths within the rift along its axis.

Due to inavailability of comprehensive completion data of boreholes, the hydrogeology of the study area is understood from the piezometric data point of view. These data assist in understanding the flow system of the area. On a regional scale, a piezometric map showed that groundwater flows from elevated areas to low lying discharge areas, and the flow occurring both laterally and longitudinally according to the rift geometry. In the area south of Suswa, the piezometric surface is deep (Table 5.1 (a)) and suggests that flow from the sides of the rift in this particular area is limited, and it is likely that the major rift faults act as low permeability barriers to flow across the rift. The model assumed in the area south of Suswa is therefore longitudinal flow paths within the rift floor from Suswa down the topographic gradient southwards (Fig. 5.14). According to the model, cold water enters the system from directions east and west of Suswa volcano. This water is heated up in the Suswa by the shallow magma body and, due to the fact that it is under high hydrostatic pressure from the cold water to the north, east and west, it flows southwards and down.

The general permeability of rocks in the rift valley is low although there is considerable variation depending on whether the rocks are fractured, weathered or are reworked volcanics. Aquifers are normally found in fractured volcanics, or along the weathered contacts between the different lithological units. Tectonic movements of the rift valley have important effects on aquifer properties, both on a small scale by creating the local fracture system which comprises many aquifers, and on the large large scale by forming regional hydraulic barrier or shatter zones of enhanced permeability. In the Suswa area, trachytes constitute a major proportion of the aquifer with permeability varying depending on whether the rock is fractured or weathered. The mean borehole yield for all aquifers around Suswa and Longonot for trachytic aquifers is 7.56 cubic metres per

hour. Boreholes in the area are shallow (less than 300 metres) and therefore the deep hydrological conditions of the area is not fully understood. However, the permeability is generally expected to fall with depth as a result of closure of fissures by the overburden stresses. Some of the boreholes drilled in the area did not actually produce water but steam and, after a few days, they caved in due to high sucking pressure from below (Table 5.1 (a)). Boreholes B1 and B2 indicated high anomalous temperatures when they were drilled. These boreholes are close to Suswa volcano and probably received water directly from Suswa where the geothermal system has its heating source.

Table 5.1 (b) shows the geological logs of two boreholes, one which is dry while the other is productive. Two boreholes drilled right at the escarpment were dry and were drilled with much difficulty as the drilling bit got stuck often.

5.6   Summary

An attempt has been made to try and correlate the geoelectric characteristics of the different layers obtained from resistivity results, the hydrogeological information obtained from boreholes, the iso-resistivity contour maps and the geology of the area. This attempt has, however, been limited by lack of sufficient reliable borehole data in the area. Only a few boreholes are available and these were drilled only to depths not exceeding 300 metres. Therefore, the correlation made between the few borehole logs and the geoelectric sections may not be quite reliable. The resistivity of a specific rock material is dependent on its chemical and physical properties and the surrounding conditions. This implies that a different rock type can be correlated to a geoelectric layer which is not representative of the actual situation. Fracturing and alteration due to thermal waters or other chemical effects may also impose a totally different geoelectric characteristic from what is expected of fresh rock.

The geology of the area has been studied by Randel and Johnson (1970), Baker (1958), Thompson and Dodson (1964), Kagasi (1983) and, more recently, by Baker et al. (1987). A geological map at a scale of 1:250 000 and geological sections have also been presented by Randel and Johnson (1970). The stratigraphic sequence of the area

Table 5.1 (a)   Records of boreholes drilled in the vicinity of the study area

LOCATION	TOTAL DEPTH(M)	TEMPERATURE(^{0}C)	COMMENTS
Ewaso Kedong village B1	originally 300. now 270	70. temp. gradient 200^{0}C/km	dry borehole east of the area
South of Suswa B2	30 - 40	emittedsteam when drilled	now dry and caved in
South-eas of Suswa B3	30 - 40	emitted steam when drilled	now dry and caved in
Suswa village B4	280	not measured	dry and caved in

Table 5.1 (b)   Records of borehole P-23 east of the area and P-27 north of Kalelewe Hill, southern part of the area (Courtesy of M.O.W.D.)

P-23	P-27
0 - 40 m Clay and volcanic gravel 40 - 50 m Lava 50 - 66 m Tuff 66 - 74 m Lava 74 - 78 m Reddish lava 78 - 82 m Clay and detritus 82 - 141 m Lava COMMENTS W.S.L. = 74 m and 102 m Tested yield = 2.14 m^3/hr Aquifer composed of reddish lava, probably trachytes and tuffs.	0 - 14 Soil and clay 14 - 27 m Broken volcanic rock 27 - 37 m Red gravel and volcanic rock COMMENTS B/H blew steam during the day and sucked air during the night.
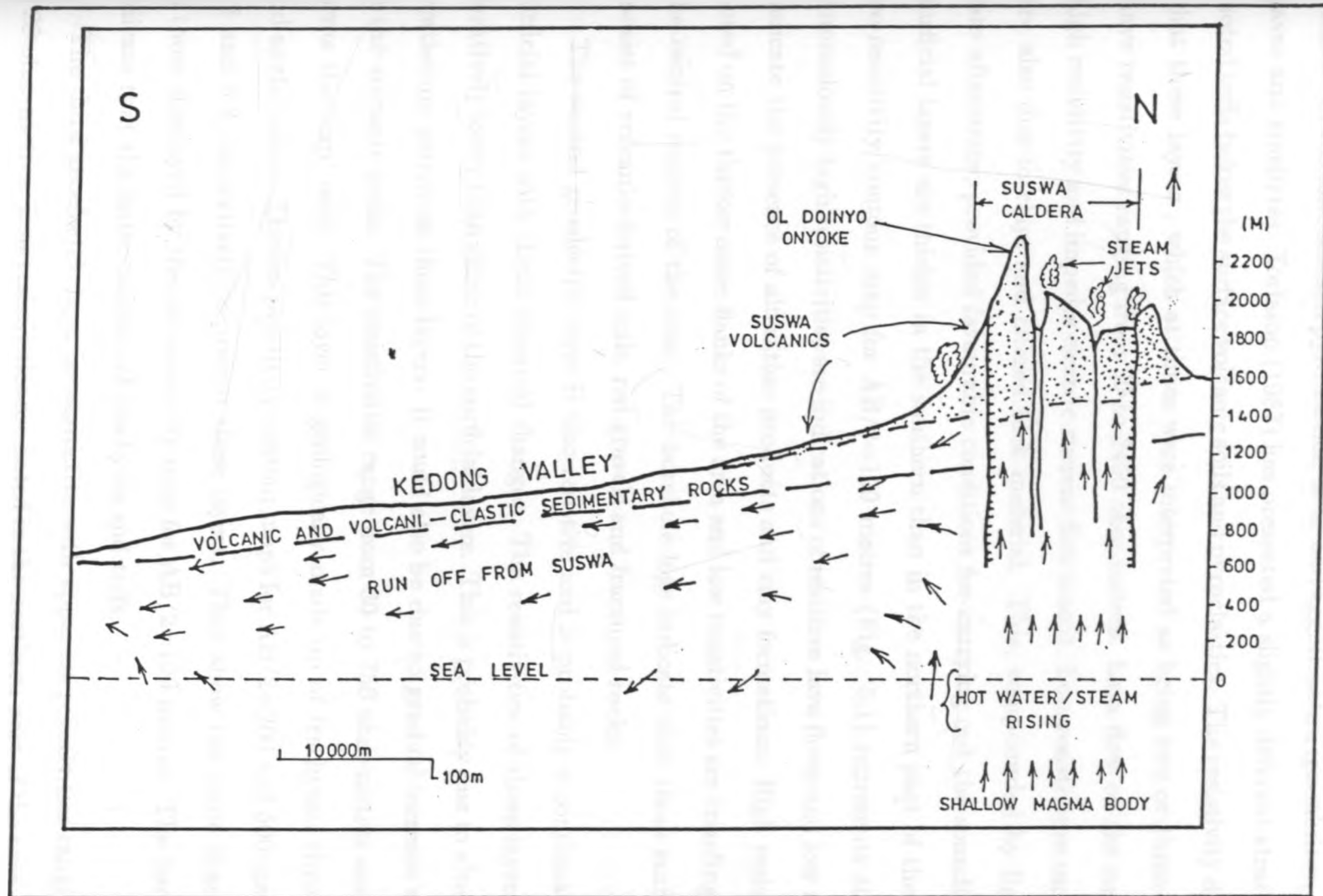
Figure 5.14   The hydrogeological model of the area south of Suswa volcano.

consists of volcanic soil and pyroclastics, lavas and agglutinates, ignimbrites, fine grained lavas and trachytes. Torfason (1987) has presented a slightly different stratigraphy. He noted tuffs below the surface volcanic soils and pyroclastics. The resistivity data indicate that these layers, which at times were interpreted as being two or three in number, have resistivities ranging from 30 to 2450 ohm-metres. Lava flow on the surface shows high resistivity and impedes electric current flow into it. Low resistivities on the surface are also due to clays and altered rock material. This, compounded by light rains in late afternoons, provided favourable conditions for carrying out the soundings. These surficial layers are thicker in the southern than in the northern part of the area. The iso-resistivity contour map for AB/2=100 metres (Fig. 5.1) represents these layers. Anomalously high resistivities are indications of resistive lava flows and low resistivities indicate the presence of alteration products and clay formations. High resistivities are noted on the thicker outer flanks of the area and low resistivities are trending N-S along the central regions of the area. The borehole logs indicate that these surficial layers consist of volcanic-derived soils, red gravels and fractured rocks.

The second geoelectric layer is also resistive and is probably a continuation of the surficial layers with slight chemical changes. The resistivities of these layers are comparatively lower than those of the surficial layers. This is probably due to alteration and weathering action on these layers. It could also be due to gradual increase of porosity in the volcanic rocks. The resistivities range from 30 to 750 ohm-metres and the layer forms the 'cap' rock. This layer is geologically made up of trachytes, rhyolites, tuffs and agglutinates. The iso-resistivity contour maps for AB/2=200 and 500 metres (Figs. 5.2 and 5.3, respectively) represent these layers. They show the same characteristics as those displayed by the iso-resistivity map for AB/2=100 metres. The borehole logs indicate that the latter consists of trachytes and tuffs.

The third geoelectric layer is conductive with apparent resistivities ranging from 4 to 28 ohm-metres. Low resistivities are noted in the northern part of the area and along a N-S direction in the central regions. The iso-resistivity contour map for AB/2=1000 metres (Fig. 5.4) displays these features clearly. The N-S trending low resistivities in the centre may be due to an underground water channel. Geologically, this layer consists of

alteration products of highly permeable tuffs, trachytes and ignimbrites which have been altered and their resistivities are further lowered by the presence of conductive minerals like chlorites, oxides and clays. Resistivities of less than 5 ohm-metres are typical of the porous volcanic materials saturated with highly conductive geothermal waters (Bibby et al., 1984). For example, at the Broadlands geothermal areas in New Zealand, where the geothermal fluids have chloride concentration of about 1200 ppm, typical resistivities are between 2 and 3 ohm-metres (Risk et al., 1984). Resistivities between 10 and 13 ohm-metres represent rhyolites as well as tuffs and trachytes showing extensive alteration. Deep trachytes found within 500 and 1000 metres are still altered as their resistivities are still around 15 to 25 ohm-metres. Resistivities higher than 20 ohm-metres are too high to be caused by the presence of conductive fluids. These could probably be thermally altered rocks whose low resistivities could be caused by the presence of alteration products such as clay. It has been noted that thin layers (5 to 40 m) of pyroclastics intercalated with several layers of ash are commonly associated with active fumaroles (Torfason, 1987), probably as the younger lavas on top are more compact and impermeable. This layer is suspected to be occuring within the conductive layer. The geological sections indicate that rhyolites and tuffs prevail at depths between 500 and 1000 metres. The hydrogeological model indicates that this layer is the aquiferous zone. It occurs at depths between 100 and 220 metres in the northern part of the area and deepens gradually southwards to more than 500 metres. Its thickness does not, however, exceed 900 metres.

The fourth and last layer is resistive and, as such, has been termed the resistive substratum or 'electric basement'. Its resistivity ranges from 50 to 640 ohm-metres. It can be stated here that only the top part of the resistive substratum has been encountered in this investigation. The resistivities are moderate and not as high as those expected of a true resistive substratum. The depth to the resistive substratum is between 1000 and 1500 metres, but the interpreted thicknesses place it between 1100 and 2000 metres. This layer is manifested in the iso-resistivity map for AB/2=2000 metres shown in Figure 5.5. This map is characterized by moderate to high resistivities which could be due to thermal alteration of the basement rocks. The higher the degree of

alteration, the lower the resistivities of a particular formation. These locations show lower resistivities compared to the others. The geological sections indicate that basalts, trachytes, welded and breciated tuffs, with a low degree of alteration, make up the resistive substratum. The true resistive substratum has resistivities over 120 ohm-metres (Geotermica Italiana, 1988).

Generally, beneath the surface pyroclastics and volcanic-derived soils, the first 2000 metres consist of rhyolites, ignimbrites, basalts and trachytes with intercalations of tuffs. The resistivities vary according to the degree of alteration, the amount, temperature and concentration of geothermal fluids. On the other hand, if the formation contains no fluids, for instance, the resistive substratum, then low resistivities might imply a higher degree of thermal alteration as the predominating factor.

Chapter 6

DISCUSSION AND CONCLUSIONS

6.1   Discussion

The analysis and interpretation in this study were based on the resistivity data obtained earlier by the M.O.E.R.D. and the present author. These data are, obviously, not sufficient to draw final conclusions. Rather, a total evaluation of the geothermal potential of a particular area, as recommended by Isherwood and Mabey (1978), should include

(a) Geologic data:

These should include borehole data and the tectonic regime of the area. Known Geothermal Resources Areas (KGRAs) commonly occur near the margins of basins in areas that contain Cenozoic volcanic rocks and active faults. The borehole logs, on the other hand, greatly improve the interpretations of resistivity data, especially in terms of eliminating equivalence that may otherwise cause ambiguities in interpretations.

(b) Data on temperature, chemistry and discharge rates of known thermal springs and wells:

Thermal wells and springs are found in most KGRAs. The chemistry of thermal water is used to appraise potential utilization problems. Reservoir temperatures are calculated using Silica and Sodium - Potassium - Calcium chemical geothermometry. Reservoir temperatures are used to access the expected geothermal energy.

(c) Geophysical data, usually including gravity and magnetic maps and shallow and deep probing electrical surveys:

The usual objective of electrical surveys is to determine if a resistivity anomaly exists and to define the approximate extent of the anomaly. Gravity data are used to estimate the thickness of the basin fill, the gross structure of the basin, including the location of major normal faults that are important in understanding the geothermal system. Permanent magnetic anomalies are associated with regional features.

(d) All engineering and economic data available relating to geothermal resources or geothermal development:

These should include the socio-economic impact such a project would have on the local communities and the feasibilities of erecting engineering structures within the site.

The present area of study falls only short of meeting these requirements. The area is within the Rift Valley of Kenya which is a basin margin with active faults. The features present in the area are almost similar to those noted at the productive Olkaria geothermal fields to the north of Suswa crater. These features include the fault trends, the subsurface morphology and geology. The volcanism in the Suswa area does not span a long time, since the earliest lava identified from the volcano date back to the Upper Pliocene Period (Kagasi, 1983; Baker et al., 1987). The basaltic and alkaline volcanism produced broad regional doming, the main one being Suswa crater. The volcanic activity within Suswa still continues as is evident from the steaming jets and the active fault zones within the area. Numerous eruption centres are common in the northern half of the area. These eruption centres are aligned to form a volcanic line or zone (Tandamara) connecting Suswa and the more active Olkaria geothermal fields.

Several thermal springs and wells are present at the extreme northern part of the area. Comprehensive data are not available on the reservoir temperature corresponding to these springs, but they have been estimated to be below 80^0 C (Geotermica Italiana, 1988). Steaming fumaroles with hissing sound, which indicate that the reservoirs are at high pressures, are within the slopes of Ol Doinyo Onyoke crater. Surface geothermal manifestations are good indications of the size of the heating source and its temperatures. Steam is normally emitted through permeable fractures in the pyroclastics and the trachytes within the Ol Doinyo Onyoke crater. The Olkaria fields have steaming jets with temperatures of over 150^0 C. There is only one fumarole in the south of Ol Doinyo

94

Onyoke crater with temperatures above 90^0 C, but emitting little steam. Open fissures exist in the southern slopes of the crater and, in some parts, steam is emitted under high pressure from these fissures. The general impression is that the geothermal activity in the south of Suswa area is less than in the Olkaria region. The probable reason for these diverse differences is that some of the magma responsible for heating the Olkaria fields vented northwards from Suswa crater, where there was an easy passage. This, therefore, depleted the Suswa reservoirs of the heating source. This is supported by the fact that there seems to be a connecting volcanic axis or zone (Tandamara) between Suswa and Olkaria fields. The eruptive centres are aligned from Suswa to Olkaria and the distribution of surface geothermal manifestations are also elongated in the same direction. On the other hand, no hot spring or well was noted on the southern half of the area. Absence of steaming springs at the surface in the southern part of the area, despite the presence of geothermal waters beneath, suggests the occurrence of impermeable layers, consistent with clay mineralization of the surface layers. Surface alterations indicate that parts of the central region of the area were also steaming not so long ago. These surface alterations include clays, the presence of sulphur and altered lavas (rhyolites and trachytes).

The low temperature and high pressure geothermal reservoirs at the slopes of Ol Doinyo Onyoke are probably within the plateau trachytes and other Pleistocene formations. The N-S trending fractures cutting the lower part of Suswa and Ol Doinyo Onyoke volcanoes (the underlying trachytes) offer good permeability which is further increased along contacts of lava and pyroclastics. These features are the same as those noted in Olkaria fields. High temperature geothermal reservoirs like those in Olkaria are commonly bordered by low temperature geothermal areas like Suswa. Temperatures do not normally exceed 150^0 C in low temperature areas but are between 200 and 350^0 C in high temperature areas (Gudmundsson, 1982).

The resistivity data alone could not provide the above information on the geothermal characteristics of the area. The resistivity of a specific rock material is varied depending on its chemical and physical properties and the surrounding conditions. The chemical nature of a rock is not discerned by the resistivity data alone. Geothermally

productive areas are characterized by resistivity lows relative to the surrounding formations. The average formation resistivity at Cerro Prieto geothermal fields (Wilt et al., 1981), for example, is 2.0 ohm-metres or less, increasing to 4.0 ohm-metres within the zones enclosing the production intervals. Apparent resistivities noted at the slopes of Ol Doinyo Onyoke were generally around 10 ohm-metres. The least noted apparent resistivity was 4.0 ohm metres at ST02. Analysis carried out at Cerro Prieto fields suggested that the increase in resistivities was primarily due to the formation of reduced porosity zones caused by hydrothermal metamorphism. This could also be the reason for the increased resistivity around Olkaria fields and Ol Doinyo Onyoke crater. Formation resistivity was also noted to reduce when the temperatures reached a certain level at Cerro Prieto fields (Razzo et al., 1980). Nevertheless, an increase in the porosity of the formation or in salinity of the fluids has the same effects. In many geothermal areas such as Cerro Prieto fields in Mexico, Battazor in Nevada, USA, and Olkaria in Kenya, near surface resistivity lows appear to correspond to deeper geothermal reservoirs. Resistivity lows are associated with most geothermal systems and often the extent of the resistivity low is the only evidence available to indicate the possible extent of the geothermal anomaly. Low resistivities occur also due to the water table being close to the ground surface (Bibby et al., 1984). In Suswa area, the northern part of the area is characterized by resistivity lows, especially at the slopes of Ol Doinyo Onyoke while all the southern half can be outrightly dismissed as an area of geothermal potential since it is characterized by resistivity highs and absence of any surface geothermal manifestations. Low resistivities in the north could be indicative of conductive (saline) geothermal fluids while low resistivities in the south could be due to clay mineralization of the surface formations. The areas of groundwater and geothermal potential can, therefore, be demarcated as the northern half of the area. A geothermal reservoir, generally, corresponds to a low resistivity zone because of a combination of various characteristic factors - porosity, salinity and temperature. However, a low resistivity anomaly does not necessarily signal a geothermal reservoir. It is difficult to isolate which of these factors is the dominating one unless an integrated study is done. The other characteristic factors which also influence resistivity but can be discerned by

gravity are fracturing and alterations due to chemical effects and/or thermal energy. These latter factors may impose different geoelectrical characteristcs from what is expected of fresh formations. Because variations of resistivity and thickness for a given layer might only be due to differences in the degree of alteration, it could be improper to correlate along the cross-sections one geoelectrical horizon to a well defined lithological formation. This limits the use of borehole logs as means of correlation with geoelectric sections. This is further compounded by the fact that the ratio of 1:1 for probing depth versus AB/2 spacing is not valid for large AB/2 separations. A totally different geoelectrical layer might, therefore, be wrongly correlated to a well defined lithological layer obtained from borehole logs. This limitation necessitates the use of an integrated study by different geophysical methods and geochemical analysis.

Gravity and magnetic data are important in supplementing the resistivity data. The gravity data are used to estimate the thickness of the basin fill and locations of major faults that are important in understanding geothermal systems. Geothermal-related anomalies in the basins are most commonly residual gravity highs that are interpreted to reflect densification of porous sediments, structural highs or anomalous geometry of fault zones. Gravity studies within the eastern rift have resulted in various models being proposed. Notable ones are by Baker and Wohlenberg (1970) and Fairhead (1976). The former interpreted the positive residual anomaly which parallels the axis of the rift as an intrusion zone reaching within 2 kilometres of the surface in places. Fairhead (1976) interpreted the gravity high in two various extremes and then considered a combination of the two. First, the gravity high was assumed to be caused entirely by partial infill of the rift by dense lavas overlain by an interbedded mixture of trachytes, phonolites and basalts. The computed thickness of the infill was estimated to 2.5 kilometres. Secondly, the gravity high was assumed to be caused entirely by a linear dyke injection zone intruding rift volcanics. The depth to the top of the model intrusion zone was assumed to be 3.5 kilometres which agreed well with seismic refraction studies. A combination of these two models, which is more appropriate and satisfies the gravity data, incorporated the dyke injection and rift infill by dense lavas. Geothermal anomalies relate to regional magnetic lineaments and zones suggestive of structures within the basement (Isherwood

and Mabey, 1978). Future work should also incorporate magnetic measurements so that a refined model can be achieved.

6.2 Conclusions

6.2.1 General

Potential groundwater zones are expected within weathered and/or fractured volcanics or contact zones of different lithological units. Geothermal targets are also located in such formations, but they further require a resistive 'cap' rock necessary to contain great pressures caused by steaming fluids. Low resistivities are generally associated with weathered and fractured formations, formations containing water or fluids, conductive minerals, clayey formations and high temperature zones. An integrated geophysical, geochemical and geological investigations gives an insight on the influencing parameter(s) in specific areas.

6.2.2 Groundwater potential

The groundwater potential of the area south of Suswa volcano is generally moderate. Successful boreholes within the vicinity of Suswa have a mean yield of about 7.56 cubic metres per hour and out of 48 boreholes drilled, only 4 were dry. Successful boreholes are drilled away from the escarpment where the major faults act as barriers for groundwater flow. The average depth of the boreholes is about 280 metres and water is struck from 200 to 280 metres. Shallower boreholes are drilled close to the volcano where the water table is shallow. But such boreholes produced steam and dried after a few days. The aquifer is composed of weathered and/or fractured trachytes and tuffs, and also at contact zones of the different volcanic units. These aquifers were depicted by low resistivities ranging from 4 to about 20 Ωm. This corresponds to the middle conductive layer underlain by the resistive substratum. The groundwater flow pattern is such that lateral flows from the escarpment to discharge areas on the rift floor, and axial flow away from the rift floor, leads to longer, deeper flow paths along grid faults and the rift axis southwards. The implication here is that boreholes on the southern part of the

study area drilled to depths of up to 350 metres should realize better yields than those in the northern part. This is so because boreholes in the south should trap most of the water from Suswa and from the escarpments. However, much deeper boreholes might be unsuccessful since permeability is expected to fall rapidly at greater depth as a result of closure of fissures by overbudden stresses.

6.2.3   Geothermal potential

Known Geothermal Areas (KGRA's) have been noted to have resemblance to each other (Isherwood and Mabey, 1978) and are therefore guidelines to potential geothermal areas. The geothermal potential of the study area was understood from geophysical studies compared with those carried out at Olkaria fields. The studies were initiated because the area has a considerable concentration of high temperature and thermal upflow proved by the geothermal manifestation, for example, steam jets, fumaroles and altered ground. Potential geothermal areas are normally within or adjacent to large ring structures, for example, Olkaria and Suswa caldera.

Chemical data collected in Suswa area (Clark et al., 1990) have suggested that much of the groundwater and fluids in the Suswa area is relatively local in origin, and by the use of stable isotope data, some of the water has been traced to Lake Naivasha. Further geochemical analysis of the geothermal fluids at Suswa indicates that all the fluids can be explained in terms of a mixing series of rift wall meteoric water and water from Lake Naivasha. This implies good reservoir recharge necessary for geothermal fields.

The extreme northern parts of the study area, within the caldera and just on the slopes of Ol Doinyo Onyoke crater, are considered potentially active geothermal areas. These areas have a concentration of steaming jets and fumaroles and the resistivity studies indicate low resistivities (4.0 to 10 Ωm) within these zones. The resistivity values are expected to be much less within the inner caldera.

Such low resistivities may not be entirely due to the high temperature geothermal fluids, but at least they are indicative of a probable zone for further exploration. It is therefore recommended that the area within the Suswa caldera should be further studied and a refined model constructed. Such studies should include integrated geophysical

methods and chemical and geochemical analysis of the fluids in and around the Suswa caldera. Resistivity studies alone have resulted in the identification of three geoelectric layers:-

(i) the resistive upper layer forming a 'cap' rock necessary for a geothermal area,

(ii) the middle conductive layer of low resistivity. This layer, which was interpreted as weathered and/or fractured trachytes and tuffs, forms the aquiferous zone where potential groundwater and geothermal targets are located, and

(iii) the top part of the basement also referred to as the resistive substratum.

The above can be further proved and refined by integrated geophysical studies.

REFERENCES

AFTAB, K., MAGURE, P., HENRY, B., and HIGHAM, M., 1986, KRISP '85, An international seismic investigation of the Kenya Rift, **Geology Today 1986**, 139-144.

BAKER, B. H., 1958, Geology of the Magadi area, Geological Survey of Kenya Report No. 42.

BAKER, B. H., MITCHELL, J. G., and WILLIAMS, L. A. J., 1987, Stratigraphy, geochronology and volcano-tectonic evolution of the Kedong-Naivasha-Kinangop region, Gregory Rift Valley, Kenya, (Unpublished).

BAKER, B. H., MOHR, P. A., and WILLIAMS, L. A. J., 1972, Geology of the eastern rift system of Africa, Geological Society of America, Special Paper No. 136.

BAKER, B. H., and WOHLENBERG, J., 1971, Structural and evolution of the Kenya Rift Valley, **Nature 229**, 538-542.

BALFOUR, BEATTY and CO., 1968, Electrical Resistivity Survey in Kenya Rift Valley, Unpublished report to the East African Power and Lighting Co. Ltd.

BANWELL, C. J., 1970, Geophysical techniques in geothermal exploration, **Geot- hermics 2, special issue 2**, 781-798.

BARONGO, J. O., 1989, Application of transient airborne electromagnetic and ground resistivity methods to geological mapping in tropical terrains, Ph.D. thesis, McGill University.

BHATACHARYA, B. B. ,and SEN, M. K., 1981, Depth of investigation of collinear electrode arrays over homogeneous anisotropic half-space in Direct Current methods, **Geophysics 46**, 768-780.

BHATACHARYA, P. K., and PATRA, H. P., 1968, Direct Current Geoelectric Sounding, Elsevier Publishing Co., Amsterdam.

BHOGAL, P. S., 1978, The Electrical resistivity method of geophysical prospecting and its application to Geothermal exploration in the Rift Valley of Kenya, Ph.D thesis, University of Nairobi.

BIBBY, H. M., DAWSON, G. B., RAYNER, H. H., STAGPOOLE, V. M., and GRAHAM, D. J., 1984, The structure of the Mokai geothermal field based on geophysical observations, **Journ. of Volc. and Geothermal Res. 20**, 1-20.

CATALDI, R., LAZZAROTTON, A., MUTTLER, P., SQUARCI, P.. and STEFANI, G., 1978, Assessment of the Geothermal potential of central Tuscany, **Geothermics 7**, 91-131.

CLARK, M. C. G., WOODHALL, D. G., ALLEN, D., and DARLING, G.. 1990, Geological, volcanological and hydrogeological controls on the occurrence of geothermal activity in the area surrounding Lake Naivasha, Kenya, M.O.E.R.D./B.G.S. Technical Co-operation, 87-135.

COMPAGNIE GENERALE DE GEOPHYSIQUE., 1963, Abaques de sondage electrique, E.A.E.G., The Hague.

COMPAGNIE GENERALE DE GEOPHYSIQUE., 1963, Master curves for electrical sounding, 2nd Ed., E.A.E.G., The Hague.

DOBECKI, T. L., and ROMIG, P. R. 1985, Geothermal and groundwater geophysics, **Geophysics 50**, 2627-2628.

DOBRIN, M. B., 1978, Introduction to geophysical prospecting, 2nd Edition, McGraw Hill Co., New York.

FAIRHEAD, J. D., 1976, The structure of the lithosphere beneath the Eastern Rift, East Africa, deduced from gravity studies, **Tectonophysics 30**. 269-298.

FAIRHEAD, J. D., and GIRDLER, R. W., 1972, The seismicity of the East African Rift System, **Tectonophysics 15(1/2)**, 115-122.

FURGERSON, R. B., 1972, Electrical resistivity survey of the Olkaria Prospect, Kenya, Unpublished report of the UNDP/EAPL project, Kenya Power Company.

GEOTERMICA ITALIANA S.R.L., 1988, Integrated Geophysical Survey in the Menengai and Suswa-Longonot areas of the Kenya Rift Valley, D.T.C.D., U.N. and M.O.E.R.D., Kenya Government.

GHOSH, D. P., 1971, The application of filther theory to the direct interpretation of geoelectrical resistivity sounding measurements, **Geophysical Prospecting 19**, 192-217.

GHOSH, D. P., 1971, Inverse filter coeffiecient for the computation of apparent resistivity standard curves for a horizontally stratified earth. **Geophysical Prospecting 19**, 769-775.

GRANT, R. S., and WEST, G.F., 1965, Interpretation Theory in Applied Geophysics, McGraw Hill Book Co., New York.

GROUP SEVEN INC., 1971, Electrical resistivity survey in the Rift Valley of Kenya, Unpublished report of the UNDP/EAPL project, Kenya Power Company.

GUDMUNDSSON, J. S., 1982, Low temperature geothermal energy use in Iceland, **Geothermics 11**. 59-68.

INMAN, J. R., RYU, J. and WARD, S. H., 1973, Resistivity inversion, **Geophysics 38**, 1088-1108.

ISHERWOOD, W. F., and MABEY, D. R., 1978, Evaluation of Battazor known geothermal resource area, Nevada, **Geothermics 7**, 221-229.

JACKSON, D. D., 1972, Interpretations of inaccurate, insufficient and inconsistent data, **Geophys. J. Roy. Astr. Soc. 28**, 97-109.

JACKSON, D. D., 1979, The use of apriori data to resolve non-uniqueness in linear inversion, **Geophys. J. Roy. Astr. Soc. 57**, 137-157.

KAGASI, J. 1983, The volcanic petrology and geological structures of Mt. Margaret -Kijabe hill area, Kenya Rift Valley, M.Sc. thesis, University of Nairobi.

KELLER, G. V., 1971, General recommendations concerning electrical surveys of geothermal prospects in the Rift Valley Province of Kenya, Unpublished report of the UNDP/EAPL project, Kenya Power Company.

KELLER, G. V. and FRISCHKNECHT, F. C., 1966, Electrical Methods in Geophysical Prospecting, Pergamon Press, London.

KOEFOED, O., 1968, The Application of the Kernel Function in Interpreting Geoelectrical Resistivity Measurements, Geoexploration Monographs, Series 1 - No. 2, Stuttgart, Gebruder Borntraeger.

KUNETZ, G., 1966, Principles of Direct Current Resistivity Prospecting, Geopublication Associates, Berlin, Borntraeger.

LANCZOS, C., 1961, Linear Differential Operators, Van Nostrand Co., London.

MARQUARDT, D. W., 1963, An algorithm for least squares estimation of non-linear parameters, **J. Soc. Indust. Applied Math. 11**, 431-441.

MEIDAV, T., 1960, An electrical resistivity survey for groundwater, **Geophysics 25**, 1077-1095.

MOONEY, H. M., and WETZEL, W. W., 1956, The potentials about a point electrode and apparent resistivity curves for two-, three-, and four-layer earth, University of Minnesota Press, Minneapolis, 243 plates.

MWANGI, M. N., 1981, Resistivity survey for groundwater in Msambweni, Kenya, M.Sc. thesis, University of Nairobi.

NDOMBI, J. M., 1978, Geology, gravity and resistivity studies of Olkaria Geothermal

fields, Kenya, Ph.D. thesis, Stanford University.

O'NEILL, D. J., 1975, Improved linear filter coefficients for application in apparent resistivity computations, **Bulletin of the Australian Society of Exploration Geophysicists 6**, 104-109.

O'NEILL, D. J., and MERRICK, N. P., 1984, A digital linear filter for resistivity sounding with a generalized electrode array, Gephys. Pros. 32, 105-123.

ORELLANA, E., and MOONEY, H. M., 1966, Master tables and curves for vertical electrical sounding over layered structures, Interciencia, Madrid, 34 plates.

PETRICK, W. R., PELTON, W. H., and WARD, S. H., 1977, Resistivity inversion applied to crustal resistivity sounding data from South Africa, **Geophysics 42**, 995-1005.

RANDEL, R. P., and JOHNSON, R. W., 1970, Geological map of Suswa area, Degree Sheet No. 51 NW quarter 1:250 000, Mines and Geological Department, Kenya.

RAZZO, A. M., ARELLANO, C. F., and FONSECA, L. H., 1980, CFE resistivity studies of Cerro Perieto Geothermal fields, **Geothermics 9** 7-14.

RISK, G. F., MACDONALD, W. J. P., and DAWSON, G.B., 1970, D.C. resistivity survey of the Broadlands geothermal regions, New Zealand, **Geothermics 2, special issue 2**, 287-294.

ROONEY, D., and HUTTON, V. R. S., 1977, A magnetotelluric and magnetovariational study of the Gregory Rift Valley, Kenya, **Geophys. J. R. astr. Soc. 51**, 91-119.

RUST, W. M. Jr., 1940, Typical electrical prospecting methods, **Geophysics 5**, 243-249.

SAGGERSON, E. P., 1971, Geological map of Nairobi area, Degree sheet No. 51 NE quarter, Mines and Geological Department, Kenya.

SAVAGE, J. E. G., and LONG, R. E., 1985, Lithospheric structure beneath the Kenya Dome, **Geophys. J. R. astr. Soc. 82**, 461-477.

SKINNER, N. J., 1977, Recent geophysical studies of Kenya Rift Valley, **Contemp. Phys.**, 455-470.

SLITCHER, L. B., 1933, The interprtation of the resistivity prospecting method for horizontal structures, **Physics 4**, 59-68.

SURVEY OF KENYA, 1970, The Kenya Atlas, Survey of Kenya, Nairobi.

TELFORD, W. M., GELDART, L. P., SHERIFF, R. E., and KEYS, D. A., 1990, Applied Geophysics, 2nd Edition., Cambridge University Press, London.

THOMPSON, A. O., and DODSON, R. G., 1963, Geology of Naivasha area, Geological Survey of Kenya Report No. 55.

TORFASON, H., 1987, Geothermal and Geological survey of Mt Suswa, Kenya, D.T.C.D. and U.N.

VOSOFF, K., 1958, Numerical resistivity analysis - Horizontal layers, **Geophysics 28**, 536-556.

WIGGINS, R. A., 1972, The general linear inverse problem, implications of surface waves and free oscillation for the earth structure, **Rev. Geophys. Space Phys. 10**, 251-285.

WILT, M. J., GOLDSTEIN, N. E., and RAZZO, M. A., 1980, LBL Resistivity studies of Cerro Prieto Geothermal fields, **Geothermics 9**, 15-26.

WILT, M. J., and GOLDSTEIN, N, E., 1981, Resistivity monitoring at Cerro Prieto Geothermal fields, **Geothermics 10**, 183-193.

ZOHDY, A. A. R., 1965, The auxillary point method of electrical sounding interprtation, and its relationship to Dar Zarrouk parameters, **Geophysics 30**, 644-660.

ZOHDY, A. A. R., EATON, G. P., and MABEY, D. R., 1980, Applications of subsurface Geophysics to groundwater investigations. Techniques of water resources investigations of the United States Geological Survey, **Geophysics 45**, 5-55.

Area: SUSWA					KS 020 195				V.E.S. Number

Operator: N.O.O Prime Nant Tir.   Altitude (m): 1926   S.A

Date 17-06-87   AB Azimuth 120   ST 01

Observations:

AB/2	MN/2	ΔV (m volts)	I (m Amperes)	ᴷᴵᴬᴺ	ρ (ohm)	NOTES
3	1	1525	115	12·6	167·1	
5	1	310	1025	37·7	114·0	
7	1	165	100	75·2	124·4	
10	1	50·9	93	155·5	134·6	125·4
10	2·5	215	93	58·9	136·2	
15	2·5	86	88	137·5	134·6	
20	2·5	70	107·5	247·6	134·2	
30	2·5	44	105	561·6	134·7	
40	2·5	30·5	170	1001·6	120·8	
50	2·5	14·25	157·5	1557	131·2	144·9
50	10	41·8	151·5	377	157·5	
70	2·5	4·7	112·5	3075	128·5	139·7
70	10	22·5	112·5	754	150·2	
100	10	28	410	1555	144·1	
150	10	10·25	272·5	3519	132·6	7.
200	10	7·1	42	230	255	6266	103·5/103·2	101·35	07·8
200	40	36·5	45·5	420	255	1508	42·9/44·9·35	
300	10	2·6	40·5·9	14122	177	67·2
300	40	7·75	-1·5	3·12	58·5	56·9
400	40	4·8	7·5	6220	45·2	
500	40	4·2	9·45	9755	40·6	40·4
500	100	10·2	560	7770	40·1	
750	40	7·815	610	22027	31·6	21·5
750	100	2·25	6·0	8679	32·0	
1000	40	0·31	445	35207	26·9	21·5
1000	100	4·77	445	15551	26·9	
1500	100	0·36	0·45	420	5·0	35186	26·9/44	24·42	27·6
1500	250	1·40	255	580	5·0	13744	25·35	24·5
2000	100	0·183	·137	220	4·2	62675	27·43/27·1	27·15	27·3	27
2000	250	0·184	·76	345	4·20	26760	27·44/27·4	27·13	27265
2500	400			96018		
2500	250	0·36	0·21	510	5·0	38877	27·c/29·5·c 27·0
3000	250	0·23	0·30	510	1·6	56156	21·5/32·8 22·5
3000	400			34715		
4000	250	0·174	0·190	470	475	100138	37·1/44 130·5
4000	400			62204		
5000	250			156667		
5000	400			97546		

GEOTHERMAL PROJECT KEN 82/002.

Area	SUEUA	BJ CSS, 660	VES Number S102

Operator: Odhot Mfanty ...	Altitude (m): 1610
Date: 5/08/87	AB Azimuth: 70
Observations: Δ 23	SOITAMRUT

AB/2	MN/2	ΔV (m volts)	I (m Amperes)	$K = \pi\left(\frac{AB\;AN}{MN}\right)$	ρa (Ωm)	NOTES
3	1	16.0	37	12·6	6503	
5	1	770	44	37 7	831.4	
7	1	430	39	75 4	928	
10	1	810	45	155 5	1071.2	
10	2·5	720	46	58 9	921.6	
15	2·5	320	69	137·5	898	
20	2·5	260	69	247·4	860.5	
30	2·5	66	71	561·6	522	
40	2·5	60	110	1001·4	564.1	
50	2·5	26.5	125	1567	892.2	
50	10	157.5	185	377	320.9	
70	2·5	12.5	162.5	3075	236.5	
70	10	53	160	754	249.8	
100	10	8.15 13.75	79 135	1555	160	158 159
150	10	5.1	757.5	3519	113.9	
200	10	2.18	177.5	6268	77	
200	40	9	177.5	1508	76.5	
300	10	0.48	160	14122	42.6	
300	40	1.01	160	3472	39.4	
400	40	2	440	6220	28.3	
500	40	0.37	127.5	9755	93.7	
500	100	0.91	127.5	3770	25	
750	40	0.5	420	22027	26.2	
750	100	1.35	420	8679	27.9	
1000	40	0.8 1.1	960 1300	39207	33.6	83.1 32.3
1000	100	2.2 3	940 12	15551	36.5	35.9 36.2
1500	100	0.37	281.5	35186	45.5	
1500	250	0.77	289.5	13744	37.8	
2000	100	0.29 0.38	390 510	62675	47.7	47.9
2000	250	2.64 0.8	390 500	24740	40.5	59.6 40.1
2500	100	—	—	98018	— £	
2500	250	0.96 1.25	520 1100	38877	45.5	44.0 44.8
3000	250	0.8 0.73	660 860	56156	48.78	47.7 48.2
3000	400			34715		
4000	250			100138		
4000	400			62204		
5000	250			156687		
5000	400			97546		

GEOTHERMAL   PROJECT   KEN   82/002.

Area:	Susura-longonot			BJ D73, 663			V.E.S Number
Operator: M'S3, U··· 2.J1'· ···				Altitude (m):	1610		SE
Date	15/5/87			AB Azimuth	60		ZF 5703
Observations	Soitam ut 132, A 330						

AB/2	MN/2	ΔV (m volts)	I (m Amperes)	$K = \pi \left(\frac{AM \cdot AN}{MN} \right)$	ρ a(nm)		NOTES
3	1	1550	62	12·6	315·0		
5	1	61·0	79	37·7	315·0	-	
7	1	218	42·5	75·4	307·0		
10	1	132	76·5	155·5	268·3		
10	2·5	325	76·5	58·9	250·2		
15	2·5	160	105	137·5	216·1		
20	2·5	69	90·5	247·4	188·6		
30	2·5	33	125	561·6	148·3		
40	2·5	1813	115	1001·4	157·9		
50	2·5	10·125	105	1567	151·1		
50	10	400	105	377	143·6		
70	2·5	3·85	92	3075	128·7		
70	10	15	92	754	122·9		
100	10	7·9	140	15·55	86·6		
150	10	1·07	55	3519	64·0		
200	10	0·25	42	6268	53·7		
200	40	1·2	42	1508	43·1		
300	10	0·17	8·1	14122	29·6		
300	40	0·572	80	3472	24·8		
400	40	0·56	195	6220	17·8		
500	40	2·3	420	9755	15·0		
500	100	1·96	420	3770	17·6		
750	40	0·34	500	22027	16·5		
750	100	1·025	500	8679	17·8		
1000	40	0·53	1300	39207	17·5		
1000	100	1·475	1300	15551	20·0	R -
1500	100	0·573	0·81	580	1120	35186	21·4/24·2	23·6
1500	250	1·25	2·14	820	1180	13744	26·0/27·3	27·1
2000	100	0·29	0·315	620	740	62675	28·3/26·6	27·5
2000	250	0·76	0·46	620	740	24740	30·3/30·0	30·15 ··
2500	100	—				98018	—	
2500	250	0·44	2·70	1050	740	38877	34·8/30·4	34·6
3000	250	0·47	0·58	710	900	56156	37·0/36·2	36·6
3000	400	—		—		34715	—	
4000	250					100138		
4000	400					62204		
5000	250					156687		
5000	400					97546		

GEOTHERMAL PROJECT KEN 82/002

Area:	SUSUA (south) - L	BJ 036,637	V.E.S. Number

Area: SUSUA (south) - L BJ 036,637   V.E.S. Number

Operator: PIC Kilele Hamzi Zio Plieiro   Altitude (m): 1605

Date: 7-05-87   AB Azimuth: 120

Observations: (A)cone 29   Ol Doyn.o 11
On the slope of Susua volcano; presence of several
surface geological disomogeneities

AB/2	MN/2	ΔV (mvolts)	I (m Amperes)	K=(AM.AN/MN)	ρ (ohm)	NOTES
3 1	1	860		41	12·6	258.1	
5 u	1	475		60	37·7	298.5	
7 u	1	180		36	75·4	314.2	
10 1	1	46		28	155·5	255.5	
10 1	2·5	110		28	58·9	231.4	
15 u	2·5	170		115	137·5	203.3	
20 u	2·5	1025		1225	247·4	207.0	
30 1	2·5	50		115	561·6	246.2	
40 u	2·5	19.5		76	1001·4	263.9	
50 u	2·5	165		105	1567	246.2	
50 u	10	78		105	377	280	
70 1	2·5	16.5		162.5	3075	276.4	
70 1	10	48		160	754	320.5	
100 u	10·	18.5	16.5	.90	83	15·55	3·196/3·38	216.7
150 u	10	7.1	7.6	62	21.5	3519	372.3/326	273.5
200 1	10	4.5		89		6268	316.9	
200 1	40	20		89		1508	338.7	
300	10	2.65		1225		14122	282.4	
300	40	10.5		125		3472	281.6	
400	40	4.95	5.65	122	136	6220	252.4	258·4 ⎰ 255.4
500	40	1.7u		105		9755	159.5	
500	100	5		105		3770	189.5	
750	40	0.7	0.96	390	500	22027	39.5/40.3 ⎰ 40.9	
750	100	2.18	2.69	390	500	8679	47.3/46.7 ⎰ 47.0	
1000	40	0.23	0.29	400	525	39207	22.5/21.8 ⎰ 22.2	
1000	100	0.62	0.71	400	526	15551	24.1/24.0 ⎰ 24.1	
1500	100	0.16	0.48	495	630	35186	25.6/25.8 /25.2 ⎰ 25.2	
1500	250	0.375	1.25	495	680	13744	24.9/25.3 25·1 ⎰ 25.1	
2000	100	0.R	0.27	460	60·	62675	26.6 /26.4	
2000	250	0.0	0.417	460	46·3	24760	25.3/25.2	n5/in /25.5
2500	100	3—	2—	—		98018	—	
2500	250	0.37	0.8	50·	1075	38877	28.8/29	Av.0·95/1280 R.29.9
3000	250	077		1280	1670	56156	338/36.1	0665/Raa /326
3000	400	—		—		34715		
4000	250	825	0·43	650	/100	10013B	39.2/19.1	
4000	400	—		—		62204		
5000	250	—		—		156687		
5000	400		•	—		97546		

Area	Suswa Longonot	AJ 052, 630	V.E.S Number
Operator: HG, Francisco		Altitude (m): 1650	82
Date 20-05-87		AB Azimuth 90	
Observations: SUSWA (OL DOINYO) 258 A10			

AB/2	PN/2	ΔV (m volts)	I (m Amperes)	$K=\pi(\frac{AM\,AN}{MN})$	ρ(αlpm)	NOTES
3 /	1	405		81	12·6	163 33	
5 "	1	420		905	37·7	474 96	
7 4	1	210		82	75·6	193	
10 /	1	95		74 ·	155 5 ·	199 3	
10 /	2·5	255		75	58·9	202 .9	
15 /	2·5	120		88.5	137·5	186 4	
20 /	2 5	675		95	247 6	175 8	
30 /	2 5	32		105	561·6	171. 2	
40 /	2 5	2025		105	1001 6	193. 1	
50 /	2·5	11		94	1567	183.4	
50 /	10	865		93.5	377	219 7	
70 /	2·5	63		120	3075	161.4	
70 /	10	30		120	754	188.5	
100 /	10	7.5		80	15 55	141 9	-
150 /	10	4.7		101.5	3519	85.91	
200 /	10	21		1775	6268	74.15	
200 /	40	10.25		121 5	1508	87 02	
300 4	10	0.955		230	14122	58 6	
300 5	40	4 3		230	3472	64. 9	
400	40	4 32	2.225	265	480	6220	31.1	30 2
500	40	1.425		560	9755	24.8	
500	100	4.8		560	3770	32 3	
750	40	0.125	0.46	120	132	22027	23.1	24 7 / 36.4
750	100	0.602	0.402	120	132	8679	29 4	31.42 ; 33 41
1000	40	—		—		39207	—	Enel Sv Sta
1000	100	0.093	0.1	38	62	15551	38 1/37	
1500	100	1.35	1.625	450	1600	35186	41.3/208	
1500	250	3	8.7	1150	1600	13744	35.9/363	
2000	100	1.05	086	1520	1250	62675	43.6/43	
2000	250	2 375	1.95	1520	1250	24740	38 7/38 6	··
2500	100			—		98018	—	
2500	250	1.36	1.13	1375	1100	38877	38 6/60	1.395/ 1370 / 39 6 3
3000	250	0 41	0.5	520	670	56156	44 6/42	3 41.5
3000	400	—		—		34715		
4000	250					100138		
4000	400					62204		
5000	250					156687		
5000	400					97546		·

GEOTHERMAL PROJECT KEN 82/002.

110

Area	SUSUVA			BJ 064 640		V.E S Number
Operator:				Altitude (m): 1670		
Date				AB Azimuth 735		
Observations:						

AB/2	MN/2	ΔV (m volts)	I (m Amperes)	$K=\left(\frac{AM\,AN}{MN}\right)$	ρ (ohm m)	NOTES
3	1	460		27.5	12.6	35.7	
5	"	1	160	13c	37.7	48.6
7	,il 1	115	14.2	75.4	60.2	
10	, 1	63	157.3	155.5	64.2	
10	, 2·5	160	15.5	58.9	61.8	
15	" 2·5	58	92	137.5	81.4	
20	,ii 2·5	27.2	63	247.4	81.4	
30	, 2·5	1°.	59	115 260	561.6	928.92
40	" 2·5	22.5	9.0	1001.4	22.4	
50	,il 2·5	10	9.10	1567	24.6	
50	,i 10	44	90.5	377	80	
70	, 2·5	3	160	3075	57.6	
70	, 10	13.21	155	754.	63.3	
100	" 10	30	9.5	1555	51	
150	,ii 10	5.1	46.5	3519	38.5	
200	10	1.64	1.32	320	353	6268	33.1 33.5
200	40	3.35	6.1	5.5	350	1508	1.8 12.5
300	10	0.66	2.8	230	41.5	14122	23 21.5
300	40	2.285	3.8	32.5	53.5	3472	45.5
400	40	1.45	9.15	450	115	6220	20.10.8
500	40	2.32		350		9755	2.4
500	100	1.86		350		3770	20
750	40	0.7	2.85	520	220	22027	4..4 9.9
750	100	1.325	1.57	520	720	8679	26.1 20.3
1000	40	9.0	0.44	250	1110	39207	23 23.3
1000	100	1.2	1.65	2.3	1140	15551	93.5 19.3
1500	100	0.2	0.46	520	760	35186	2.5 126.0
1500	250	—	—	—	—	13744	
2000	100	3.4		0.30		62675	23.2
2000	250	1.35		820		26740	20
2500	100	0.276	0.22	9.20	700	98018	20.5 30
2500	250	0.26	0.52	9.20	200	38877	32.11 29.4	3D 1
3000	250	0.42	0.61	360	10.0	56156	35.5 33.9	24.7
3000	400	—	—	—	—	34715	—
4000	250	.	.			100138	
4000	400					62204	
5000	250					156687	
5000	400					97546	

GEOTHERMAL PROJECT KEN B2/002

Area: SUSUA Lonfount (Soitaueru9)					V.E.S Number 85 5107	
Operator: XC, GB, Nicola, Field Altitude (m): 1510						
Date 29 - 04 - 87 AB Azimuth 40						
Observations: On the axis between SU SUA and Soitaurut / Vo leames c?						

AB/2	MN/2	ΔV (m volts)	I (m Amperes)	K·π($\frac{AM.AN}{MN}$)	ℓa(nm)	NOTES
3 ı	1	1400	99	12 6	178 2	
5 ıı	1	630	99	37 7	210	
7 ın	1	360	99	75 4	274.2	
10 ı	1	167.5	99	155·5	263.1	
10 ı	2·5	490	99	58·9	291.5	
15 ıı	2·5	1225	685	137·5	265.9	
20 ııı	2·5	650	805	247.4	199.8	
30 ı	2·5	165	540	561·6	150.8	
40 ıv	2·5	58	460	1001·4	132 0	
50 ıvı	2·5	59	755	1567	122.5	
50 ın	10	260	755	377	129.8	
70 ı	2·5	25	670	3075	114.7	
70 ı	10	105	670	754	118.2	
100 ıv	10	66	670	15 55	106.8	
150 ın	10	18	670	3519	94.5	
200	10	8.7	670	6268	81.3	
200	40	36	670	1508	81·0	
300	10	2.75	670	14122	58·0	
300	40	11.15	670	3472	57. 8	
400	40	15.5	12.25	1860	150+	6220	58.8/58.6	Problem: geological...
500	40	0.835	170	9755	47.9	
500	100	2.175	170	3770	48·2	
750	40	1.125	690	22027	35.9	
750	100	2.878	690	8679	35.5	
1000	40	—	680	39207	—	
1000	100	1·6¹	680	15551	345	
1500	100	0 44	670	35186	23 2	\ 717
1500	250	1175	670	13744	24.1	/
2000	100	0.393	950	62675	25.3	\ 26
2000	250	1 080	950	24740	26.8	/
2500	100	—	—	98018	—	
2500	250	0.71	1000	38877	27.6	
3000	250	0.7125 0.73	1330	1330	56156	30.1/30 8	044 / 800 / 30. 9
3000	400	0.41 0.53	1010	1330	34715	40.9/40.1	
4000	250			100138		
4000	400			62204		
5000	250			156687		
5000	400			97546		

GEOTHERMAL PROJECT KEN 82/002.

Area: SUSUA LONGONOTO   BJ 119,652
Operator: AC, Pietro & Maurizio   Altitude (m): 1510 m
Date 5-05-87   AB Azimuth. 40°
Observations: Susua 207.5   L   8   Sait 266.5   5108

AB/2	MN/2		ΔV (m volts)		I (m Amperes)		$K=\pi\left(\dfrac{AM\cdot AN}{MN}\right)$	ρa (am)	NOTES
3	1	I	700		45		12.6	180	
5	1	II	375		62		37.7	228.0	
7	1	III	220		58		75.4	286	
10	1	I	152		67		155.5	352.8	
10	2.5	I	400		67		58.9	351.6	
15	2.5	II	355		125		137.5	390.5	
20	2.5	III	153	175	87	85	247.4	235.1/229	
30	2.5	I	120		145		561.6	466.8	
40	2.5	II	66.5	68	140	148	1001.4	475.6/460	
50	2.5	III	360		149		1567	378.6	
50	10	III	160		149		377	404	
70	2.5	I	11		125		3075	270.6	
70	10	II	49		125		754	295.6	
100	10	III	130		117.5		15.55	172.0	
150	10	III	3.3		140		3519	82.9	
200	10		11.9		95		6268	78.5	
200	40		4.9		96		1508	78.6	
300	10		0.77		137.5		14122	79.1	
300	40		3.1		135		3472	79.7	
400	40		1.5		160		6220	73.9	
500	40		5.1		770		9755	66.6	
500	100		13.5		770		3770	66.1	
750	40		0.45		2425		22027	44.8	
750	100		1.25		240		8679	45.2	
1000	40		1.58		2600		39207	26.0	
1000	100		6.26		2600		15551	27.6	
1500	100		0.71		1600		35186	17.8	
1500	250		5.05		1600		13744	20	
2000	100		0.45		1600		62675	18.13	
2000	250		1.16		1600		24740	20.5	
2500	100		—		—		98018		
2500	250		0.865	0.945	1600	1600	38877	23.5/23	0.915/1600/23.4
3000	250		0.645	0.720	1400	1550	56156	25.9/26.1	26.0
3000	400						34715		
4000	250		0.451	0.595	1400	1750	100138	32.25/34	33.1
4000	400						62204		
5000	250						156687		
5000	400						97546		

GEOTHERMAL   PROJECT   KEN   82/002.

Area:	Su Suo (south) – L		BJ 033,622	V.E.S Number.

Area: Su Suo (south) – L	BJ 033,622	V.E.S Number.
Operator: AC, Pietro, Mauʒizio Altitude (m) 41500 m		
Date 6-05-87 AB Azimuth 105		
Observations: Kalalerue Hill 186, Small felCai on Suoug		
(B) hice 203, SUSUA (OL Dormio)		

AB/2	MN/2	ΔV (m volts)		I (m Amperes)		K=($\frac{AB-MN}{MN}$)	ρa (nm)	NOTES
3 1	1	1000		1325		12·6	95 1	
5 "	1	320		115		37·7	104.9	
7 "	1	102.5		90		75.4	119.4	
10 1	1	165		195		155·5	131.6	
10 1	2 5	400		195		58·9	120.8	
15 "	2 5	137.5		1375		137·5	137.5	59 /
20 "	2 5	112.5		200		247.4	151.5	
30 1	2·5	70		200		561·6	196.6	
40 "	2 5	41		155		1001.4	234.6	
50 "	2·5	31		190		1567	255.7	
50 "	10	110		185		377	224.2	
70 1	2 5	16.75		170		3075	303	
70 1	10	57.5		170		754	255	
100 "	10	29.2		170		15 55	267	
150 "	10	8		140		3519	201.1	
200	10	5.3		1975		6268	168 2	
200	40	23.5		197.5		1508	177.5	
300	10	2.55		380		14122	109.6	
300	40	12.8		390		3472	116.5	
400	40	2.3	6 65	300	850	6220	47.7/687	2.25 / 325 / 47.4
500	40	1.12	0.67	300	150	9755	16.34/36.8	
500	100	3.1	1.53	300	178	3770	39.7/39.2	
750	40	0.32		440		22027	16.0	
750	100	0.88		440		8679	17.4	
1000	40	0.158		420		39207	14.7	
1000	100	0.383		420		15551	14.2	
1500	100	0 36	0.56	840	135 3	35186	15.6 / 14.5	
1500	250	1.25	2.11	840	1350	13744	20.4 / 21.5	
2000	100	0.173	0.368	720	1500	62675	15.1 / 15.4	
2000	250	0.6	1.26	720	1500	24740	18.8 / 20.9	
2500	100	0.26	0.198	1600	1125	98018	15 9 / 14 4	16 2
2500	250	0.87	0.6	1600	1125	38877	21.3 / 20.7	21·0
3000	250	0.47	0.667	1100	1550	56156	24.1/24.7	
3000	40	—		—		34715	—	
4000	250	0.60	0 37	1400	1250	100013 B	29.2/29.7	27 5
4000	400					62204		
5000	250					156687		
5000	400					97546		

GEOTHERMAL   PROJECT   KEN 82/002.

Area:	SUSVA				BJ 081,630	V.E S Number
Anerator: Λ.C. G?, :C .... ,? Altitude (m) 1425						84 23
Date 22/5/87			AB Azimuth NS			
Observations:						STIU

AB/2	MN/2	ΔV (mvolts)	I(m Amperes)	$K=\left(\frac{AM.AN}{MN}\right)$	ρ(alam)	NOTES
3	1	1300	45.3	12 6	360	-
5	1	530	28.5	37.7	510.0	
7	1	360	85	75.4	764.6	
10	1	186	45.0	155.5	642.7	
10	2.5	460	44.5	58.9	608.9	
15	2.5	232.5	60	137.5	532.8	
20	2.5	94.5	59.5	247.4	392.9	
30	2.5	27	60	561 6	252.7	
40	2.5	15	66	1001.4	227.5	
50	2.5	7.5	52.5	1567	223.8	
50	10	31	52 5	377	222.6	
70	2.5	7.9	110	3075	220 8	
70	10	31	110	754	212.5	
100	10	16.25	116	15 55	217.8	
150	10	4	74.5	3519	189	
200	10	9.7	103	6260	164 3	165.5
200	40	14 25	103	1508	165.7	
300	10	0 63	75	14122	118.6	1 $\frac{5}{7}$
300	40	2 66	24 5	3472	124	1
400	40	3.15	210	6220	93.3	
500	40	4.725 2.12	243 292	9755	69.3	70.8 70.0 71.7
500	100	4.7 5.7	243 290	3770	72 9	74.1 73.5
750	40	0.62	420	22027	21.75	
750	100	1.43	430	8679	29.3	
1000	40	0.326 0.45 525	737	39207	22.2	23 9 22.0 ~2
1000	100	0 29 1 46 = 75	737.5	15551	24.4	24 5 24.3
1500	100	0.72 0 53 1410	825	35186	92 8	22 60 22.7
1500	250	1.66 4 25 1090	825	13744	20 9	20 82 20 7
2000	100	0.36 0.41 1000	>20	62675	22.6	21.3 22.0
2000	250	0.2 1.06 1000 1950		24740	21.6	19.8 50 078 9m
2500	100	—	—	98018	—	—
2500	250	0.47 0 58 760 950		38877	24.3	23 8 ~ 25 0 51
3000	250	0.24 0.42 760 950		56156	25.1	24.8 0 Pm
3000	400	—	—	34715	—	
4000	250	0 2 0.26 670 525		10013 8	59.89	31.8 1 690 AV
4000	400			62204		
5000	250			156687		
5000	400			97546		

GEOTHERMAL   PROJECT   KEN 82/002.

Area:	Sosuwa - Lon500not	BJ 112 .630	V.E.S Number
Operator: AC . Mauridio		Altitude (m) 1440	
Date 19 - 05 - 87		AB Azimuth 0	
Observations: Soilowtuf 50 E			

AB/2	MN/2	ΔV (in volts)	I (in Amperes)	$K = \pi \frac{(AB-AN)}{MN}$	ρ (a(nm))		NOTES	
3	1	460	61	12.6	95.51			
5	1	205	62	37.7	124.68			
7	1	122.5	56	75.4	164.93			
10	1	82	57	155.5	223.70			
10	2.5	205	57	58.9	211.83			
15	2.5	105	505	137.5	285.89			
20	2.5	56	39	247.6	355.24			
30	2.5	61	82	561.6	417.7			
40	2.5	405	102	1001.4	397.6			
50	2.5	73.5	95	1567	387.62			
50	10	95.5	93	377	387.13			
70	2.5	5.35	77	3075	233.45			
70	10	34.5	77	754	337.83			
100	10	18	102.5	1555	223.03			
150	10	7.6	110	3519	243.13		-	
200	10	5.5	160	6268	215.46			
200	40	19.5	155	1508	189.7			
300	10	2	160	14122	201.7			
300	40	6.9	160	3472	121.12			
400	40	4.6	163.5	6220	170.8			
500	40	1.925	122.5	9755	159.1			
500	100	5.2	122.5	3770	160.0			
750	40	2.35	530	22027	90.91			
750	100	6.5	530	8679	92.97			
1000	40	1.05	700	39207	52.2			
1000	100	2.82	700	15551	62.6		A	
1500	100	0.50 0.8	800 1090	35186	25.9	25.8	25.85
1500	250	1.55 2.1	802 1090	13744	26.6	26.5	26.5
2000	100	0.42	1200	62675	22.5		
2000	250	1.1	1200	24740	22.3		
2500	100	0.223 0.313	880 25.6	98018	24.9	25.6	25.5
2500	250	0.576 0.776	880 1200	38877	25.4	25.1	
3000	250	0.664 0.53	1360 1060	56156	27.7	28.1	
3000	400	—	—	34715	—		
4000	250	0.38 0.30	1075 860	100138	35.4	35.1	
4000	400	—	—	62204	—		
5000	250			156687			
5000	400			97546			

GEOTHERMAL PROJECT KEN B2/002

Area: Suswill Swoipi
Operator: .... Altitude (m): 1240
Date 14/01/88
AB Azimuth /.
Observations: 1 Airly , Cn,

AB/2	MN/2	ΔV (in volts)	I (in Amperes)	(CW/AM/AN/MN)	C a (in m)	NOTES
3 ,	1	610		38	12 6	169.1	
5 «	1	545		18.5	37 7	111 1	
7 «	1	8.5		65	75 6	98 6	
10 «	1	63-	49	57	68 5	155 5	117/115	
10 «	2·5	130 6	115	64.5	56 5	50 9	120 8/11	
15 «	2·5	55 5		53 5		137·5	143 6	
20 »	2·5	75		110		247 6	168·7	
30 «	2·5	25	30	83	99	561 6	169 1/17	
40 »	2·5	215	17 25	125	103	1001 6	172/162	7 - 16.9 2
50 »	2·5	30 6		261		1567	164 9	
50 »	10	112 1		285		377	181 9	
70 «	2·5	154		340		3075	122 9	
70 «	10	31.5		345		754	161 8	
100 «	10	17 0	21.9	220	212 0	1555	120 2	129 4 125 0
150 »	10	9 8	340			3519	101 6	
200 «	10	6.5	3.6	355	245 .	6268	79 5	78 - 71
200 «	40	26·0	21 6	255	245 .	1500	60 4	111 1
300 «	10	1.03		241		16122	59 1	
300 »	40	6.4		241		3472	90 3	
400 »	40	5.06		440		6220	71 4	
500 «	40 -	2 6	15	495	74.	9755	51.2	45 8 49 3
500 «	100	6.5	9.25	175	200	3770	49.6	49 3
750	40	·91	6	89 .		22027	24 5	
750	100	3.28		211		8679	24 3	
1000	40	0·27	0·2	57 0	420	35207	18 4	18 2. 18 5 18 25
1000	100	0·66	0·49	525 0	420	15551	13 8	12 3 13 0
1500	100	0·15		350 0		35186	15 1	
1500	250	0·511		255 2		13744	20 2	
2000	100	0·16	0·2	540	790	62675	164 5	15·9
2000	250	0·25	0·51	540	790	26760	17·4 ×	16·0
2500	100	0		—	—	98018	—	
2500	250	0·212		445		38077	16·5	
3000	250	0·1178	0·42	305		56156	21·6	20 5 21
3000	400					34715		
4000	250					100138		
4000	400					62204		
5000	250					156687		
5000	400					97546		

GEOTHERMAL PROJECT KEN 82/002.

Left Sheet

Area:	Susua - Longonot			BJ 032 601		V.E.S. Number

Operator: Lc - Mauririio Pietro · Altitude (m): 1350
Date: 8 - 05 - 87 · AB Azimuth: E-W
Observations: Eol da ue rec + 26 52°, Small J. on the slope of Susua 18 · SUSUA 7,

AB/2	MN/2	ΔV (mvolts)	I (m Amperes)	$K = \pi \frac{AM \cdot AN}{MN}$	ρ a(am)	NOTES
3	1			12·6		
5	1	1725	260	37·7	280	
7	1	850	260	75·4	246.5	
10	1	745	510	155·5	227.2	
10	2·5	2180	540	58·9	251.8	
15	2·5	325	220	137·5	203 1	
20	2·5	210	260	247·4	199.8	
30	2·5	225	600	561·6	210.6	
40	2·5	136	660	1001·4	206.3	
50	2·5	84.5	660	1567	200.6	
50	10	360	660	377	205.6	
70	2·5	36	585	3075	186.4	
70	10	150	595	754	190.1	
100	10	77.5	850	15 55	141.8	
150	10	23.5	920	3519	89.4	
200	10	3.45	725	6268	81.7	
200	40	45	725	1508	93.6	
300	10	6.5	810	14122	78.5	
300	40	18.6	860	3472	80.7	
400	40	7·6 9.3	800 1075	6220	52.5/63	57
500	40	4·3 4.75	1070 1140	9755	39.2/60.6	39.9
500	100	13·5 14.9	1070 1140	3770	47.6/49.7	46.5
750	40	1·30	1150	22027	25.8	
750	100	3.95	1150	8679	20	
1000	40	0.54	1160	39207	18.7	
1000	100	1.58	1160	15551	21.4	
1500	100	0.5	950	35186	18.6	-
1500	250	1.27	950	13744	18.4	
2000	100	0.46	1390	62675	19.8	
2000	250	1.05	1390	24740	18.7	
2500	100	—	—	98018	—	
2500	250	0.57 0.62	070 1160	38877	20.7/20.8	
3000	250	0.67 0.522	1100 1240	56156	24.7/23.6	
3000	400	—	—	34715	—	
4000	250	0.29 0.33	925 1025	100138	31.5/32.2	0.31 980/31.4
4000	400			62204		
5000	250			156687		
5000	400			97546		

GEOTHERMAL PROJECT KEN 82/002

Right Sheet

Area:	SUSUA - L		/BJ 616 066		V.E.S. Number

Operator: Lc. GB Mauririio, Pietro Niesen · Altitude (m): 1380
Date: 28 - 04 - 87 · AB Azimuth: 35°
Observations: 15 km from Fore SL 16

AB/2	MN/2	ΔV (mvolts)	I (m Amperes)	$K = \pi \frac{AM \cdot AN}{MN}$	ρ a(am)	NOTES
3	1	2900	156	12·6	234.2	
5	1	1275	156	37·7	308.1	
7	1	800	156	75·4	386.7	
10	1	4003	156	155·5	458.5	
10	2·5	1200	156	58·9	453.1	
15	2·5	800	218	137·5	504.6	
20	2·5	590	277	247·4	527	
30	2·5	235	277	561·6	474.4	
40	2·5	300	730	1001·4	411.5	
50	2·5	100	540	1567	290.2	
50	10	450	540	377	314.2	
70	2·5	28	540	3075	159.4	
70	10	125	540	754	174.5	
100	10	28.5	540	15 55	82	
150	10	3.2	620	3519	46.5	
200	10	6.15	620	6268	42.0	
200	40	19	670	1508	46.2	
300	10	24.7	695	14122	34.5	
300	40	7.65	695	3472	38.2	
400	40	4.1	730	6220	34.9	
500	40	3.3	950	9755	33.9	
500	100	7.88	950	3770	31.3	
750	40	0.88	690	22027	28.1	
750	100	908	690	8679	26.2	
1000	40	0.487	835	39207	22.9	
1000	100	0.98	735	15551	20.8	
1500	100	0.63	1150	35186	19.5	
1500	250	1.68	1150	13744	20.1	
2000	100	0.444 0.53 R	1825 1380	62675	22.2/23.5	230
2000	250	1.66 1.28 M	1935 1380	24740	22.5/22.9	221
2500	100	—		98018	—	
2500	250	1.03 0.83 R	1670 1300	38877	26/24.8	
3000	250	0.557 0.705	1160 1400	56156	27/21.3	
3000	400			34715		
4000	250			100138		
4000	400			62204		
5000	250			156687		
5000	400			97546		

GEOTHERMAL PROJECT KEN 82/002.

Area:	Siswa - Longonot	/ BJ 614125		V.E.S Number

Operator: O B AC Hoot Ho... D. Altitude (m): 1450
Date: 29 - 4 - 87   AB Azimuth N - S
Observations: 320° OL Doinyo Onioke (top) +5 Longonot (for)

AB/2	MN/2	ΔV (mvolts)	I (m Amperes)	Km(AMAN/MN)	ρ(ohm)	NOTES
3	1	1430	16·45	12·6	1095·3	
5	1	155	6·5	37·7	855	
7	1	153	15·6	75·4	739·5	
10	1	65	18·5	155·5	571·6	
10	2·5	174	18·5	58·9	554·0	
15	2·5	72	21·25	137·5	301·9	
20	2·5	38·5	115	25·2	122	247·4	249·3 / 241·3	2453
30	2·5	14·2	89·5	561·6	202·6	
40	2·5	7·8	7 8	39·5	39·5	1001·4	197·7	
50	2·5	5·65	42·5	1567	208·3	
50	10	21·9	43·5	377	194·3	
70	2·5	3·55	47·5	3075	229·8	
70	10	13·5	47·5	754	214·3	
100	10	14·0	90	1555	241·9	
150	10	24·5	300	3519	267·4	
200	10	15	300	6268	313·4	
200	40	61·	300	1508	306·6	
300	10	11	460	14122	337·7	
300	40	44	460	3472	332·1	
400	40	42	790	6220	330·7	
500	40	8·75	310	9755	275·3	
500	100	19·3	310	3770	234·7	
750	40	5·1	885	22027	126·9	
750	100	11	880	8679	108·5	
1000	40	—	—	39207	—	
1000	100	17·	3·125	490	870	15551	343/56·8	355·1
1500	100	0·652	675	35186	32·0	
1500	250	1·375	672	13744	28·1	
2000	100	0·426	960	62675	27·8	
2000	250	0·916	0·539	905	860	24740	25·0 / 25·9	
2500	100	0·222	780	98018	27·9	
2500	250	0·53	780	38877	26·4	
3000	250	0·36	700	56156	29	
3000	400	—	—	34715	—	
4000	250	0·429	0·518	1160	1440	100138	36·4 / 36·8	
4000	400	—		62204		
5000	250			156687		
5000	400			97546		

GEOTHERMAL   PROJECT   KEN 82/002

Area:		South of Mt Suswa					V.E.S. Number.
Operator:		GITAU, CHIAMA		Altitude (m):	1420		ST. 16
Date	19/4/88			AB Azimuth	I — W.		
Observations:							

AB/2	MN/2	ΔV (m volts)	I (m Amperes)	$K=\frac{AB-MN}{MN}$	ρ_a (ohm)	NOTES	
3	1	920	12.5	12 6	726		
5	1	610	2.	37 7	820		
7	1	365	3?	75 6	818		
10	1	192	3 6	155·5	736	} 710.5	
10	2·5	416	3 6	58 9	785		
15	2·5	126	4° 5	137 5	527		
20	2·5	24	0.5	247·6	407		
30	2·5	46	66	561·6	391·4		
60	2·5	10.2	100	1001 6	328		
50	2·5	2·75	17·75	116	0,7	1567	338/335	0.115	325.8
50	10	01.	21·5	112		377	331/358	
70	2·5	5.2	6·5	56.5	25	3075	279	} 281.0
70	10	2 6	20·5	9.5	7.	756	283	
100	10	8·75	12·75	21	75·5	1555	235/371	} 236
150	10	6.75	16.5	3519	226		
200	10	2.3	62.5	6268	219	} 212.0	
200	40	9.4	62.5	1508	210		
300	10	2.85	25r	14122	161	} 160.5	
300	40	11.5	250	3672	160		
400	40	3.5	152.5	6220	130		
500	40	1.5	5.65	430	680	9755	90	95	108.4
500	100	18·5	12	425	56	3770	121	123.5	
750	40	10.5	4	315		22027	92	} 97.2
750	100	19	315	8679	52.5		
1000	40	0.25	6.10	415	565	39207	191	256	20.34.4	25.2
1000	100	0.775	1.05	415	565	15551	25.0	25.9	
1500	100	0.325	775	35186	14.8	} 17.6	
1500	250	1.15	775	13766	20.4		
2000	100	0.18	68	62675	16.2	} 19.2	
2000	250	0.428	6.55	24760	22.2		
2500	100	0.055	500	98018	18 6		
2500	250	0.32	500	38877	24.9		
3000	250	0.24	500	56156	27.0		
3000	400			36715			
4000	250			100138			
4000	400			62204			
5000	250			156687			
5000	400			97546			

GEOT PROJECT KEN 82/002

AB/2	MN/2	ΔV (mvolts)	I (m Amperes)	$K=\pi(\frac{AB-MN}{MN})$	ρa (nm)	NOTES
3	1	680		199		12·6	43·7	
5	1	330		210		37·7	59·2	
7	1	975	250	265	193	75·4	78·2	78·1
10	1	122		187		155·5	101·4	
10	2·5	800		157		58·9	315	
15	2·5	275		300		137·5	126	
20	2·5	270	235	235	420	247·4	134/38	
30	2·5	61	85	215	310	561·6	159/159	
40	2·5	42		275		1001·4	152·9	
50	2·5	28·5		315		1567	141·8	
50	10	121		315		377	144·5	
70	2·5	10·5		272		3075	118·7	
70	10	45	41	260	255	754	130·5/121	J 125·
100	10	16·5	15·25	255	234	1555	100·6/104	
150	10	8·2	5·3	400	255	3519	92·1/73	
200	10	2·25		270		6268	52·2	
200	40	9·8		265		1508	55·8	
300	10	0·52		207·5		14122	32·3	
300	40	2·2		227·5		3472	33·6	
400	40	0·68		132		6220	23·2	
500	40	0·303		122·5		9755	16·2	
500	100	0·8		152·5		3770	16·5	
750	40	·338	·32	592·5		22027	11·9	
750	100	·85		600		8679	12·3	
1000	40	·189		740		39207	10·0	
1000	100	·50		740		15551	10·6	
1500	100	·09	·116	395	885	35186	8·0/10·3	Av=9·1
1500	250	0·8		38		13744	10·4	
2000	100	·283		1490		62675	11·9	
2000	250	·7		1490		24740	11·6	
2500	100	·135		920		98018	14·4	
2500	250	·48	·334	920	915	38877	18·8/14·9	760/0·1mv	15·354
3000	250	·30	·37	1000	117	56156	16·8/16·2	
3000	400					34715		
4000	250					100138		
4000	400					62204		
5000	250					156687		
5000	400					97546		

GEOTHERMAL PROJECT KEN 82/002.

116

Area:	Svong				U.T 082 593		V.E.S. Number
Operator	Mwangi Ngugi / G. kw				Altitude (m): 1370		EJF
Date	22/2/90				AB Azimuth E-W		18
Observations:	Good ground conditions — faired at person night						

AB/2	MN/2	ΔV (in volts) (in amperes)				K (AMAN MN)	ρ(calc)	NOTES
2	1					4.0	4.44.64	
5	1	0.10	0.17	0.54	6.76	37.7	150.77	
7	1	5.82	6.88	5.90	5.93	75.6	446.58	
10	1	3.25	3.32	2.34	3.25	155.5	570.57	519.8
10	2.5	1.78	2.81	1.50	3.51	58.9	618.55	
15	2.5	3.55	3.64	3.68	3.68	137.5	506.60	
20	2.5	1.91	1.54	1.97	1.99	247.6	487.33	
30	2.5	0.77	0.X	0.77	0.78	561.6	421.14	
40	2.5	0.34	0.26	0.42	0.43	1001.6	409.45	
50	2.5	0.18	0.19	0.21	0.21	1567	330.62	329.6
50	10	0.52	0.55	0.42	0.55	377	328.58	
70	25					3075	NOT DONE	
70	10	0.28	0.40	0.33	0.34	754	260.52	
100	10	0.11	0.13	0.14	0.15	1555	227.28	
150	10	0.03	0.0	0.0	0.06	3519	206.8	
200	10	0.01	0.02	0.02	0.03	6268	187.37	180.8
200	40	0.09	0.11	0.12	0.12	1508	188.74	
300	40	0.01	0.02	0.03	0.03	3472	105.180	
400	40	0.008	0.01	0.01	0.02	6220	85.443	
500	40	1.12	6.31	6.78	6.81	9755	56.62	
500	100	6.90	6.90	6.8	6.49	3770	59.83	m2
750	100	3.25	3.93	3.79	3.21	8671	78.77	m26
1000	40					39207		DONE
1000	100	1.28	1.31	1.24	1.25	15551	20.88	mR
1500	100					35186		not pass out
1500	250					13744		to rains and
2000	100					62615		thunderstorms
2000	250					24740		
2500	100					98018		
2500	250					30877		resistivity
3000	250					56156		also due to luck
3000	400					34715		of personel
4000	250					100138		and radio calls
4000	400					63204		
5000	250							
5000	400					97546		

GEOTHERMAL PROJECT KEN 82/002.

Area:	Eburra		BJ 030 588				V.E.S. Number.
Operator	Amani Amani/Gutura		Altitude (m): 1300				19
Date	23 2 90		AB Azimuth E - W				
Observations:	Bluf grassland - Scattered Thickets - light brown soil						

AB/2	MN/2	ΔV mV/I in Amperes				K MN	ρ ohm	NOTES
3	1	21.9	22.8	23.6	23.7	12.6	294.5	
5	1	9.81	4.52	5.11	5.11	37.7	192.3	
7	1	1.56	1.72	1.80	1.86	75.4	140.2	
10	1	0.61	0.64	0.61	0.69	155.5	106.9	106.4
10	2.5	1.69	1.74	1.72	1.76	58.9	103.8	
15	2.5	0.70	0.72	0.70	0.74	137.5	101.9	
20	2.5	0.38	0.41	0.42	0.42	247.4	104.4	
30	2.5	0.17	0.19	0.21	0.23	561.6	128.8	
40	2.5	0.11	0.13	0.14	0.14	1001.6	141.7	
50	2.5	78.1	76.9	77.3	77.5	1567	121.4	1n m Ω 125.3
50	10	0.30	0.32	0.34	0.34	377	129.2	
70	2.5					3073		Not done
70	10	0.15	0.18	0.19	0.20	754	148.1	
100	10	0.08	0.10	0.11	0.11	1555	171.8	
150	10	37.8	38.9	39.7	39.8	3519	140.2	1n Ω
200	10	19.5	19.8	20.0	20.0	6268	125.5	1n Ω 120.3
200	40	82.6	83.8	85.4	85.6	1508	135.1	
300	10					14133		Not done
300	40	22.7	23.1	23.6	23.8	3472	82.5	1 .. Ω
400	40	8.72	8.69	8.86	9.57	6220	55.2	1 m Ω
500	40	3.81	3.59	3.60	3.65	9755	35.6	1n .. Ω
500	100					3933		Not done
750	40	0.82	0.86	0.88	0.89	22027	19.6	
750	100					3630		Not done
1000	40	0.43	0.44	0.46	0.46	39207	17.9	
1000	100					15551		Not done
1500	100	0.29	0.40	0.42	0.92	35186	14.8	
1500	250					13244		Not done
2000	100	0.20	0.27	0.24	0.24	62675	15.2	
2000	250					26741		
2500	100					98018		
2500	250					38877		
3000	250					56156		
3000	400					34715		
4000	250					100138		
4000	400					6220		
5000	250					97		
5000	400					97546		

GEOTHERMAL   PROJECT   KEN   82/002.

Area:	Jiana			DJ 083 564			V.E.S. Number
Operator	Duad Phool Cik			Altitude (m): 1215			20
Date	24/3/90			AB Azimuth N–S			

Observations: Hard soil – short grassland with scattered bushes (thickets). A hot day.

AB/2	MN/2	ΔV in mV				K×(ΔV/MN)	ρ(ohm)	NOTES
3 .	1	6.52	6.68	.50	6.57	12·6	56.6	
5 .	1	2.51	2.57	2.74	2.95	37·7	111·4	
7 .	1	1.55	1.62	1.72	1.76	75·6	132·5	
10 .	1	1.32	1.26	1.38	1.29	155·5	216·7	205.5
10 .	2·5	2.92	2.12	2.25	2.20	56·9	194·3	
15 .	2·5	1.62	1.98	2.04	2.06	137·5	250·8	
20 .	2·5	1.12	1.43	1.54	1.62	247·6	298·8	
30 .	2·5	0.81	0.84	0.87	0.87	561·6	488·6	
60 .	2·5	0.42	0.44	0.46	0.4	1001·6	462·4	
50 .	2·5	0.23	0.26	0.27	0.28	1567	443·2	all	
50 .	10	0.96	1.10	1.14	1.16	377	428·9	NB done
70 .	2·5					3075		
70 .	10	0.31	0.35	0.35	0.27	754	283·5	
100 .	10	0.09	0.10	0.11	0.12	1555	184·4	
150 .	10	0.01	0.02	0.03	0.04	3519	140·0	
200 .	10	16.8	15.0	9.4	19.2	6260	120·2	
200 .	60	78.1	78.3	78.5	81.6	1508	115·5	
300 .	10					14122		NB done
300 .	60	17.4	17.6	17.9	18.0	3472	62·4	
600 .	60	6.98	7.09	7.14	7.15	6220	44·5	
500 .	60	2.81	2.89	2.94	2.96	9755	28·9	
500 .	100	2.91	6.99	7.08	7.11	3770	26·8	
750 .	11					22027		NB done
880 .	200					8679		
1000 .	11					39207		
1000 .	100	2.88	0.90	0.92	0.94	15551	14·6	
1500 .	100					35186		
1500 .	250					13766		
2000 .	100					62675		
2000 .	250					24766		
2500 .	100					92018		
2500 .	250					38877		
3000 .	250					56156		
3000 .	600					34715		
6000 .	250					100130		
4000 .	600					62206		
5000 .	25					156607		
5000 .	600					97566		

Left Form

Area: (illegible) BJ 115 582   **V.E.S. Number:** 57

Operator: Rwod / Dandi / Cuku   **Altitude (m):** 1410   **AB Azimuth:** E-W

Date: 25/3/90

Observations: Grassland with scattered short thickets. Good ground conditions (rained at night).

AB/2	MN/2	ΔV (Resistivity / Impedance)				K(AM AN/MN)	P(alam)	NOTES
3	1	8·5	8·21	8·18	8·81	12·6	514·1	(not surface)
5	1	15·79	15·88	16·27	16·18	37·7	628·8	very soft on
7	1	7·21	7·77	8·31	8·47	75·4	655·2	land
10	1	2·98	3·24	3·42	3·43	155·5	532·3	vegetation
10	2·5	8·89	9·22	9·26	9·28	58·9	548·5	528·9
15	2·5	2·93	3·28	3·56	3·71	137·5	514·3	
20	2·5	1·88	2·01	2·04	2·05	247·6	506·6	
30	2·5	0·54	0·61	0·79	0·83	561·6	411·7	
40	2·5	0·12	0·31	0·41	0·42	1001·4	411·7	
50	2·5	0·1	0·19	0·22	0·24	360·6	360·6	257·5
50	10	0·61	0·79	0·91	0·95	377	354·4	
70	2·5					3075		Not done
70	10	0·19	0·25	0·37	0·40	754	297·8	
100	10	0·14	0·13	0·19	0·15	1555	229	
150	10	58·7	60·0	60·78	60·98	3519	214·4	in ml
200	10	28·9	30·4	23·1	33·3	6268	208·7	207·6
200	40	30·6	34·5	36·5	37·1	1508	206·5	
300	10					14122		Not done
300	40	60·1	51·5	52·8	52·4	3472	187·9	
400	40	18·9	19·7	21·7	22·7	6220	140·8	
500	40	7·79	11·52	12·10	11·53	9755	111·7	105·2
500	100	23·3	24·3	25·7	26·2	3770	98·6	
750	40					22027		
750	100					8679		Not done
1000	40					39207		
1000	100	1·63	1·74	1·87	1·94	15551	30·1	in ml
1500	100					35186		Not done
1500	250					13744		
2000	100	0·20	0·25	0·33	0·5	62675	24·7	in ml
2000	250					24760		Not done due to Tme
2500	100					98018		
2500	250					38877		
3000	250					56156		
3000	400					34715		
4000	250					100138		
4000	400					62;		
	250					156·1		
5000	400					97546		

GEOTHERMAL PROJECT KEN 82/002.

Right Form

Area: (illegible) BJ 047 552   **V.E.S. Number:** 87 / 22

Operator: (illegible) / Dandi / Cuku   **Altitude (m):** 1225   **AB Azimuth:** N-S

Date: 26/3/90

Observations: Flat Flat — short grassland with scattered thickets. Fence (?)

AB/2	MN/2	ΔV (Resistivity / Impedance)				K(AM AN/MN)	P(alam)	NOTES
3	1	2·68	2·75	2·82	2·87	12·6	36·2	
5	1	1·48	1·40	1·38	1·37	37·7	52·1	
7	1	1·09	1·12	1·15	1·14	75·4	86·6	
10	1	0·65	0·68	0·72	0·72	155·5	112·6	105·7
10	2·5	1·62	1·64	0·7	0·68	58·9	98·7	
15	2·5	0·81	0·84	0·88	0·87	137·5	120·5	
20	2·5	0·60	0·75	0·52	0·56	247·4	212·0	Change to 130 (in/eq)
30	2·5	0·11	0·14	0·17	0·18	561·6	97·1	
40	2·5	0·09	0·10	0·11	0·11	1001·4	109·2	
50	2·5					1567	—	Not done.
50	10	0·20	0·23	0·21	0·23	377	90·5	
70	2·5					3075	—	Not done
70	10	108	111·5	110·1	121·1	754	91·3	in ml
100	10	52·2	55·9	57·1	56·2	1555	87·3	
150	10	20·2	20·2	20·4	20·3	3519	72·3	in ml
200	10	7·99	8·31	8·41	8·65	6268	54·2	
200	40					1508	—	Not done
300	10	3·87	3·57	3·81	3·23	14122	45·1	
300	40	12·2	12·9	13·4	12·6	3472	47·4	46·5
400	40	5·01	5·19	5·22	5·24	6220	72·6	
500	40	2·02	2·14	2·16	2·17	9755	21·1	21·8
500	100	5·78	5·87	5·76	5·77	3770	22·5	in ml
750	40					22027	—	
750	100					8679	—	
1000	40					39207	—	
1000	100	0·68	0·69	0·71	0·72	15551	11·17	
1500	100					35186		
1500	250					13744		Not done due to rike and lack of communication, Gobli (?) make up and down as time was limited. Thunderstorm threatening.
2000	100					62675		
2000	250					24760		
2500	100					98018		
2500	250					38877		
3000	250					56156		
3000	400					34715		
4000	250					100138		
4000	400					62204		
5000	250					15.		
5000	400					97546		

GEOTHERMAL PROJECT KEN 82/002.

Left sheet

Area: Huwa   BS 106 555
Operator: [illegible] / [illegible]   Altitude (m): 1385
Date: 27/3/90   AB Azimuth: N-S
V.E.S. Number: 57 / 23
Observations: Slightly hilly surface – short grasses, soft [...] brown soil – hot day.

AB/2	MN/2	ΔV				K(MN AB/MN)	ρ(calc)	NOTES
3	1	8.91	1.58	2.01	3.03	12.6	28.2	reading
5	1	1.28	1.32	1.33	1.32	37.7	50.1	
7	1	0.82	0.84	0.87	0.89	75.6	66.7	N/a m
10	1	0.47	0.49	0.52	0.53	155.5	82.7	
10	2.5	1.40	1.01	0.43	0.47	58.9	N.4	82.6
15	2.5	1.41	0.50	0.53	0.55	137.5	75.5	
20	2.5	0.22	0.24	0.28	0.26	247.4	65.2	
30	2.5	0.1	92.2	3.31	93.1	561.6	52.3	
40	2.5	45.5	44.4	049	45.2	1001.4	45.3	m n l
50	2.5	24.3	25.1	256	25.8	1567	40.3	
50	70	47				3.1		NO slope
70	25					3075		
70	10	46.3	46.9	46.5	470	754	75.5	
100	10	16.2	16.7	19.5	17.7	1555	20.6	
150	10	7.9	8.0	8.0	8.2	3519	28.8	m n l
200	10	3.5	3.7	4.1	4.0	6260	26.1	
200	40					1508		
300	10					14122		
300	40	5.12	5.92	5.7	5.62	3472	20.2	m n l
400	40	5.3	5.7	2.8	29	6220	15.1	
500	40	1.09	1.33	1.15	1.13	9755	14.3	
500	100					3770		NO slope
750	40		4			22027		
750	100					8679		
1000	40	0.11	0.19	0.27	1.2	39207	11.5	m n l
1000	100					15551		
1500	100					35186		
1500	250					13744		
2000	100					62675		
2000	250					24740		
2500	100					98018		
2500	250					38877		
3000	250					56156		
3000	400					34715		
4000	250					100138		
4000	400					62204		
	0					156687		
5000	400					97546		

Right sheet

Area: [illegible]   BS 106 585
Operator: [illegible] / [illegible]   Altitude (m): 1320
Date: 27/3/90   AB Azimuth: N-S
V.E.S. Number: 57 / 24
Observations: Slightly grassland, scattered thicket. [...] light brown soil.

AB/2	MN/2	ΔV				K(MN AB/MN)	ρ(calc)	NOTES
3	1	8.8	12.4	2.6	2.6	12.6	158.1	
5	1	2.41	2.49	3.51	3.7	37.7	142.1	
7	1	1.17	1.28	1.41	1.44	75.6	108.7	
10	1	0.98	0.50	0.51	0.52	155.5	58.2	81.9
10	2.5	1.37	1.39	1.41	1.43	58.9	83.6	
15	2.5	0.81	0.46	0.47	0.47	137.5	65.0	
20	2.5	0.13	0.19	0.21	0.21	247.4	52.8	
30	2.5	87.1	87.3	90.1	90.2	561.6	50.5	m n l
40	2.5	47.7	48.5	49.5	49.6	1001.4	49.7	m n l
50	2.5	31.7	32.1	52.1	52.8	1567	51.5	m n l
50	70					3.1		
70	2.5	19.1	19.3	19.4	19.5	3075	59.8	m n l) 60.7
70	10	80.9	81.3	81.5	81.6	754	61.5	m n l
100	10	42.5	44.5	44.5	44.9	1555	69.8	m n l
150	10	22.3	21.1	21.1	21.1	3519	34.4	m n l
200	10	11.73	11.59	11.97	12.12	6260	35.2	m n l
200	40					1508		
300	10					14122		
300	40	16.9	16.1	16.2	16.2	3472	56.6	m n l
400	40	7.75	8.10	8.10	8.17	6220	50.5	m n l
500	40	2.29	2.91	4.00	2.02	9755	39.2	m n l
500	100					3770		
750	40		4			22027		
750	100	2.01	1.21	1.33	33	8679	20.2	m n l
1000	40					39207		
1000	100	1.19	1.20	1.10	1.20	15551	18.7	m n l
1500	100					35186		
1500	250					13744		
2000	100					62675		not done
2000	250					24740		
2500	100					98018		to done at
2500	250					38877		tension
3000	250					56156		
3000	400					34715		
4000	250					100138		
4000	400					62204		
5000	250					156687		
5000	400					97546		

Plate 1   The murram road running round the foot of Soitamrut. Ol Doinyo
Onyoke is at the background.

OL Doinyo Onyoke

Soitamrut

119

Plate 2   A general view of the area from ST23 facing north.

Plate 3   Part of the crew with the Maasai boy who was the field guide.

Plate 4   Close-up of the Terrameter with the Booster 'slaved' to the SAS 300 Terrameter.

Plate 5   Locating the sounding station where the Terrameter is positioned.